A Physiological and Psychometric Evaluation of Human Subconscious Visual Response and Its Application in Health Promoting Lighting

by

Garen V. Vartanian

A dissertation submitted in partial fulfillment
of the requirements for the degree of
Doctor of Philosophy
(Macromolecular Science and Engineering)
in the University of Michigan
2016

Doctoral Committee:

Assistant Professor Kwoon Y. Wong, Co-Chair
Associate Professor Pei-Cheng Ku, Co-Chair
Professor L. Jay Guo
Professor Jinsang Kim

Dedication

This dissertation is dedicated to my family and friends, both near and far, without whom this endeavor would have seemed impossible. I would like to thank my parents in particular for their unending love and support (in more ways than one).

Acknowledgement

The journey that has lead to the writing of this thesis was fraught with difficult choices and much uncertainty, but its final conclusion has brought much more clarity to its author, and one hopes, the field of study which is the focus of this work.

I would like to thank senior lab mates Drs. Greg McGraw, Brian Lassiter, and Kyle Renshaw for passing on their valuable experiences as research engineers and scientists early on in my tenure and for showing me how to (and how not to) proceed with the execution of scientific research: in a well thought out and efficient manner. I also want to thank them for helping set the foundations that facilitated the realization of instrument design as pertaining to my thesis work, long after they had graduated.

I would further like to thank my research advisors, Professors Kwoon Wong and Pei-Cheng Ku, without whom I may not have extended my stay past the no man's land of the terminal masters degree. Their faith in my progress and my ideas is the deciding factor in my remaining in the program to its completion. My departmental advisors, Rick Laine and Nonna Hamilton, provided additional personal and financial support and showed me what it takes to run a great program: passion and genuine concern for the success of its student body.

I would like to extend a special thank you to Scott Almburg, who is in charge of the electronics module at the Kellogg Eye Center. A masters degree of Electrical Engineering specializing in Solid State Electronics acquainted me with challenging mathematical and physical concepts, often seen only in the most modern of electronics devices. Scott, however, provided me with the missing piece in my electronics skillset, extensive practical knowledge and know-how. I have to thank him for learning how to design and spec a device board and its various components, wire it, utilize low level language to program its controllers, manage device power, and do some old fashioned trouble shooting – and there was the occasional exactoblade and elbow grease duty to dislodge overzealous solder flux, preventing the destruction of many months' work. For that mentorship and help with the construction of numerous devices, I thank you Scott, you are truly the fifth Beatle. I would also like to thank Scott Szalay, who is charged with running the machine shop at Kellogg eye center. He helped in the design and build of custom instruments, often with beautiful results.

Lastly, I would like to thank the people I've met in Ann Arbor along the way – too many to list, who've helped enrich my life's education in areas outside that of my formal expertise. In particular, I thank Sasha Cai Lesher Perez, Iverson Bell, III., Remy Elbez, Alyssa Mouton, and Erik Yusko.

Preface

The material enclosed in this dissertation balances on the intersection of multiple disciplines. These disciplines are psychophysics, vision science, and lighting engineering. This thesis explores what impact lighting has on human subconscious visual response and how this knowledge can be combined in an interdisciplinary nature to provide solutions to the deficits inherent in artificial light. That is, what effect will intermittent light have on the visual response, and by extension human physiology, when compared to steady light presentations? Will pulsing light produce an exaggeration of response? Can a differential dynamic response be used to overcome health deficits that have been induced by modern lighting environments? Conversely, are current lights and electronic displays too stimulating in the evening and how should their output be reduced?

The interplay of these 3 scientific fields will be better understood in the introductory section of this thesis. Vision science is a broad field encompassing electrophysiology of the retina, higher cortical processes involved in vision, clinical work in ophthalmology, molecular biology, and genetics. There is some overlap between psychophysics and vision science when it comes to the phenomena of conscious visual perception as it pertains strictly to humans. Psychophysics is a field that interests itself in the quantification of physiological responses to physical stimuli, almost exclusively in the human domain. It pertains to all human senses, such as touch, taste, smell, sound, but

focuses mostly on our most complex sensation, the perception of light, i.e., our conscious visual response. Lighting engineering focuses on the development and application of artificial lighting in order to illuminate our surroundings. Psychophysical metrics are employed by lighting engineers to ensure lights adhere to certain standards, e.g., minimum brightness requirements, color appearance, and color rendering abilities with respect to the environment that is to be illuminated.

The novel approach undertaken here incorporates data from subconscious visual response studies into psychophysical modeling and lighting engineering. Subconscious vision is a relatively recent focus of the vision science community, brought on by the discovery of a previously unknown retinal photoreceptor dedicated to subconscious visual regulation and subsequent major advances in the study of subconscious visual processes over the past decade. Ironically, our chief focus in the concluding study of this thesis has been to minimize perception of changes in the lighting environment, as it pertains to psychophysics.

We seek to integrate subconscious visual response metrics into the world of lighting design with the hopes that those who suffer from light-deficit induced depression, daytime fatigue, poor alertness levels, and poor sleep quality can increase their productivity and enjoy their days while going about their daily routines – without having to stare at the sky for hours a day! For the lighting and electronics industry, we hope our study of subconscious stimulative thresholds at night will better inform their design guidelines for health conscious products.

Table of Contents

List of Figures

Chapter 1 – Introduction

The human visual system is an incredible sensing mechanism. Not only is it incredibly refined, but also dominant, accounting for the majority of sensory processing in humans(Medina 2008; Stein 2006). A surprising half of the human cortex is delegated to visual processing(Toga 2015). It should come as no surprise then that the branch of science devoted to perception, psychophysics, is dominated by the study of vision and the phenomena of color. Nor should it be surprising that health outcomes have been increasingly tied to visual function. The techniques developed in psychophysics have been utilized to make many of the observations found in this thesis. Before getting into the health implications of light and what psychophysics is exactly, it is best to give a brief overview of the human visual system as related to the research material in this dissertation.

The Human Eye: Structure and Function

Gross Anatomy

The human eye consists of numerous structures (see Figure 1.1). Externally, a central aperture, the pupil, is clearly visible and provides an entrance for light from our environment(*Webvision: The Organization of the Retina and Visual System* 2016; Malacara 2011). The iris is the pigmented muscle surrounding the pupil. The muscles of

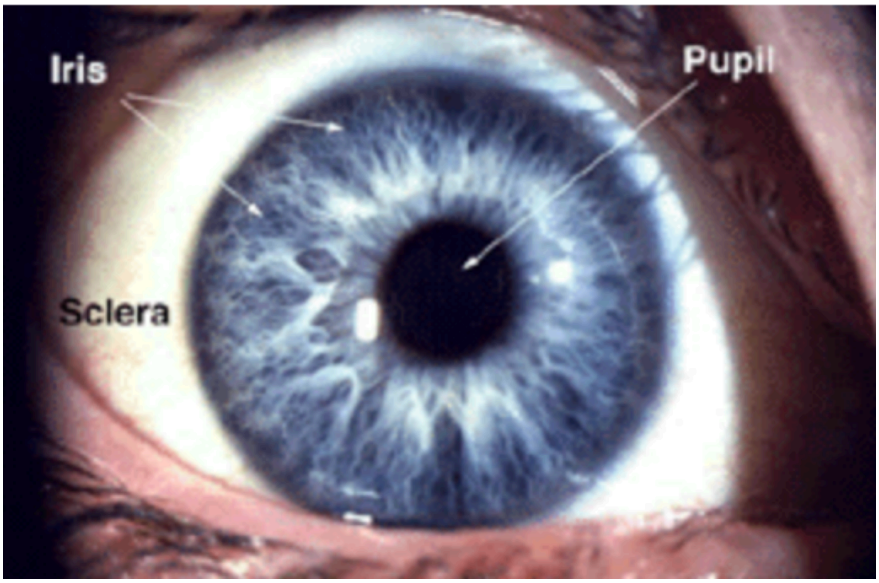

Figure 1.1 External structures of the human eye(*Webvision: The Organization of the Retina and Visual System* 2016).

the iris constrict and dilate such that the size of the pupil is affected. It limits the amount of light that can enter the eye, although an important function is depth of focus modulation. The sclera is the "white of the eye" and provides the mechanical support, forming the majority of the outer wall of the eyeball. Continuous with the sclera is the transparent surface covering the iris and pupil. This structure is known as the cornea and forms a raised surface (see Figure 1.2). The cornea provides most of the optical focusing power allowing for image formation on the photoreceptor mosaic located in the back of the eye, the retina(Malacara 2011). With the aid of specialized muscles, the lens depicted in the illustration provides additional adjustment in the focusing of light for proper image rendering. Fluids of varying viscosity fill in the space between these structures. The pigment epithelium is located in the backwall of the eye. It surrounds the cells of the outer retina and provides cellular support to the retina.

The Retina and Classical Photoreception

The retina is essentially an extension of the brain and a direct window to the outside world(Dowling 2012). Photoreceptors that are responsive to light form the sensory neurons around which all supportive structures of the eye are formed. The pioneering vision scientist and Nobel laureate, Ramon y Cajal, described the neural cell types of the vertebrate retina as early as the late 19th century (see Figure 1.3a), and as early as the first decade of the 20th century, Helmholtz postulated that the photoreceptors subserving image-forming vision can be attributed to the rods and three cone subtypes of the outer retina (see Figure 1.3b)(Helmholtz 1911). The outer retina consists of rod and

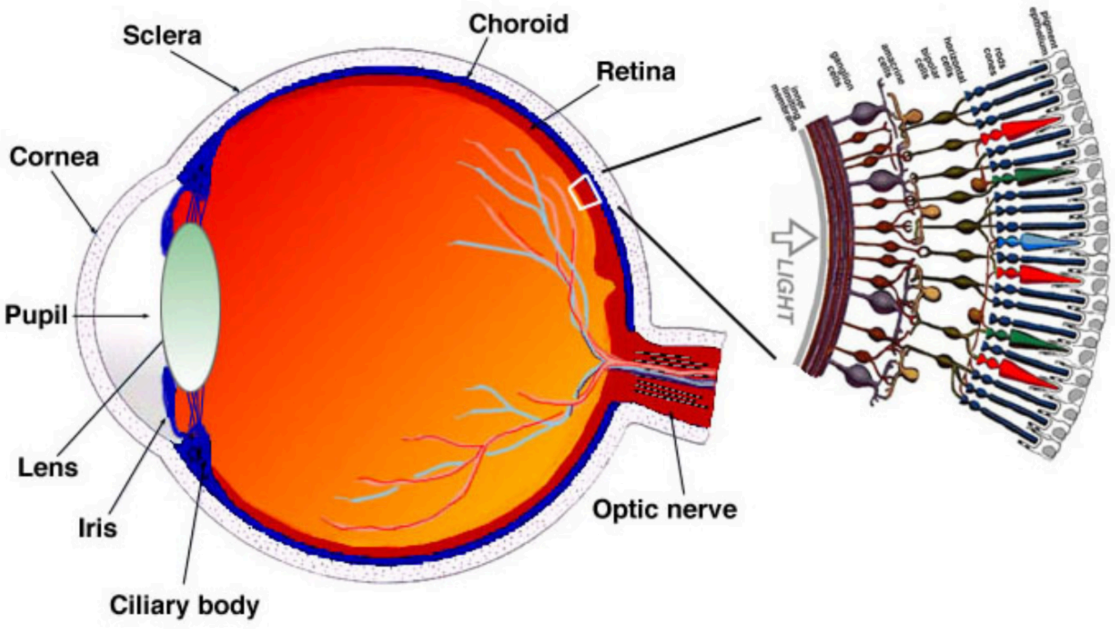

Figure 1.2 An illustration of the human eye(*Webvision: The Organization of the Retina and Visual System* 2016).

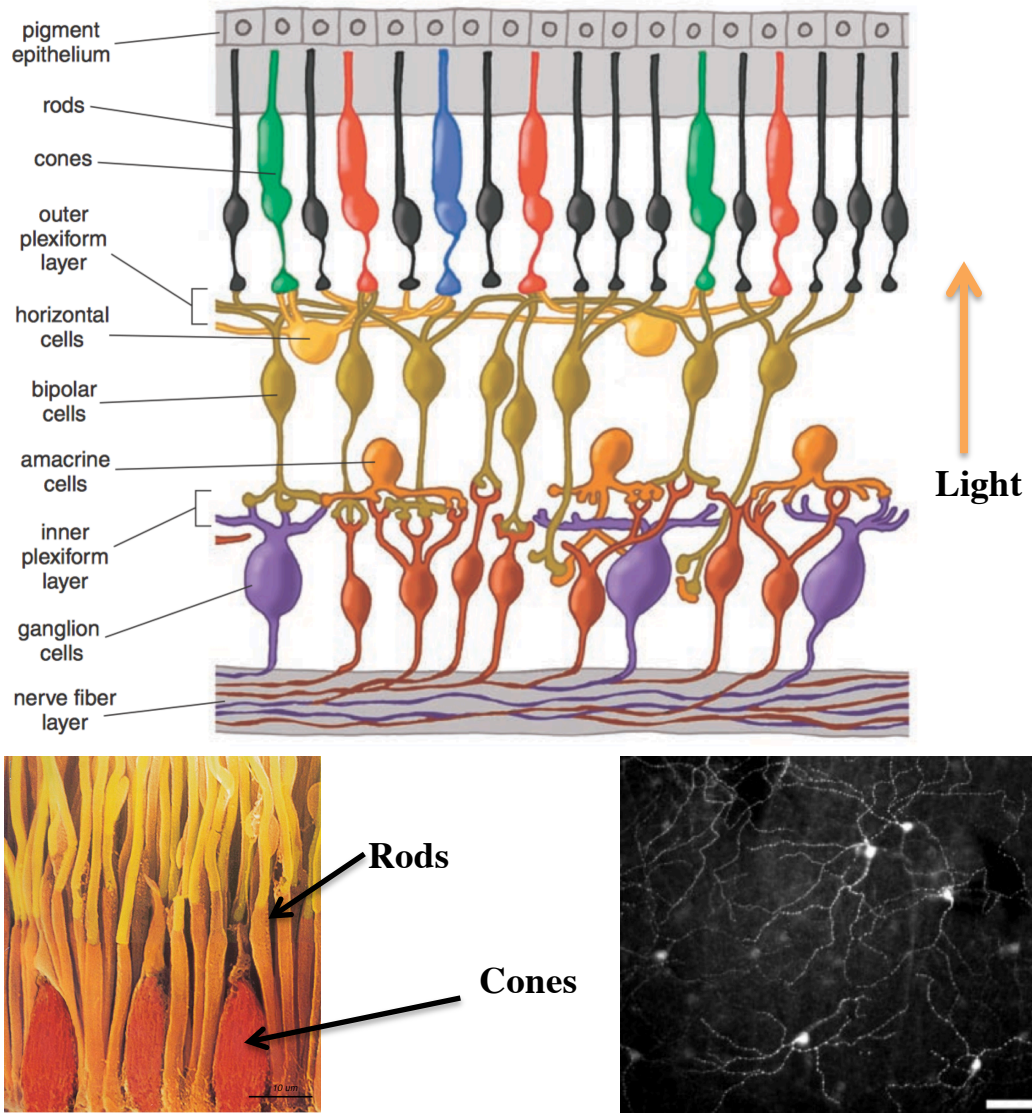

Figure 1.3 Cells of the human retina. The vertically aligned cells in this depiction form clearly delineated layers (top). The outer retina consists of rods and cone cells. These photoreceptors mediate conscious vision. Their signals are sent through bipolar cells to ganglion cells, which ultimately relay visual signals to brain centers involved in visual processing. The pigment epithelium is located in the back of the eye. The pupil is located behind the nerve fiber layer and light crosses through the retina before impinging upon the rod and cone photoreceptors. A scanning electron micrograph image of cones and rods from a primate retina (bottom left)(*Webvision: The Organization of the Retina and Visual System* 2016). The extensive processes of the ipRGCs. Scale bar is 100 microns (bottom right)(Provencio, Rollag, and Castrucci 2002).

cone cells. Their signals are sent through bipolar cells to ganglion cells, which ultimately relay visual signals through the optic nerve to brain centers involved in visual processing. The retina can be considered an inverted structure, with the tips of the photoreceptors in the outer retina pointing away from the direction of light. Therefore, light must travel through retinal layers in order to interact with the active segments of the cone and rod photoreceptors.

In primate retina, there is a specialized region that provides high acuity visual function. This region is known as the fovea(Dowling 2012). The inner layers of the retina are diverted in the foveal region so that light scattering is reduced en route to the rods and cones. Blood vessels are absent in this region as well as the subclass of cones, which are sensitive to blue light (again in order to reduce the scattering effects of short wavelength light and enhance acuity). The fovea makes reading of the small print on this page possible.

The region in and around the central fovea is known as the macula. The macula has a yellow pigmentation known as the macula lutea. This pigmentation protects the fovea by absorbing UV and deep blue radiation. As a result of the distinct organization of foveal photoreceptors and the macular pigmentation, two separate color matching functions have been devised for predicting color appearance in humans depending on the degree of viewing angle from observer to object(Schanda 2007). The color matching functions are described further below.

It is now known that the human retina contains 3 classes of photoreceptors: rods, cones, and intrinsically sensitive retinal ganglion cells. Each of the classes have

photopigments with spectral absorption profiles that vary from each other. The cones are further divided into 3 subclasses each with photopigments that have different spectral absorption profiles.

Rods are utilized in nocturnal settings where light levels are very low, but provide poor object discrimination. This is a result of the synaptic organization of the rods, as the outputs of individual rod photoresponses are summed together with responses from neighboring rod cells. Rod spectral absorption sensitivity peaks at close to 500 nanometers. This summation of signal boosts the sensitivity of rod vision, but comes at the cost of image detail.

Under daylight conditions, cones are active, but not rods, since the highly sensitive rod responses have been saturated(Hecht 1987). Cones also sum their signals to a lesser degree in the periphery of the retina, however, in the fovea, cones output their signal one-to-one to the ganglion cell layer(Dowling 2012). The three cone types display different peak spectral sensitivities, enabling color discrimination (see Figure 1.4). As such, humans and other animals that encode color with 3 distinct photoreceptor-types are known as trichromats. The three cone subclasses have opsin photopigments, which are maximally sensitive to short, medium, or long wavelengths of light. These subclasses are commonly known as blue, green or red cones, respectively. Cones responses are often abbreviated as S, M, and L. The basis of color discrimination is derived from the spectral differences of the 3 cones types. Neural processes mediating color contrast are complex,

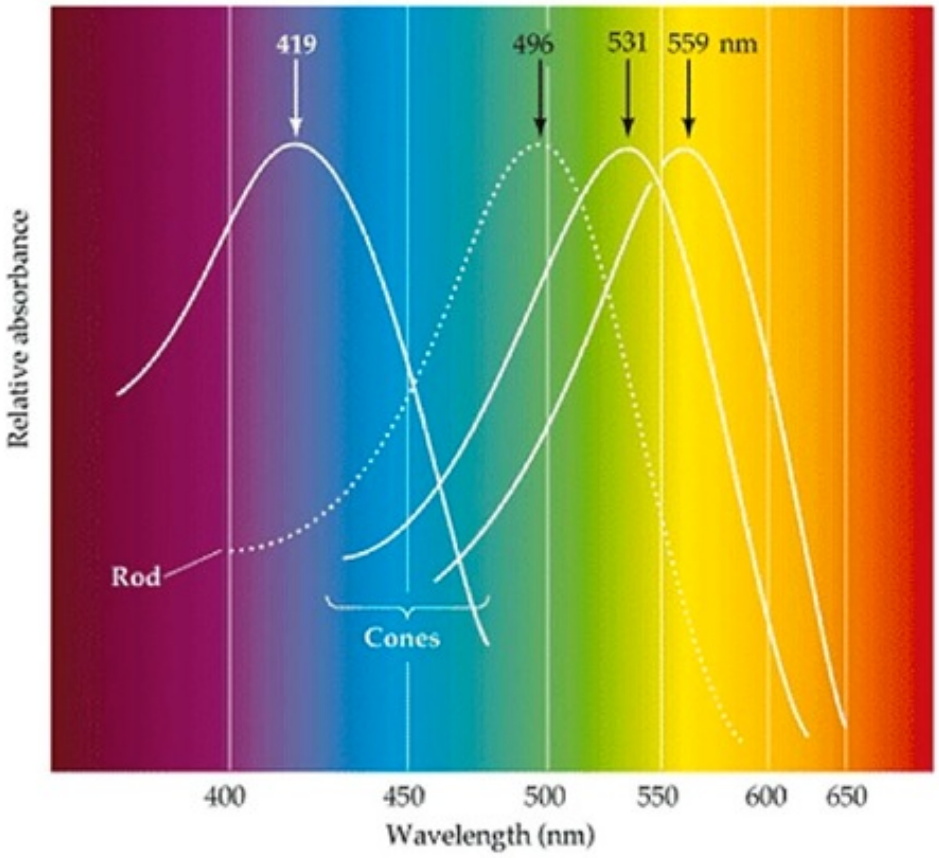

Figure 1.4 The relative spectral absorbance spectra of human rods and cones. Peak absorption wavelengths (in nanometers) are indicated with arrows(*Webvision: The Organization of the Retina and Visual System* 2016).

including subtractive and additive interplay of cone response at the retinal and cortical levels, but color is essentially a function of response ratio of the 3 cone types to stimuli.

A New Class of Photoreceptor: The intrinsically photosensitive retinal ganglion cell (ipRGC)

In the 20th century, it was noted that loss of visual function didn't preclude animals or even some blind humans from maintaining a circadian rhythm(Czeisler et al. 1995; García-Fernández, Jimenez, and Foster 1995; Freedman et al. 1999). This physiological regulation by light was errantly attributed to residual rods and cones in the visual system that were too sparse to contribute to conscious visual perception, but sufficient for regulation of subconscious processes. In 2002, the existence of a novel class of photoreceptors was confirmed, intrinsically photosensitive retinal ganglion cells (ipRGCs) containing melanopsin photopigment(S Hattar et al. 2002), which form the primary conduit for subconscious, non-image-forming physiological responses to light (see Figure 1.5). ipRGCs are able to respond to light directly via melanopsin, as well as via inputs from rod and cone photoreceptors.

ipRGCs were found to play the critical and diverse role in non-image forming vision with direct regulation of pupillary light reflex and circadian entrainment among the well-defined outputs regulated(Berson, Dunn, and Takao 2002; S Hattar et al. 2002). Demonstrations of these non-image-forming responses include the pupillary light reflex(Gamlin et al. 2007), suppression of nocturnal melatonin secretion(G. C. Brainard et al. 2001), and photoentrainment of circadian rhythms (e.g. sleep/wake cycle) (see Figure 1.6)(K. Y. Wong, Graham, and Berson 2007).

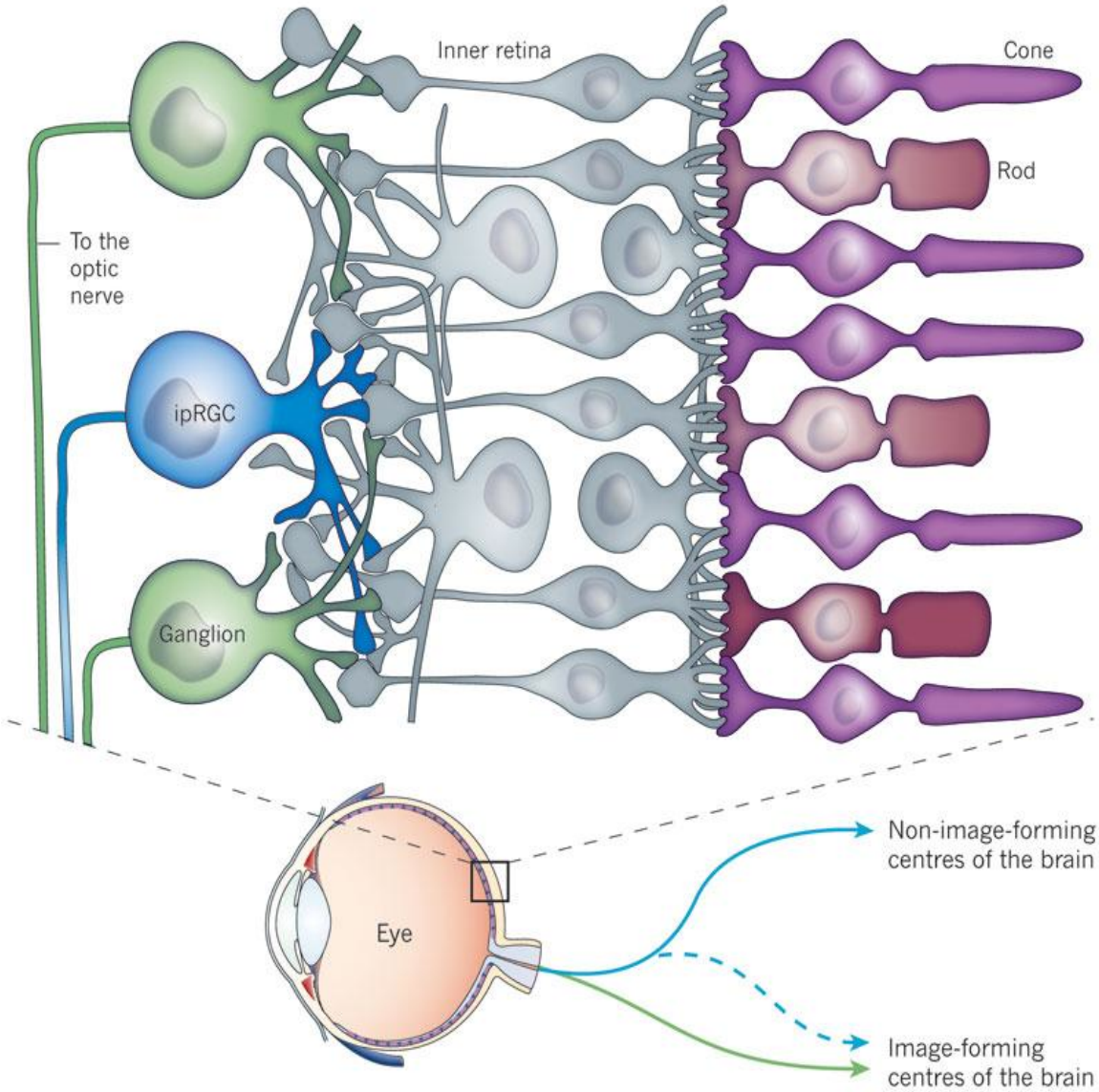

Figure 1.5 A special class of ganglion cell, the intrinsically photosensitive retinal ganglion cell (ipRGC). ipRGCs provide non-image forming responses to light, regulating physiological processes. They contain their own intrinsic photopigment, melanopsin, and are thus considered true photoreceptors(Lok 2011).

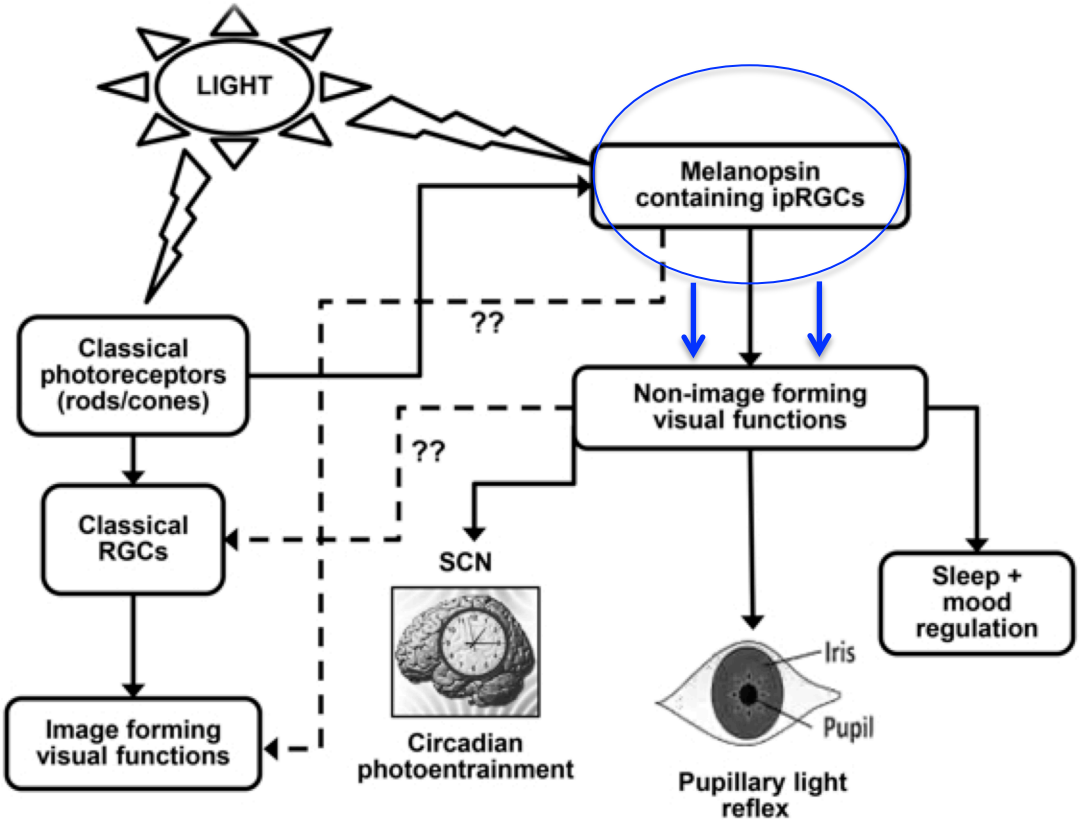

Figure 1.6 ipRGCs trigger subconscious, non-image-forming visual responses separate from conscious visual perception. Several examples of subconscious outputs regulated: the regulation of sleep and mood, pupillary light reflex, and synchronization of our circadian clock to the light/dark cycle. It is not known to what extent conscious vision is influenced by responses from ipRPCs (http://photobiology.info/Sengupta.html).

As early as 1962, Bouma noticed that the pupillary light response peaked at 490 nm(Bouma 1962). He was able to rationalize this result be fitting a linear combination of the S-cone and rod response curves. Now these findings can be explained by a photopigment, melanopsin. This discovery helps explain numerous subconscious physiological responses in a definitive manner. Gamlin showed that the ipRGC pathway drives the pupillary light response, whose spectral sensitivity is shown to peak at 482nm(Gamlin et al. 2007). Brainard and colleagues showed an ipRGC-mediated action spectrum for acute melatonin suppression, which peaked between 446 and 477 nm (see Figure 1.7)(G. C. Brainard et al. 2001). Neither of their mathematical fits to these sensitivity values can be explained by the absorption profiles of any of the rods and cones, thus signifying the dominant role melanopsin plays in mediating these processes.

Unlike the rods and cones which are found in the outer retina, ipRGCs are in the inner retina (ganglion cell layer) and are absent from the fovea(Dacey et al. 2005). These intrinsically photosensitive ganglion cells constitute no more than a few percent of all ganglion cells in mammals(Bailes and Lucas 2010). ipRGCs have a distinct anatomy for photon capture when compared to rods and cones. Rod and cone cells have single cylindrical, narrow outer processes and are roughly 2 and 1.5-6 microns in diameter, respectively(*Webvision: The Organization of the Retina and Visual System* 2016). ipRGCs have extensive processes branching out for hundreds of microns, which seem to be suitable for a broad-capture, integrating photoreceptive system (see Figure 1.3b and c)(Provencio, Rollag, and Castrucci 2002).

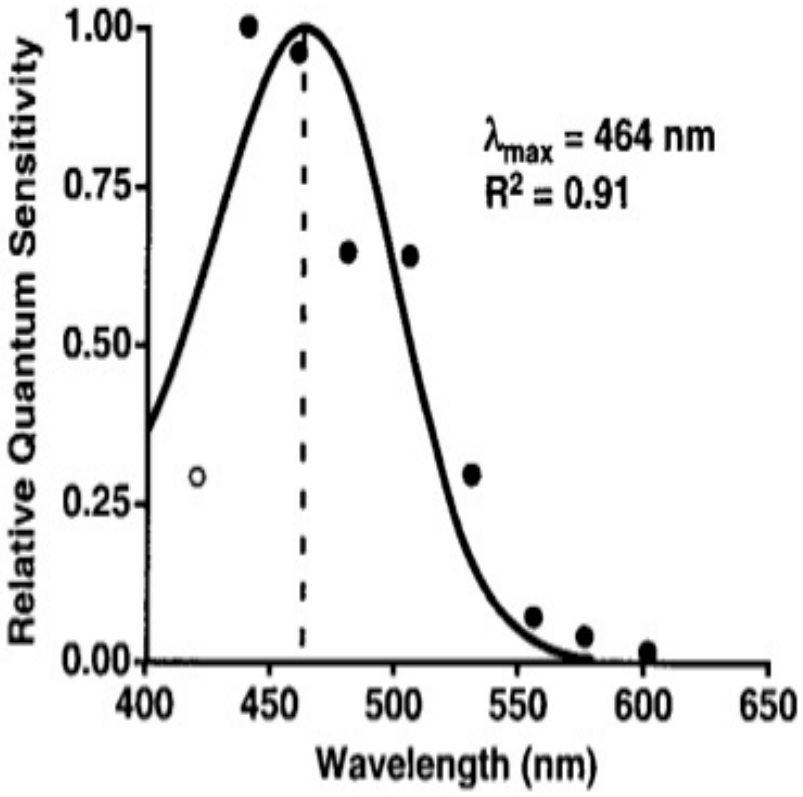

Figure 1.7 Action spectrum for melatonin suppression via ipRGCs in humans. The light-mediated suppression of melatonin levels as measured in blood peaks at a sensitivity of approximately 464 nm. The fit presented in this figure closely resembles the absorption profile of the melanopsin photopigment(G. C. Brainard et al. 2001).

Deviations from proper daytime light exposure can result in unhealthy outcomes, such as jet lag and seasonal affective disorder (SAD)(Rosenthal et al. 1984), and perhaps even general depressive disorders(Naus et al. 2013). Further discussion of health impacts of light are presented in the last section of this introduction.

The contributions of ipRGCs to conscious vision is a matter of ongoing research. In 2007, Zaidi et al. showed that under very bright blue light conditions, certain blind subjects can perceive the presence of light utilizing what is postulated to be a primitive brightness detection circuit in the visual system(Zaidi et al. 2007). How strongly this channel of perception contributes to vision in sighted individuals is yet to be determined.

Visual Psychophysics

What is Psychophysics?

How is it that a person can step from a darkened room into blinding brightness, and within a matter of seconds, is able to see perfectly well? How come one's environment appears to be tinted blue after staring at a pink object for some period of time? As the intensity of a lamp is increased, how much brighter will it appear to an observer for every incremental increase in intensity? How the perceptual attributes of sensations relate to the physical stimuli that produce them is the study of psychophysics. A large component of this field is focused on quantification of perceived stimuli and is sometimes specifically referred to as quantitative psychology or psychometric physics.

Psychophysics studies all the senses as related to human perception. It is part psychology, part physiology, part mathematics, and involves the philosophy of why we perceive. Quantifying psychophysical phenomena is a matter of determining the appropriate measurement techniques to retrieve unconfounded data and then determining the most appropriate way to interpret the results. This goes beyond mathematical fitting: the question of absolute versus relative scales is equally important.

Quantifying Sensation Response Magnitude

One of the first scientists to propose a mathematical relation between sensation and stimulus magnitude was Fechner in 1860(Fechner 1860). Fechner's logarithm law is expressed as:

$$\psi = k \log \left(\frac{\phi}{b}\right)$$

where ψ is sensation magnitude, ϕ is stimulus magnitude, b is the magnitude of absolute threshold of sensitivity, and k is a proportionality constant. As becomes apparent, a stimulus with intensity b has a magnitude perception of zero. Then the magnitude aroused by stimulus intensity 10b is k, by stimulus 100b is 2k, and stimulus 1000b is 3k and so on. Fechner states, "As stimulus increases geometrically, sensation intensity increases arithmetically"(Marks 1974, 6). Fechner's motivation is to provide units by which sensory magnitude can be measured, just noticeable difference (JND). JND's units are therefore equal in subjective magnitude.

There was much controversy related to this proposed law and it is in fact an oversimplification, but it generally holds true that senses are felt on a geometric scale and rarely are sensations perceived as linear. Brentano made a modification to Fechner's rule, such that JNDs grow in size as sensory magnitude is increased(Brentano 1874). This resulted in reformulating the relationship between perception and stimulus as a power law. Ultimately, many magnitude estimations for various sensation experiments were fit with a simple power law:

$$\psi = k\phi^{\beta}$$

β is found by plotting sensation magnitude by stimulus intensity on a double-logarithmic plot. Some example betas for psychophysical functions are warmth (small area), 1.5; warmth (large area), 0.7; loudness (3150 Hz tone), 0.67, brightness (short flash), 0.5; brightness (long flash), 0.33 (see Figure 1.8)(Marks 1974). It is important to note there is no psychophysical function that is comprehensive for any particular sensation.

It is correct only to speak of a response function in the context of all other relevant variables. For example, we can see that the increase in brightness to increasing flash intensity is more rapid for short flash duration than for long flash durations. This may also depend on whether the subject is in a dark room or if his surroundings are well illuminated. Then the question can be asked whether the room is illuminated with white light or one that is clearly colored. It soon becomes clear that the environmental variables can become overwhelming, and a very large number of studies have been undertaken in order to make sense of the complex environment to which our sensory systems have been designed to perceive.

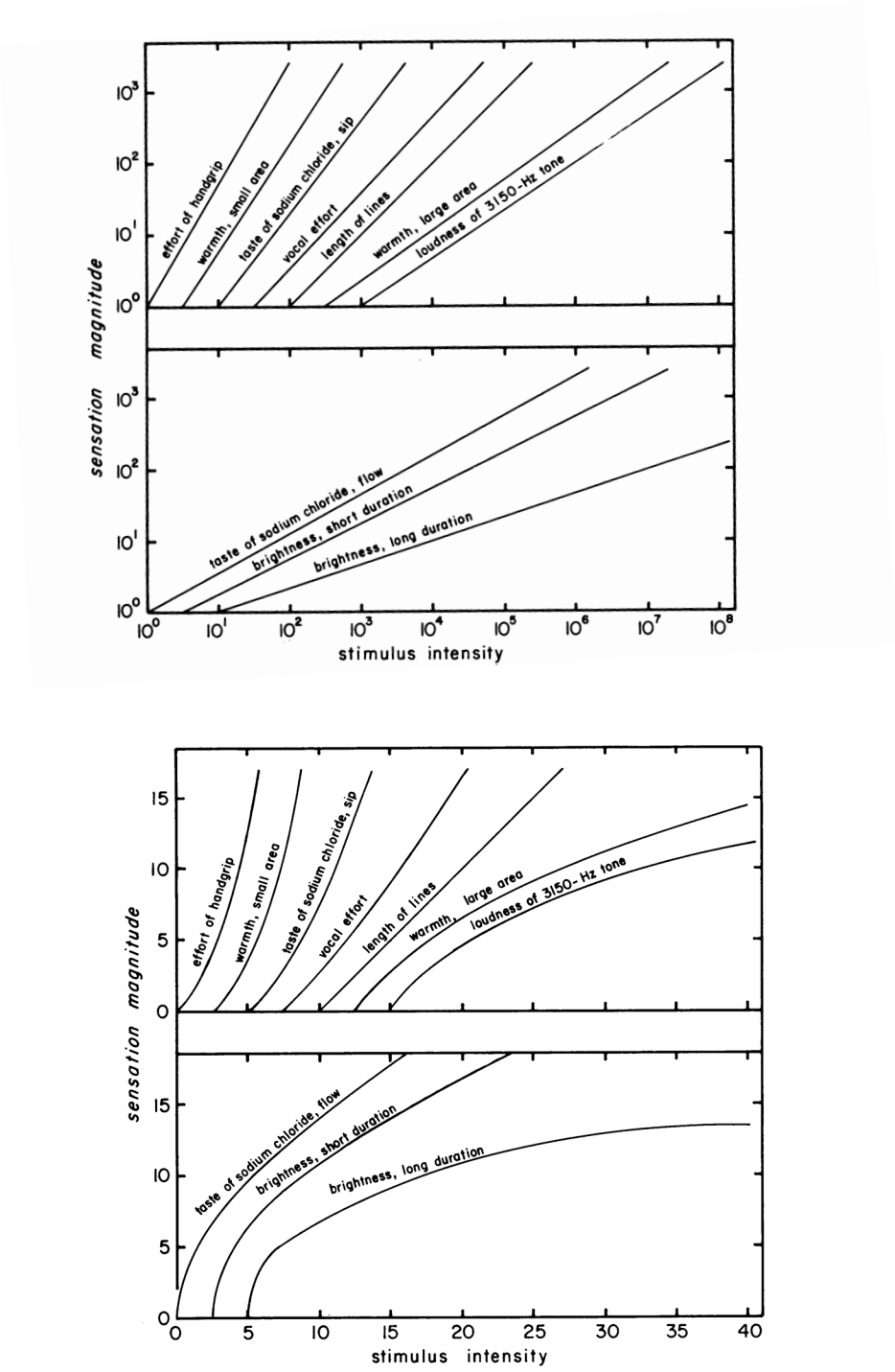

Figure 1.8 Sensory perception increases as stimulus intensity increases according to a simple power law. Seven psychophysical functions have been plotted on a double-logarithmic scale (upper panel) and shown on a linear plot for comparison (lower panel)(Marks 1974). Note that the fitting parameters can change under different test conditions.

In order to unclutter our thinking in the design of light stimuli, we focus on the most relevant factors determining response magnitude. We see that visual response is more sensitive to short flashes than long flashes.

Scaling

One's first instinct is to assume that absolute scales provide the most meaningful, or powerful indication of an effect, however most sensory perceptions are highly context and contrast sensitive. In the case of measuring pupil response sensitivity to light presentations, the measured data can be presented in absolute values, e.g., the diameter of the pupil as light is introduced. However, a more meaningful presentation of the data can be provided by interpreting this measurement with respect to the dark-adapted pupil size, that is, with respect to a subject's pupil size when it is most dilated. With the latter approach, a percentage of diameter change can be calculated and provides a more insightful value for determining level of activation of this subconscious visual process.

Summation and Adaptation

When a stimulus is presented, there is usually a two-stage response. These two sensation modalities can be independent to varying degrees. The first stage is a quick increase in sensory magnitude. The second stage is a diminution of the sensation over time, usually reaching an asymptotic value. The first stage is called summation, and the second stage is called adaptation(Marks 1974). This is a double phenomenon that is well observed in visual response.

The human eye has an incredible dynamic range due to its ability to adapt to light over a logarithmic scale for just over 11 orders of magnitude (see Figure 1.9)(Stockman and Sharpe 2006). This is due to both pigmentation bleaching in the photoreceptors themselves and neuronal processes in the retina and the brain(Dowling 2012). As previously mentioned, our eye is more sensitive to brief flashes of light than longer pulses. This effect is observed not just in brightness perception, but in physiological responses to light such as pupil constriction(Joshua J. Gooley et al. 2012; Vartanian, Zhao, and Wong 2015) and circadian rhythm resetting(Munch et al. 2012; Zeitzer et al. 2011; Rimmer et al. 2000). These results can be attributed to prevention of light adaptation, and we will use this behavior to our advantage in the design of health-promoting lighting.

Color Science

Color Matching and Color Models

During the early twentieth century, it became apparent that physical measurement of light source power (in Watts) did not correlate with the source's visibility. Illuminants that have the same power output can produce very different brightness. In order to determine the relative brightness of the spectrum of light at each wavelength, brightness matching experiments were conducted wherein a reference monochromatic was presented and the relative intensity of each wavelength of light was then determined. In 1924, it

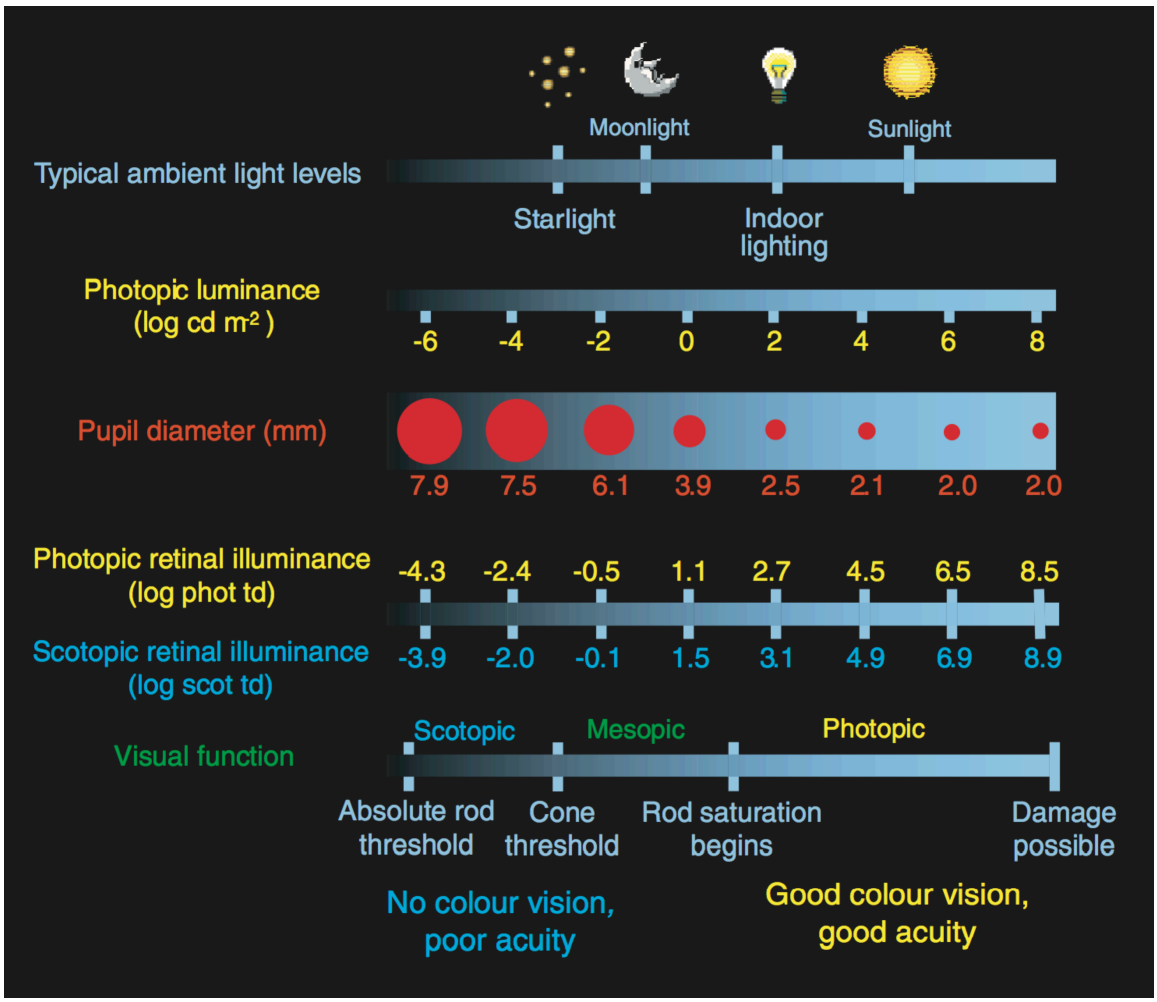

Figure 1.9 Illumination levels. Typical ambient light levels are compared with photopic luminance (log cd m^{-2}), pupil diameter (mm), photopic and scotopic retinal illuminance (log photopic and scotopic trolands respectively) and visual function. Trolands are candela m^{-2} multiplied by pupil area in mm^2. The scotopic, mesopic and photopic regions are defined according to whether rods alone, rods and cones, or cones alone operate. The conversion from photopic to scotopic values assumed a white standard CIE D65 illumination (based on the design of Hood and Finkelstein, 1986)(Stockman and Sharpe 2006).

was determined that 555 nm (green-yellow) light stimulated the average observer's perception of brightness most strongly and that the value of 1 W of monochromatic at this wavelength would have a value of 683 lumens/W. All other wavelengths were scaled acoordingly(CIE No. 86 1990). The resulting function made it possible to quickly and easily convert radiometric units into physiological units. This function is known today as the CIE standard photometric observer. It is denoted V_λ (Berns 2000). (For known limitations of this function (see G Wyszecki and Stiles 1982).)

Soon after, color matching experiments were undertaken involving three reference primaries. The primaries selected had wavelengths of 436, 546, and 700 nm, roughly corresponding to blue, green, and red. Observers were required to match to blend the light output of these three primaries until a color match was made to a monochromatic test color. This was done in 5 nm increments across the visible spectrum. The R, G, and B–red, green, and blue matching values–at each wavelength were transformed into an easy to use system, called the X, Y, Z system with color matching functions x_λ, y_λ, and z_λ. This system is popularly referred to as the 1931 standard observer or the 2º observer and is assumed to represent the color matching results of an average human observer with normal color vision (CIE No. 15.2 1986). y_λ was defined as equivalent to V_λ.

The X, Y, and Z values derived from the color matching functions are called the tristimulus values. In order to calculate them, one must integrate spectral profile of an object or illuminant with each of the color matching functions:

$$X = \int_{380\,nm}^{780} S(\lambda)\bar{x}(\lambda)d\lambda$$

$$Y = \int_{380\,nm}^{780} S(\lambda)\bar{y}(\lambda)d\lambda$$

$$Z = \int_{380}^{780} S(\lambda)\bar{z}(\lambda)d\lambda$$

where S(λ) is the spectral luminance of the object.

The experiments utilized above covered only a 2º angle of vision. With better experimental techniques in the 1950s, 10º fields of view were employed as well. The color matching functions of the 10º observers varied slightly due in part to the changes in the periphery of the retina of cone distribution and its lack of macular pigmentation. This color matching data set is known as the 1964 supplementary standard observer or the 10º observer and is recommended for use whenever viewing conditions exceed a 4º field of view (see Figure 1.10 and Figure 1.11)(G Wyszecki and Stiles 1982). The ten degree observer is utilized in our studies mainly since our focus is on lighting; it is much more appropriate for the wide field illumination conditions.

Tristumulus values, containing three outputs, exist in a three dimensional space. By using projections, a two-dimensional color map can be produced. This map is known as the chromaticity diagram. The magnitudes of the tristumulus values are lost in this process and we are left with ratios, as such:

$$x = \frac{X}{X + Y + Z}$$

$$y = \frac{Y}{X + Y + Z}$$

$$z = 1 - x - y$$

Color information in this form is known as chromaticities. Hue and chroma information remain intact during this transformation. Hue is the attribute of visual perception in which a surface appears to be similar to one of the colors, red, green, yellow, blue, or any combination thereof(CIE No. 17.4 1987). Chroma is the attribute of color perception, which denotes the degree to which a color moves from a gray towards a hue of matching lightness. For exhaustion, lightness is the attribute by which a color is perceived to be equivalent to a grey that ranges from black to white.

The CIE chromaticity diagram provided a simple tool for mapping the colors of objects using specific color coordinates. However, the spacing between the colors on the map were not scaled uniformly with respect to human perception(Schanda 2007). A variety of transformations of the chromaticity space took place with the intention of providing a mapping more representative of human color discrimination. The CIE 1960 u,v uniform color space (UCS) was designated and became obsolete soon after its adoption. However, it is still used in the calculation of color rendering index (CRI) as part of the 1964 U*V*W* space (discussed below).

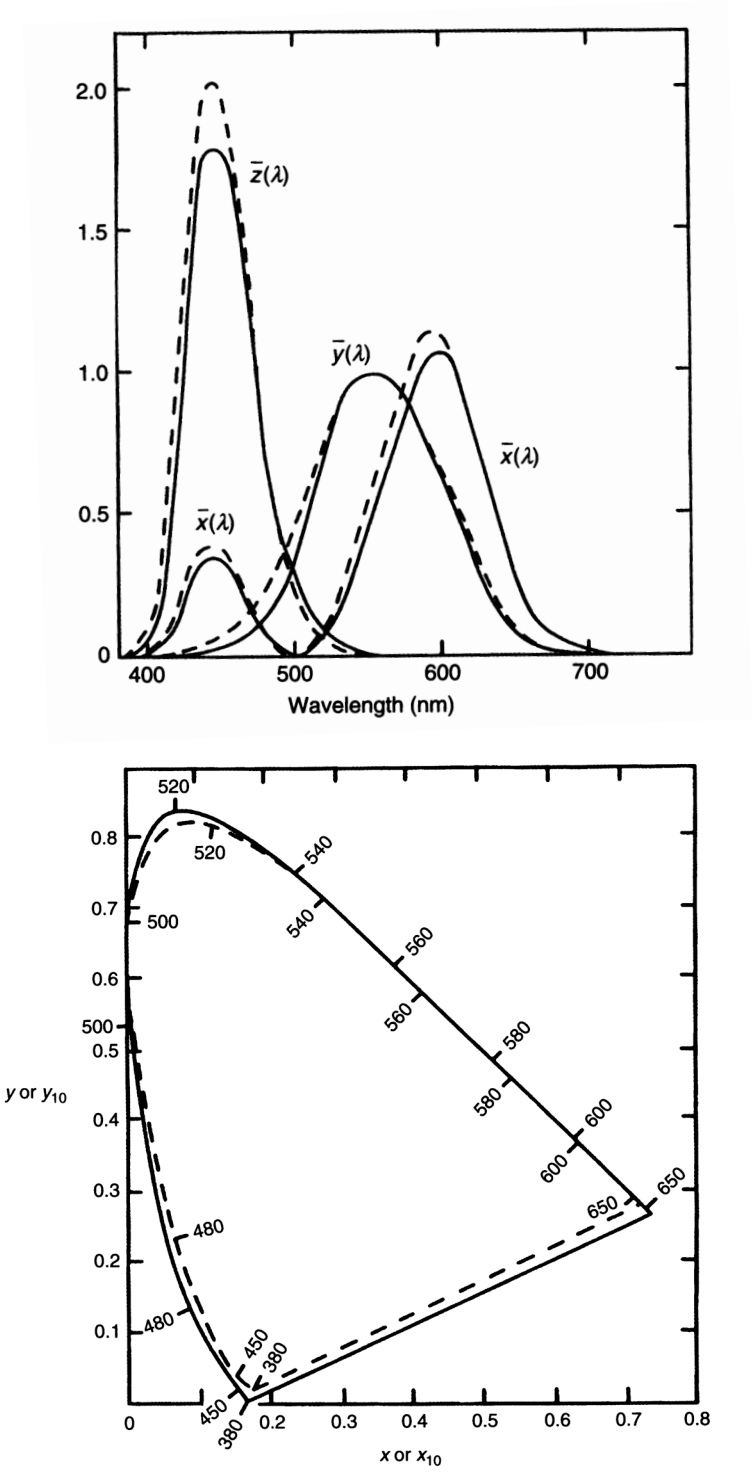

Figure 1.10 The CIE color matching functions. The 1931 Standard Colorimetric Observer or 2º observer (solid lines) and the 1964 Supplementary Colorimetric Oberver or 10º observer (dashed lines) (top panel). The CIE chromaticity diagram plotted as a function of the 2º observer (solid lines) and 10º observer (dashed lines)(reproduced from Hunt and Pointer 2011).

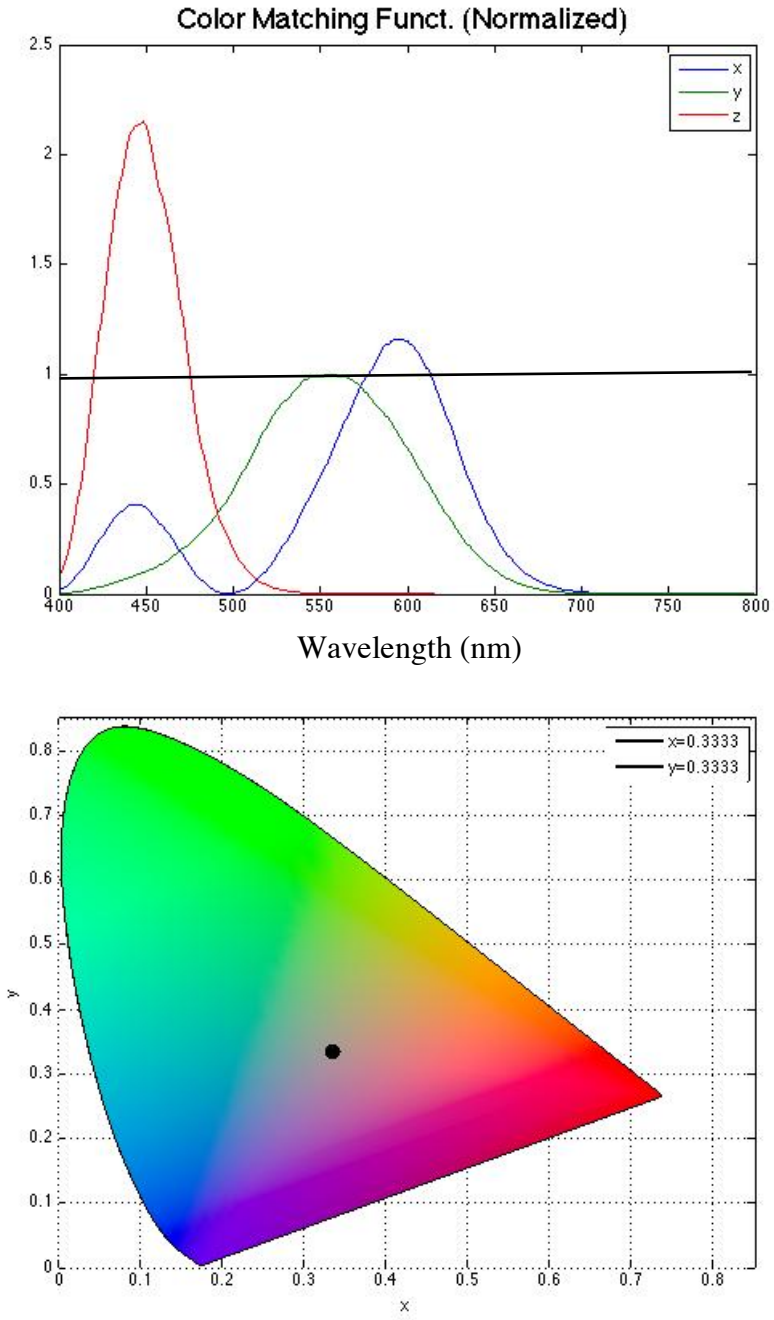

Figure 1.11 Color matching functions and chromaticity diagram. These are the x_{10}, y_{10}, and z_{10} color matching functions of the 1964 CIE supplementary observer or 10° observer (top panel). The equienergy spectrum(black line) is integrated with the color matching functions. The y axis is given in arbitrary radiometric units. The matching functions are specified such that the equienergy spectrum results in X = Y = Z. The tristimulus values are projected onto a two dimensional chromaticity plane, removing the luminance value of the object, but maintaining hue and chroma information (bottom panel). The equienergy point is plotted (black dot).

By 1976, work towards an improved uniform chromaticity diagram led to the development and adoption of the L*, a*, b* space by the CIE (CIELAB)(CIE No. 15.2 1986). The new space provided a more accurate mapping of colors within the space. It also reintroduced a third dimension, lightness, which provided the relative brightness of an object compared to the brightest white object in the environment. The coordinate system is cylindrical with L* mapped on the z-axis.

$$L^* = 116\,(Y/Y_n)^{1/3} - 16$$

$$a^* = 500\left[(X/X_n)^{1/3} - (Y/Y_n)^{1/3}\right]$$

$$b^* = 200\left[(Y/Y_n)^{1/3} - (Z/Z_n)^{1/3}\right]$$

X_n, Y_n, and Z_n are the color coordinates of the illuminant as it reflects off a white surface, known as the white point. Since color values are plotted with respect to the white point, the color mapping is dependent on the color coordinates of the illuminant. This condition has the consequence of making the appearance of CIELAB color specifications dependent on lighting context, and thus CIELAB is considered a primitive color appearance model (CAM), after which many CAMs were to follow (see Figure 1.12)(see M. Fairchild 2013).

Color Constancy – and Inconstancy

You may have noticed that when an illuminant changes, the colors of objects change

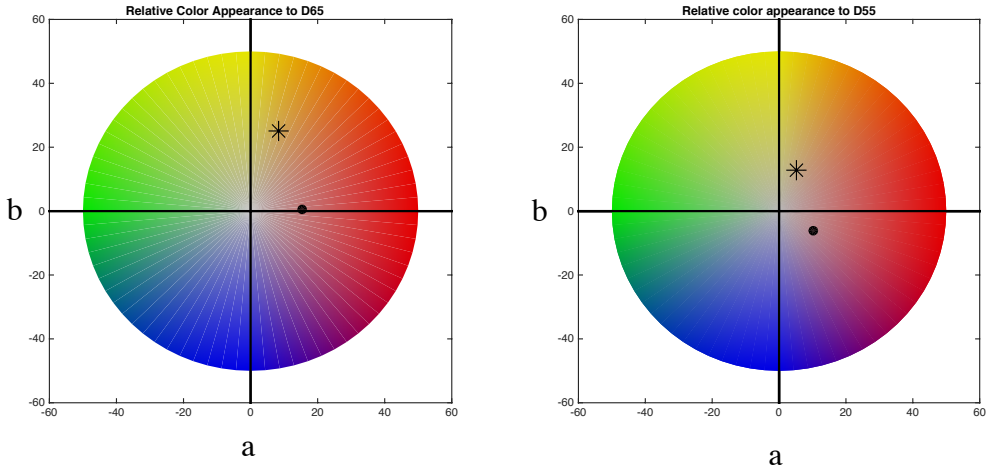

Figure 1.12 Color appearance in CIELAB changes based on white points. A red and orange illuminant are compared under midday daylight (D65) (left panel) and morning daylight (D55) (right panel). As daylight shifts towards the blue end of the spectrum from morning to midday, a simulated illuminant near a window will change in appearance from whitish to reddish in appearance. This is due to chromatic adaptation. In the morning, red cones are more adapted to the higher red content in morning daylight and thus less responsive to the orange or reddish content of the simulated illuminant giving them a less tinted appearance (right panel).

slightly. This can occur when switching from sunlight to room lighting or even during the setting of the sun itself. However, our visual system is very adept at maintaining the general color appearance of objects. If the change in illuminant is subtle, you may not notice any perceptible changes in color. Color constancy is the tendency of object colors to remain constant as the level and color of illumination changes. There is a combination of retinal and cortical processes which make constancy possible. The psychological adaptation to a change in illumination is known as discounting the color of the illumination(Berns 2000). An important component of this adjustment is chromatic adaptation, which are the changes in individual cone adaptation levels to compensate in part for changes in the spectral content of the illuminant.

Color vision is evolutionarily advantageous, since it provides an additional visual channel. This is in addition to luminance contrast, which provides grayscale information based on darkness and lightness contrast. However, it still has limitations since spectral information is reduced to 3 channels. Since conscious visual perception is mediated by the three cone visual response under normal lighting conditions, different stimuli with dissimilar spectral power distributions can still look equivalent to an observer if both spectra produce an equivalent response among the 3 cone channels. Cone metamers have differing spectral power distributions, but appear to have the same color. For example, orange monochromatic light can be similarly represented by a mixture of green and red light. Metamerism can fail under certain circumstances. For example, an object that is metameric with another object under one illuminant can look dissimilar to another object when placed under a different illuminant. This is an issue that the color industry looks to

avoid. For example, it is desirable for a sample to behave predictably in that it matches a reference item under one illumination condition and should be able to maintain its appearance when moved into a different environment (see Figure 1.13). A car paint that appears acceptable in the factory, should maintain its appearance when operating outside under a variety of lighting conditions. That is, the car paint should be as color inconstant as possible.

Under the assumption that CIELAB is a relatively uniform color space with good correlation to real life perceived differences in color, the CIE recommended using CIELAB as a measure of color differences. However, it became apparent that Euclidean distances in CIELAB are poorly correlated with visual judgments(Robertson 1978). Numerous transforms were proposed by the colorant industries and CIE throughout the next several decades (for reference see Hunt 2011). The most recent recommendation by CIE is difference equation CIEDE2000(CIE No. 142 2001). Each iteration of color difference equation further improvement in correlation between subjective perception and calculated distance, especially for small color differences.

A color inconstancy index (CII) has much utility, as in the example of designing a car paint with reliable coloration. This is not a question of metamerism, since we are comparing one sample with itself. This is a question of color stability. All color difference formulae (such as CIEDE2000) are designed to be evaluated in a daylight illuminant(Mori et al. 1991), almost always D65(M. Fairchild 2013; Hunt and Pointer 2011; Berns 2000; Schanda 2007). The D in D65 signifies an approximate spectrum of

Figure 1.13 Color inconstancy and color quality. An object has the tendency to change color under different illumination conditions. The degree to which this is occurs can be approximated using psychometric indices such as the Color Inconstancy Index (top panel). Reproductions of colors used in the calculation of the CIE general Color Rendering Index (CRI) (middle panel) (Reproduced from (M. Fairchild 2013) and (Hunt and Pointer 2011). Color Quality Scale (CQS) employs more saturated reflectance color samples(Davis and Ohno 2010).

sunlight viewed at sealevel. The two numbers that follow are the thousands and hundredths place in value specifying the blackbody temperature of the spectrum, in this case 6500 K(Schanda 2007). In order to predict the amount of color inconstancy for a sample under illuminant shift from Illuminant A to Illuminant B, the color coordinates of the sample under both conditions must be transformed to their corresponding colors under daylight illumination. Corresponding colors are pairs of color stimuli that look alike when one is seen in one set of adaptation conditions, while the other is seen under the other adaptation condition, namely a different illumination setting.

In order to calculate a corresponding color, we need to use a chromatic adaptation transform (CAT). A chromatic adaptation formula was first proposed by Von Kries(Von Kries 1911, 366–369). The adaptation offered a simple gain model, in which the cones response adapt to the new white point, i.e., when the source illuminant is changed:

$$D = \begin{bmatrix} \frac{L_{r,B}}{L_{r,A}} & 0 & 0 \\ 0 & \frac{M_{r,B}}{M_{r,A}} & 0 \\ 0 & 0 & \frac{S_{r,B}}{S_{r,A}} \end{bmatrix}$$

where $L_{r,B}$ stands for the long (red) cone response for Illuminant B, $L_{r,A}$ stands for the long (red) cone response to the Illuminant A. M and S stand for middle (green) and short (blue) cone response, in turn. Given a sample with cone stimulus values L_1, M_1, and S_1 under illuminant A, the required LMS values to maintain color constancy under illuminant B are

$$\begin{bmatrix} L_B \\ M_B \\ S_B \end{bmatrix} = D \begin{bmatrix} L_A \\ M_A \\ S_A \end{bmatrix}$$

The output vector provides the corresponding color required to maintain object color constancy under the second illuminant, Illuminant B. It is critical to point out the often missed observation that corresponding color *is not* the same as taking an object's reflectance spectra to a second illuminant and then calculating color coordinates via color matching functions. If the latter method provides the same values as the CAT, then there is perfect color constancy, which is in actuality quite rare.

The most recent CAT is the CAT02, which comes from the CIECAM02 color appearance model. It has modified or "sharpened" cone fundamentals, which provide better agreement with experimental discrimination data, and also has inputs for the nature of the environmental surround, level of luminance, and the degree of adaptation(M. Fairchild 2013).

The CAT02 is utilized in calculation of CIEDE2000 in Chapter 4 of this dissertation. There we seek to build a dynamic light that maintains the same level of cone excitation while "pulsing" the melanopsin photopigment. It is employed in an uncommon manner since the color inconstancy we gauge takes place under an illuminant whose spectrum changes, but who's LMS cone excitation levels remain fixed. This is an interesting use of CII. A CAT is still required to map the color coordinates of our test color samples onto CIELAB with D65 as the reference illuminant. From there we will make determinations as to the suitability of numerous lighting designs for use in general

lighting by seeking dynamic lighting states that will minimize the CII for our test color samples.

Color Rendering by Light Sources

In addition to minimizing perceptible color change in our environment, we must ensure that objects in our surrounding look pleasant under illumination when designing our light. The advent of fluorescent lamps brought the idea of a color rendering index (CRI) to the forefront, since fluorescent lamps came with a large variety of spectral power distributions Any change in spectral power distribution could vary the appearance of object colors drastically. A light that can fully and "accurately" reproduce a color with respect to a reference illuminant is considered a good renderer of color. The CIE definition of color rendering is: "The effect of an illuminant on the colour appearance of objects by conscious or subconscious comparison with their colour appearance under a reference illuminant"(Hunt and Pointer 2011, 144). Roughly, CRI describes how well an illuminated object's color compares to its appearance under daylight. In a sense, this is a fidelity index if one considers natural lighting settings as the true representation of color rendering in daily experience.

The lighting industry uses the CIE General Color Rendering Index (CRI) as an indicator of illuminant quality. The CIE provides 14 test color samples selected from the Munsell color system as standards with which to measure illuminant performance compared to a daylight reference (see Figure 1.13)("Method of Measuring and Specifying

Colour Rendering Properties of Light Sources" 1995). The CIE Special Color Rendering Index is given by

$$R_i = 100 - 4.6d_i$$

where d_i is the Euclidean distance in CIE 1964 U*V*W* space between color coordinates that represent the sample when illuminated by the test source and by the CIE D-illuminant closest to it in the 1960 u,v UCS. If the correlated color temperature of the test source falls below 5000 K, a Planckian radiator with equivalent temperature is used. The CIE General Color Rendering Index is calculated as such:

$$R_a = 100 - 4.6\left(\frac{d_1 + d_2 + d_3 + d_4 + d_5 + d_6 + d_7 + d_8}{8}\right)$$

where d_1 to d_8 are the Euclidean distances used in calculating the first 8 special rendering indices. Only the first 8 are used in calculating CRI. Upon inspection of the first 8 color samples, it becomes apparent these are color samples of medium chroma(see Figure 1.13). Samples 9 through 12 are of high chroma. Sample 13 is meant to represent Caucasian skin color and sample 14 is leaf green. A von Kries type adaptation is used to find the corresponding color of the samples under test source illumination into the reference illuminant space.

CRI was designed with the fluorescent lighting industry in mind. The procedure for calculating CRI came almost half a century ago, before the preparation of more accurate color spaces and CATs. The aforementioned are just a couple of its numerous shortcomings. The 1960 uniform color space used by CRI is in fact nonuniform and CIELAB was recommended as a replacement(CIE No. 15 2004). The von Kries-type

CAT is also somewhat inaccurate and performs more poorly than CAT02(CIE No. 160 2004, 160). None of the 8 samples used in calculating CRI are highly saturated. This can be problematic, especially with narrowband sources like RGB light emitting diodes (LEDs). These sources have narrow peaks and broad valleys and can appear to perform quite well with desaturated colors, hiding the deficiencies that would arise with the rendering of certain saturated samples. Although light sources can perform poorly with saturated objects even though they perform well with desaturated samples, the converse is never true. The general CRI uses simple averaging of 8 color differences, which doesn't sufficiently penalize a light source if it performs poorly on a few color samples. Color rendering is limiting as it is a measure of color fidelity, but the pleasantness of the light may be a more deterministic quality in determining performance. Any deviation of an object's color appearance from that of daylight is considered poor, however, increases in object saturation result in better visual clarity and increase perceived brightness(Hashimoto et al. 2007; A. Neumann et al. 2011).

Davis and Ohno proposed a new lighting index called Color Quality Scale (CQS) which improved on the shortcomings of CRI(Davis and Ohno 2010). In addition to the shortcomings addressed above, CQS is also scaled between 0-100. CRI may produce negative values. CQS calculations are undertaken with a new set of color samples (see Figure 1.13).

*****

The latest color difference formulas, CIEDE2000, CRI, and CQS, provide us with a good metric for understanding the qualities of light as we move ahead with the design of an illuminant with better health in mind.

Lighting Designs for Better Health

Application of Subconscious Visual Response to Non-invasive Light Therapy

The physiological and health impacts of light have been a topic of renewed interest in the 21st century. This is in large part due to the discovery of ipRGCs. Synchronization of an organism's master clock to the daily light/dark cycle is known as circadian photoentrainment and is important for the maintenance of healthy physiological processes. The sensitivity of circadian rhythms to light resetting has important implications for the impact of lighting technologies on health. Seasonal Affective Disorder (SAD), also known as winter blues, was one of the first disorders recognized as related to changes in light exposure duration(Rosenthal et al. 1984). SAD is a potentially debilitating condition in which the shortening of the daytime photoperiod induces depressive symptoms in susceptible populations. Rosenthal, who coined the term Seasonal Affective Disorder, found that exposure to very bright white light resulted in significant improvement in the depressive symptoms of those suffering from SAD. The psychiatric changes that result in SAD are likely caused by sensitivities to circadian rhythm shifts(Lam and Levitt 2000).

Both animal models and clinical trials have shown a strong circadian rhythm phase shift in response to blue lights with a global maximum at ~480nm, where the peak sensitivity of the melanopsin pigment lies(K. Y. Wong, Graham, and Berson 2007; Lockley, Brainard, and Czeisler 2003). Further studies have shown that light therapy using steady blue light would require about one fifth of the irradiance recommended for therapy utilizing bright white lights to achieve equal efficacy(Glickman et al. 2006; Meesters et al. 2011). At the very least, it seems that blue light is the most important spectral component in any future protocol involving light therapy.

ipRGCs regulate numerous other non-image forming visual processes. Nocturnal ipRGC stimulation triggers the acute suppression of melatonin release. Melatonin is a hormone that regulates the sleep/wake cycle and is secreted from the pineal gland during nighttime. Its levels in the bloodstream start to climb in the evening hours and trigger sleepiness. As mentioned above, an action spectrum for acute melatonin suppression, peaks between 446 and 477 nm(G. C. Brainard et al. 2001), and the pupillary light response, has a peak spectral sensitivity at 482nm(Gamlin et al. 2007). These results are relevant for two reasons. Firstly, they show that the outputs to the various subconscious visual centers are regulated by the same photoreceptor. Secondly, these parallel effects allow a fast and noninvasive way to gauge the potential efficacy of specific protocols on further therapeutic trials. In other words, measuring pupil reflexes would be a high throughput method for measuring maximization of subconscious stimulation to dynamic photic stimuli. For example, one can use pupillary constriction as a metric to determine the effectiveness of a certain light protocol on circadian photoentrainment and/or light

therapy. Whether or not the responses of these various systems are closely correlated remains to be seen.

In addition to SAD, it is important to note that modifications in light schedule can result in numerous other disorders. Shifts in the light/dark cycle can result from evening shift work or travel across time zones. These events can result in "jet lag", including daytime fatigue, alternating complaints of insomnia and hypersomnia, emotional disturbances, and gastrointestinal distress(Kolla and Auger 2011). ipRGC activity is significantly reduced with aging indicating a general reduction of effective light schedule(La Morgia et al. 2011). Further impetus to develop new and powerful light therapies comes from recent findings which demonstrate a causative relationship between aberrant light towards cognitive impairment and depressive behavior in rodent models(LeGates et al. 2012; Tapia-Osorio et al. 2013; Bedrosian and Nelson 2013). Light therapy has been shown to be an effective method to alleviate generalized depressive disorders, not just SAD(Naus et al. 2013; Edgar and McClung 2013; Tapia-Osorio et al. 2013).

With these studies as a pretext, the lighting industry has moved to incorporate this recent flurry of knowledge into therapeutic light boxes utilizing blue-enriched lights. However the protocols required for effective treatment of depressive disorders currently require at least 30 minutes or more of therapy every morning(Meesters et al. 2011). These high intensity blue-light therapies could impose a blue hazard risk, such that repeated exposures at long durations could result in damage to the retina("Blue Light Hazard for Light Sources and Luminaires (IECTR62778{ED1.0}B)" 2013). Designing a faster,

lower-intensity therapy would allow the protocol to be more easily and safely incorporated into a morning routine.

One unexplored approach to improved therapeutics is to go beyond spectral tuning and into dynamic lighting design. It has been noticed that cells of the suprachiasmatic nucleus (SCN) habituate on the order of seconds during constant illumination of ipRGCs(K. Y. Wong, Graham, and Berson 2007). The SCN is where the circadian master clock is housed. A light source with a temporally varying intensity may reduce habituation and thus enhance the responses of SCN neurons. Flickering light is one possible method for enhancing ipRGC photoresponses and hence subconscious visual responses. Evidence that suggests dynamic light stimulus may enhance subconscious visual response comes from a recently published study by J. Gooley. His findings show that intermittent photic stimulation of the eye in the 0.1-4 Hz range resulted in twice the constrictive pupil response as continuous light over a 30 minute period. Gooley used green light to assess the effects of flicker frequency on pupil response, showing a maximal constrictive response at 1 Hz(Joshua J. Gooley et al. 2012). Gamlin was able to measure contributions of cones to the pupil response and found its main contributions fell rapidly within the first ten seconds of photic stimulation(McDougal and Gamlin 2010). This further supports the results by Gooley. It might be possible to enhance nonvisual light responses to low-irradiance exposures by using intermittent light to activate cone photoreceptors repeatedly in humans.

One final finding to note is the post illumination pupil response (PIPR), which is a sustained pupiloconstriction observed after cessation of a bright visual stimulus. A study comparing 470 nm blue light versus 623 nm red light revealed a PIPR to the blue light,

but not to the red light(Kankipati, Girkin, and Gamlin 2009), suggesting the PIPR is primarily melanopsin-mediated. Findings from a subsequent study make this result ultimately significant. In this recent study, significant attenuation of the PIPR was observed in subjects diagnosed with SAD(Roecklein et al. 2013). This finding provided two important insights: (1) a disruption in ipRGC photoreception may contribute to SAD; (2) attenuation in ipRGC photosensitivity impairs both the pupil reflex and other subconscious visual responses. Thus, a dynamic lighting protocol that enhances the pupil reflex by employing blue light would probably also improve other aspects of subconscious vision.

Application of Subconscious Visual Response to Lighting Design

An understanding of the significance of subconscious vision has led to development of emerging light therapies, particularly for SAD. Acknowledgement of scientific findings in this field has recently begun to penetrate industry("DIN (2009) Optical Radiation Physics and Illuminating Engineering – Part 100: Non-Visual Effects of Ocular Light on Human Beings – Quantities, Symbols and Action Spectra" 2009; "IES (2008) Light and Human Health: An Overview of the Impact of Optical Radiation on Visual, Circadian, Neuroendocrine and Neurobehavioural Responses" 2008; "CIE (2009) Ocular Lighting Effects on Human Physiology and Behaviour" 2009). However their application in general lighting is still lacking. Part of the reason for this lack of implementation is the use of well-established instruments and practices in the lighting field. Two categories for light measurement exist: radiometry and photometry(DiLaura

2011). Whereas radiometers quantify physical properties of light and energy, photometers use a weighting function, the photopic luminous efficiency function, which reflects the spectral sensitivity of long and middle wavelength sensitive cones and peaks at 555nm(Gibson 1926; Stockman et al. 2007). This measurement only takes into account the conscious perception of relative brightness, and is virtually irrelevant to subconscious vision.

A second reason for the lack of implementation of recent advances in ipRGC research is the remaining uncertainty in quantifying the variety of non-image-forming responses under one unified spectral weighting function. One complication arises from the fact that up to 5 photoreceptors are involved in modulating the subconscious visual channels. The interactions of these inputs are highly time- and context-sensitive as previously discussed. It is clear that more needs to be done to address the temporal nature of subconscious visual responses. This presents a significant hurdle for transforming research findings into lighting applications without certain knowledge of the impact of different lighting conditions on behavior and physiology.

This should not preclude lighting designers from incorporating recent studies into practical designs. It is known that architectural lighting illumination within the office and home fall within one and two orders of magnitude lower than outdoor levels(Turner, Van Someren, and Mainster 2010). Since the average American spends 87% of their time indoors, this should be significantly concerning(Klepeis et al. 2001). A recent study showed that 200 lux, which is typical of indoor light intensities, for 12 hours a day is insufficient to maintain synchronization of the circadian rhythm to the light/dark cycle(Middleton, Stone, and Arendt 2002). Surprisingly, when 1000 lux was presented

for 12 hours a day, circadian rhythms of study subjects were shifted slightly forward, suggesting to the authors that even 1000 lux was insufficient to provide complete photoentrainment of circadian rhythms.

Recent studies further show properly timed light with an appropriate spectral power distribution can enhance alertness and performance during the day. Daytime homeostatic sleep pressure can be reduced with blue light as compared to green or yellow light(Rahman et al. 2014). Correlates of alertness were measured including auditory reaction times, attention lapses, and brain wave activity vis-à-vis electroencephalogram (EEG). Another study assessed the environmental impact of blue-enriched white light at the workplace. In this blind study, workers under blue-shifted lighting showed significant improvements with increases in performance, subjective alertness, and evening fatigue(Viola et al. 2008). In another trial, subjects participated in a reading performance task after exposure to either 30 seconds of blue, white, yellow, or room light(Lehrl et al. 2007). Only 30 seconds of blue light was sufficient to demonstrate a significant difference in performance.

Rahman et al. provided objective evidence of the alerting effects of blue light by assessing brain wave activity. However, the first objective evidence of the alerting effects of blue light in humans was provided by the Vandewalle group who used functional magnetic resonance imaging (fMRI) to measure levels of activation in different brain regions(G. Vandewalle et al. 2007). Participants in the study undertook an auditory working memory task, with a concurrent 18 minute daytime exposure to either blue (470 nm) or green (550 nm) monochromatic light. fMRI measurements revealed that blue light enhanced brain responses or at least prevented the decline otherwise observed following

green light exposure in frontal and parietal cortices (implicated in working memory), and in the thalamus (involved in the modulation of cognition by arousal). The study showed the almost instantaneous effect of blue light on cognitive functions and strongly implicates mediation by a melanopsin-based photoreceptor system.

Blue-light may have significant impact on the stimulation of subconscious visual channels and should motivate novel ways to enhance lighting design. One potential approach would be based on melanopsin contrast. It has recently been shown that ipRGCs with rod and cone input blocked–meaning they respond only to melanopsin stimulus–showed a significantly higher firing rate to pulsed light than steady light (Walch et al. 2015).

To study the role of ipRGCs in the visual system, researchers have employed a technique known as silent substitution to selectively stimulate the melanopsin response by adjusting contrast, while maintaining a constant response from the rods and cones(Tsujimura et al. 2010; Cao, Nicandro, and Barrionuevo 2015; Barrionuevo et al. 2014; Viénot et al. 2012). Since conscious visual perception is primarily mediated by the three cone visual response under daytime illumination conditions, different stimuli with dissimilar spectral power distributions can still look equivalent to an observer if both spectra produce an equivalent response among the 3 cone channels. Cone metamers have differing spectral power distributions, but appear to have the same color. From this understanding arose the concept of silent substitution.

The use of silent substitution predates the discovery of ipRGCs, and its use in research dates back to 1908 in frog retina research published by M. Ishihara(Ishihara 1906). Rushton employed silent substitution in psychophysical studies with more

quantitative methods in the early 1970s(Mitchell and Rushton 1971a; Mitchell and Rushton 1971b). An analytic solution was proposed by Estévez and Spekreije along this line using linear algebraic transforms into physiological cone space in 1982 (cone response functions in lieu of color matching functions)(Estévez and Spekreijse 1982). A closely related concept was first addressed conceptually by Wyszecki in 1953 as a "metameric black" and was thus proposed as a spectral energy vector describing the difference between cone metamers–being orthogonal to the color space it is derived from(Cohen and Kappauf 1982). Though the cones response is static, these vectors affect rods and melanopsin differentially. Wyszecki's conceptual framework was further fleshed out in mathematical form using linear algebraic methods by Cohen and Kappauf, also in 1982 (for details see methods in Chapter 4)(Cohen and Kappauf 1982).

Up until recently, spectral and dynamic tuning has been fairly uncommon. This is due to the inherently restricted emission spectra and slow on/off dynamics of older lighting devices. Light emitting diodes (LEDs) have facilitated the utilization of both approaches by Estévez and by Cohen in photoreceptor research, and specifically in ipRGC research(Cao, Nicandro, and Barrionuevo 2015; Shapiro, Pokorny, and Smith 1996; Tsujimura et al. 2010; Viénot et al. 2012). A recent study shows that a combination of 7 LEDs can be used to provide a melanopsin contrast ratio of 1.53 in humans(Viénot et al. 2012). It has also been reported that pupil size, which has a strong melanopsin-driven component, does not affect perceived brightness(Fotios et al. 2010). These are encouraging findings in light of the push to enhance general lighting with an "invisible," yet dynamic stimulus, which can strongly stimulate melanopsin-driven subconscious visual channels throughout the day.

In combination with recently refined color rendering standards, such as CQS, and perception metrics (CII), it may be possible to provide precisely controlled conditions for dynamic temporal and spectral photostimulation of melanopsin without disrupting one's lighting environment, ushering in an era of lighting design not previously thought possible.

Chapter 2 – Melatonin Suppression by Light in Humans Is More Sensitive Than Previously Reported

Originally published as: **Melatonin Suppression by Light in Humans Is More Sensitive Than Previously Reported,** Garen V. Vartanian, Benjamin Y. Li, Andrew P. Chervenak, Olivia J. Walch, Weston Pack, Petri Ala-Laurila, and Kwoon Y. Wong**,** *Journal of Biological Rhythms*, **30**, 4 p. 351-354, August 2015.

Introduction

The visual system mediates not only pattern vision but also non-image-forming photoresponses, including pupillary reflexes, entrainment of circadian rhythms to the light/dark cycle, and modulation of hormone secretion. Because excessive nighttime photic stimulation of this system is harmful(Bedrosian and Nelson 2013; Amaral et al. 2014), it is important to ascertain the intensity threshold of human non-image-forming vision. To this end, researchers have assessed the photosensitivity of the circadian pathway in which retinal neurons signal through the suprachiasmatic nucleus (SCN) to the pineal gland, which secretes melatonin during subjective night. Melatonin secretion can be suppressed acutely by light, and earlier work found such suppression to be most sensitive to 460-nm light, with a threshold of ~12 log photons cm^{-2} s^{-1} (G. C. Brainard et al. 2001; Thapan, Arendt, and Skene 2001). This threshold is surprisingly high because retinal input to the SCN is now known to be mediated by intrinsically photosensitive

retinal ganglion cells (ipRGCs), which receive excitatory input from rod photoreceptors and can respond robustly to intensities as low as ~7 log photons cm^{-2} s^{-1} (Dacey et al. 2005). Mouse behavioral studies have likewise demonstrated a rod contribution to circadian photoentrainment(Altimus et al. 2010; Lall et al. 2010; Butler and Silver 2011; Morin and Studholme 2011). These new findings prompted us to reexamine the threshold for human melatonin suppression.

Methods

All procedures were approved by the Institutional Review Board at the University of Michigan and complied with the Declaration of Helsinki. Six authors of this article (4 Caucasians and 2 Asians, aged 19-37 years) served as subjects. All had normal color vision according to the Ishihara test. Each person served as a subject for 2 to 13 months, during which he or she adhered to the sleep/wake schedule in the 7-day protocol (Figure 2.1A); proper photoentrainment was confirmed daily by actigraphy (Jawbone UP and UP24 activity trackers; Jawbone, San Francisco, CA). Throughout the protocol, each subject engaged in his or her normal daytime activities from 7:30 AM to 11 PM and slept from 11 PM to 7:30 AM, except on days 5 (the "control" session) and 7 (the "photostimulation" session), when he or she was in a completely dark room from 9 to 11 PM—the pair of sessions constituted a "trial." In these sessions, the subject sat upright before a Ganzfeld dome, with the head stabilized by a chin rest and a forehead band, and used salivettes (SciMart, St. Louis, MO) to collect his or her own saliva every 20 min (Fig. 1A, asterisks). On the control night, the Ganzfeld dome remained dark, but on the

photo- stimulation night, a 460-nm LED light with a half- peak width of ~25 nm (PAR20-B36; Super Bright LEDs, St. Louis, MO) was presented from 10 to 11 PM through a ceiling aperture of the Ganzfeld dome, with intensity adjusted using neutral density filters and calibrated using an S370 radiometer (Gamma Scientific, San Diego, CA). Each saliva sample was stored immediately at 4 °C for 12 to 16 h and subsequently at –70 °C for up to 2 months, before it was subjected to a melatonin radioimmunoassay (Bühlmann Laboratories, Schönenbuch, Switzerland). Each subject generated all 12 samples in every trial. To reduce inter- and intra-assay variability, all samples from each trial were analyzed in triplicate using the same assay kit. Throughout the 7-day protocol, all subjects avoided caffeine, alcohol, bananas, beverages containing artificial colorants, over-the-counter medications, melatonin supplements, and strenuous exercise.

Detailed Procedures for the Randomization Test

The randomization test was performed to compare the "control" and "photostimulation" data values at each of the six time points for each of the three stimulus intensities(Ernst 2004). At each time point for a given stimulus intensity, each subjects' values were binned into control and photostimulation pools, and the mean of the latter was subtracted from that of the former. This difference was the first "difference score" in this test. Each subject produced one difference score, and all subjects' difference scores were averaged into a "benchmark". Thus, this benchmark represented the mean difference between the photostimulation and control data. Subsequently, all of each subject's data (i.e. control and photostimulation) for that particular time point and

stimulus intensity were randomized in order, and the mean of the second half of these numbers was subtracted from the mean of the first half, to generate a second "difference score". This randomization and subtraction were done for all subjects, generating a second difference score per subject, and all subjects' second difference scores were averaged. This averaged second difference score was compared with the abovementioned benchmark and if the benchmark was larger, a value of 0 was assigned; otherwise, a value of 1 was assigned. The randomization, subtraction, and comparison of the averaged second difference score with the benchmark were reiterated 1,000,000 times to stabilize the outcome. All the values assigned (i.e. the 0's and the 1's) were summed and divided by 1,000,000 to yield a *p*-value, with $p<0.05$ signifying statistical significance.

Results

Three stimulus intensities were examined. Each intensity was tested on 3 to 6 subjects, with each subject contributing 1 to 6 trials per intensity (see Figure 2.1 legend). The data were initially analyzed using the Wilcoxon signed-rank test, a widely used nonparametric, paired-difference test. For the lowest light intensity, 8.1 log photons cm^{-2} s^{-1}, the data from the control and photostimulation sessions were statistically indistinguishable at all time points (Fig. 2.1B, left), indicating it was too low to suppress melatonin. At 9.2 log photons cm^{-2} s^{-1}, an apparent suppression was seen as all 3 data points during light treatment fell below control values (Fig. 2.1B, center), although these data were not significantly different between the 2 nights. The 2 nights' data deviated

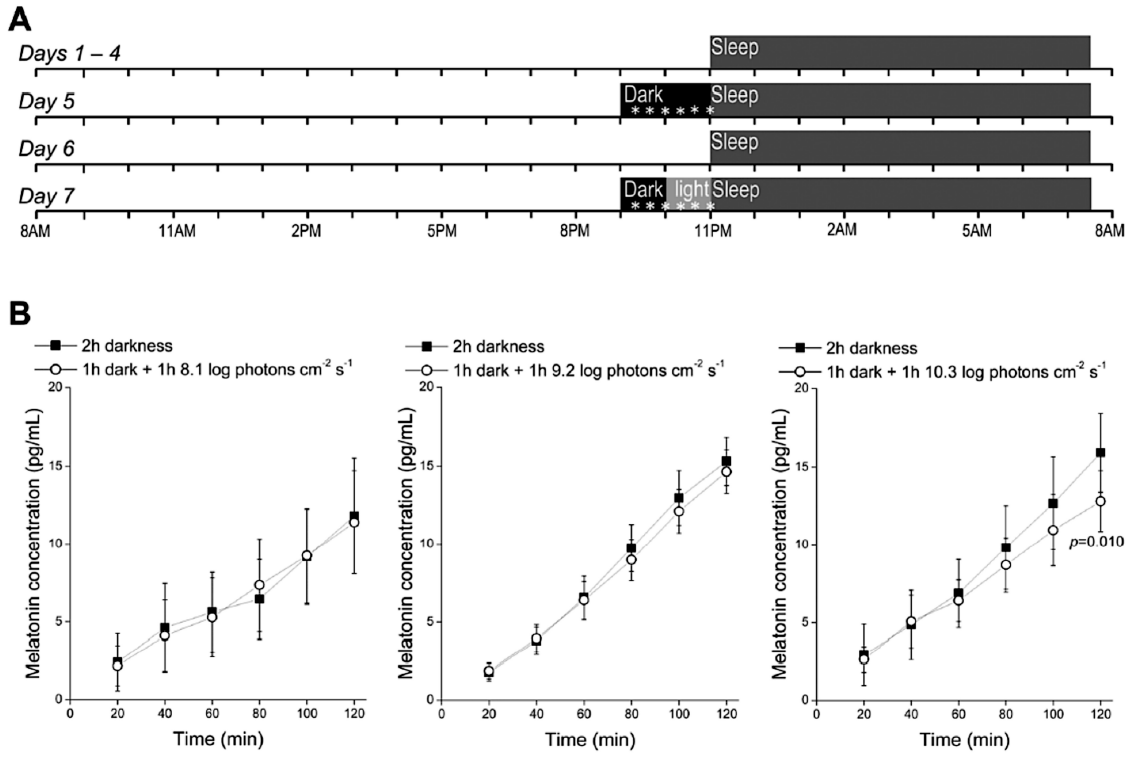

Figure 2.1 Measuring the threshold for photic suppression of melatonin. (A) The experimental protocol. Days 5 and 7 are the "control" and "photostimulation" sessions, respectively, and together they constitute 1 "trial." The asterisks represent saliva collection. (B) In each plot, the black and white curves show data averaged from all control and photostimulation sessions, respectively. Each white curve's last 3 data points were collected during light exposure. Left: Stimulus intensity was 8.1 log photons cm^{-2} s^{-1}; n = 3 subjects, who contributed 1, 3, and 6 trials. Middle: 9.2 log photons cm^{-2} s^{-1} intensity; n = 5 subjects, who contributed 2, 2, 2, 3, and 5 trials. Right: 10.3 photons cm^{-2} s^{-1} intensity; n = 6 subjects, who contributed 1, 1, 1, 1, 3, and 4 trials. The p value was calculated using the randomization test. Error bars represent SEM.

further when stimulus intensity increased to 10.3 log photons cm^{-2} s^{-1}, with a significant difference at the fifth time point ($p = 0.034$) and the final time point ($p = 0.003$) (Fig. 2.1B, right). However, the Wilcoxon signed-rank test assumes single testing of each subject, whereas our subjects often contributed multiple trials per stimulus. Thus, we reanalyzed the 10.3 log photons cm^{-2} s^{-1} data using the randomization test (Ernst, 2004), a nonparametric test compatible with our repeated-measures design. The control versus photostimulation difference became insignificant at the fifth time point ($p = 0.143$) but remained significant for the sixth time point ($p = 0.010$).

Discussion

In this study, we detected significant melatonin suppression at a light intensity about 2 log units lower than previously reported thresholds (G. C. Brainard et al. 2001; Thapan, Arendt, and Skene 2001). This difference is likely due to the higher precision of our data: all our measurements were made during the first 2 h of subjective night when melatonin level rises nearly monotonically, whereas the earlier studies were done at later time points when it fluctuates substantially. The number of subjects (6) we tested at 10.3 log photons cm^{-2} s^{-1} may seem small but is comparable to the subject numbers (5-8) that the earlier studies employed for each stimulus. There are, however, 2 plausible caveats. First, our data cannot be compared directly with the earlier studies since our photostimulation was done at early night but theirs around midnight, and the sensitivity of melatonin suppression is phase dependent (McIntyre et al. 1989). Specifically, McIntyre et al. (1989) found a higher photosensitivity at midnight than at early night,

suggesting that the 2-log-unit threshold difference between our study and the earlier ones could be an underestimate. Second, our control session always preceded the photostimulation session, whereas some laboratories prefer to randomize the order of testing. We reasoned that, had the photo- stimulation been performed first, the light exposure could induce a circadian phase shift that would interfere with the control session conducted 2 days later. Indeed, for all 3 stimulus intensities, the control and photostimulation data were nearly identical at the first 3 time points, confirming that our protocol avoided phase shifts.

Although lower than previously published values, our threshold for melatonin suppression is still at least 3 log units above the threshold for primate ipRGCs' rod-driven photoresponses(Dacey et al. 2005). While this fits the hypothesis that the human circadian system receives no excitatory rod input(Rea et al. 2005), it does not rule out such input. For example, our threshold could have been lower had the subjects' pupils been dilated by mydiatrics(Gaddy, Rollag, and Brainard 1993). Furthermore, the threshold for light pulse–induced melatonin suppression appears higher than that for circadian entrainment to light-dark cycles(Zeitzer et al. 2000; Butler and Silver 2011), suggesting that stimulus durations longer than ours could conceivably suppress melatonin at lower intensities.

Nevertheless, rods could indeed have little impact on the human circadian system. For example, nonlinearities downstream of ipRGCs could dictate the threshold for melanopsin suppression, in effect blocking low-amplitude rod-driven signals. Furthermore, retinal input to the primate SCN could be mediated by previously uncharacterized ipRGCs that receive weak rod input. Two types of primate ipRGCs have

been recorded, and both exhibited robust rod-driven light responses(Dacey et al. 2005), but 5 ipRGC types have since been discovered in rodents, of which only the M1 type innervates the SCN(Ecker et al. 2010). We learned recently that while mouse M1 cells display rod-driven photoresponses as robust as those of primate ipRGCs(Zhao et al. 2014), rat M1 cells' rod/ cone-mediated responses are far weaker(Reifler et al. 2015). The SCN-projecting ipRGCs in primates could resemble those in rats.

Conclusion

We attempted to find the true threshold of sensitivity for melatonin suppression during sleep onset and have come one step closer to elucidating the true effects of light at night on human subconscious visual response. This has significant value because of the ubiquity of laptop, tablet, and smart phone use during bedtime, which have replaced traditional print materials. The health effects of late evening light exposure are yet to be fully understood, but there are implications that such exposure can lead to morbidities, such as depression and feelings of helplessness(Bedrosian 2013), lowered testosterone, which is an effector of poor sleep and vice versa(Andersen 2011), and even increased prostate and breast cancer risk(Stevens 2009). Our findings revealed that human melatonin suppression by light presented to the eye is sensitive to at least two orders of magnitude more than previously thought at 10.3 log photons cm^{-2} s^{-1}, or 0.1 lux.

Paradoxically, human circadian rhythms can fail to photoentrain at light intensities below 80 lux(Gronfier et al. 2007) during the morning and day. A value of 80 lux is above light intensities at the eye level under typical indoor lighting

conditions(Turner, Van Someren, and Mainster 2010). This contributes to the converse issue of ipRGC understimulation during the daytime; the ability to consciously perceive our environment in typical indoor light settings, betrays the low stimulation state of subconscious vision under these same conditions–a topic that motivates the studies in the following two chapters.

Acknowledgements

We thank Josh Errickson and Prof. Kerby Shedden at the University of Michigan Center for Statistical Consultation & Research for help with statistics and Teera Parr for per- forming the radioimmunoassay. This work was funded by Research to Prevent Blindness (Career Development Award), the NIH National Eye Institute (P30 EY007003), and the Academy of Finland (253314).

Conflict of Interest Statement

The author(s) have no potential conflicts of interest with respect to the research, authorship, and/or publication of this article.

Chapter 3 – Using Flickering Light to Enhance Nonimage-Forming Visual Stimulation in Humans

Originally published as: **Using Flickering Light to Enhance Nonimage-Forming Visual Stimulation in Humans,** Garen V. Vartanian, Xiwu Zhao, and Kwoon Y. Wong, *IOVS*, **56**, 8 p.4680-4688, July 2015.

Introduction

The eye mediates both image-forming and nonimage-forming (NIF) visual functions. Whereas image-forming vision enables appreciation of spatial details, NIF vision entails largely subconscious photoresponses including the pupillary light reflex (PLR), circadian photoentrainment, and neuroendocrine regulation. Nonimage-forming photoreception is mediated by not only rod and cone photoreceptors, but also intrinsically photosensitive retinal ganglion cells (ipRGCs), which contain the photopigment melanopsin(Panda et al. 2003; Berson, Dunn, and Takao 2002; Samer Hattar et al. 2003). Nonimage-forming vision profoundly influences well-being. For example, daytime NIF photostimulation enhances alertness(Cajochen et al. 2005), improves cognitive performance(Gilles Vandewalle et al. 2013), and positively influences mood(Stephenson et al. 2012), whereas inadequate or mistimed NIF stimulation can cause sleep disturbances, depression, cognitive impairment, and certain forms of cancer(Andersen 2011; Bedrosian 2013; Stevens 2009; Turner, Van Someren, and Mainster 2010).

In a previous study, motivated by the recent awareness of the detrimental health impacts of mistimed NIF stimulation, we looked specifically at sensitivity thresholds in NIF vision at night vis-à-vis melatonin suppression measurements during sleep onset. Whereas light at night results in overstimulation, daytime environments may result in understimulation of NIF responses. We find that light adaptation impacts not only conscious vision, but subconscious vision as well(Wong 2005; Wong 2007; McDougal and Gamlin 2010). Typical daytime light levels in the home are 100 lux or less(Turner, Van Someren, and Mainster 2010), which is much dimmer than natural lighting by 20-100 times. In addition, typical measured irradiance at eye level is only 10-20% of values reported for standard surface measurements(Ryer 1997). This equates to about 10-20 lux in the typical home environment. Since human circadian rhythms can fail to photoentrain at light intensities below 80 lux(Gronfier et al. 2007), typical indoor lighting intensities during the morning and day may have significant health impacts on the general population.

Considering the health impacts of NIF photostimulation, it is beneficial to identify lighting conditions favorable for NIF vision. While extensive research has been done to demonstrate that NIF vision is most sensitive to blue wavelengths(G. C. Brainard et al. 2015; G. C. Brainard et al. 2001; Thapan, Arendt, and Skene 2001; Glickman et al. 2006; Figueiro, Bierman, and Rea 2008; Viola et al. 2008; Meesters et al. 2011; Revell et al. 2010), far less effort has been put into optimizing the temporal distribution of light. Recent reports showed that intermittent light evoked greater NIF responses than continuous light(Lall et al. 2010; Joshua J. Gooley et al. 2012; Ho Mien et al. 2014). Here, we aimed to further enhance NIF responses by finding intermittent stimuli with optimal

combinations of intensity, flicker frequency, and duty cycle. We studied the PLR, for two reasons. First, it can be measured quickly, facilitating the testing of many stimulus combinations. Second, the amplitude and time course of the PLR parallel those of ipRGC photoresponses(Gamlin et al. 2007), suggesting this behavior can serve as a readout of ipRGC activity so that a stimulus inducing a robust PLR may be inferred to excite ipRGCs potently. Because all NIF responses are driven predominantly by ipRGCs(G. C. Brainard et al. 2001; Thapan, Arendt, and Skene 2001; Güler et al. 2008; Göz et al. 2008; Hatori et al. 2008), a stimulus that strongly excites ipRGCs is likely effective for all NIF responses, and there is indeed a correlation between the PLR and other NIF photoresponses in humans(Figueiro et al. 2005; Roecklein et al. 2013; Lee et al. 2014). Thus, the findings from this study can probably be extrapolated to other aspects of NIF vision. A possible clinical application is the development of more efficient therapeutic lights for treating depression (both seasonal and nonseasonal), jet lag, and other conditions arising from improper NIF photostimulation(Rosenthal et al. 1984; Tuunainen, Kripke, and Endo 2004).

Methods

Pupillometry

All procedures were approved by the institutional review board at the University of Michigan, and adhered to tenets of the Declaration of Helsinki. Four females aged 19 to 22 years and five males aged 19 to 37 years served as subjects, after providing informed consent. Five subjects were tested in the experiments shown in Figures 3.1A

and 3 through 5. The other four contributed to the experiment shown in Figure 3.1C, and one of these generated the data shown in Figure 3.6. All had normal color vision according to the Ishihara test. The subjects' wake times ranged from 6:00 to 8:30 AM and sleep onset times from 10:00 PM to 12:30 AM. All experiments were performed between 1:30 and 6:30 PM when PLR photosensitivity exhibits insignificant circadian variation(Munch et al. 2012; Zele et al. 2011).

Pupillometry was performed in a darkroom using an infrared pupillometer (A-2000; NeurOptics, Irvine, CA, USA). This instrument's 463-nm blue LED light source was presented to either just the right eye (Figs. 3.1–7) or both eyes (Fig. 3.8) at a distance of 6.5 cm, and the left eye's PLR was imaged at 30 Hz; 463 nm is near the optimal wavelength for stimulating the human photoentrainment pathway(G. C. Brainard et al. 2001; Thapan, Arendt, and Skene 2001). This LED light was rectangular and subtended the subject's visual field 27º vertically and 34º horizontally.

As noted earlier, one potential application of this study is to inform the design of better phototherapeutic devices. Phototherapy typically entails viewing a light for 30 minutes to 2 hours(Golden, R 2005), but considering the large number of stimuli to be tested (see below), presenting each for such duration would be impractical. Thus, we started with a control experiment to ascertain whether flicker-induced PLRs would reach steady state within several minutes, and whether several minutes of prior dark adaptation would suffice. Two protocols were compared: 4-minute dark adaptation followed by 4-minute flickering light, versus 40-minute dark adaptation followed by 20 minutes of the same stimulus. We tested two frequencies, 1 and 5 pulses min^{-1}, both with a 12% duty cycle (i.e., the stimulus was lit 12% of the time per flicker cycle), and measured the PLR

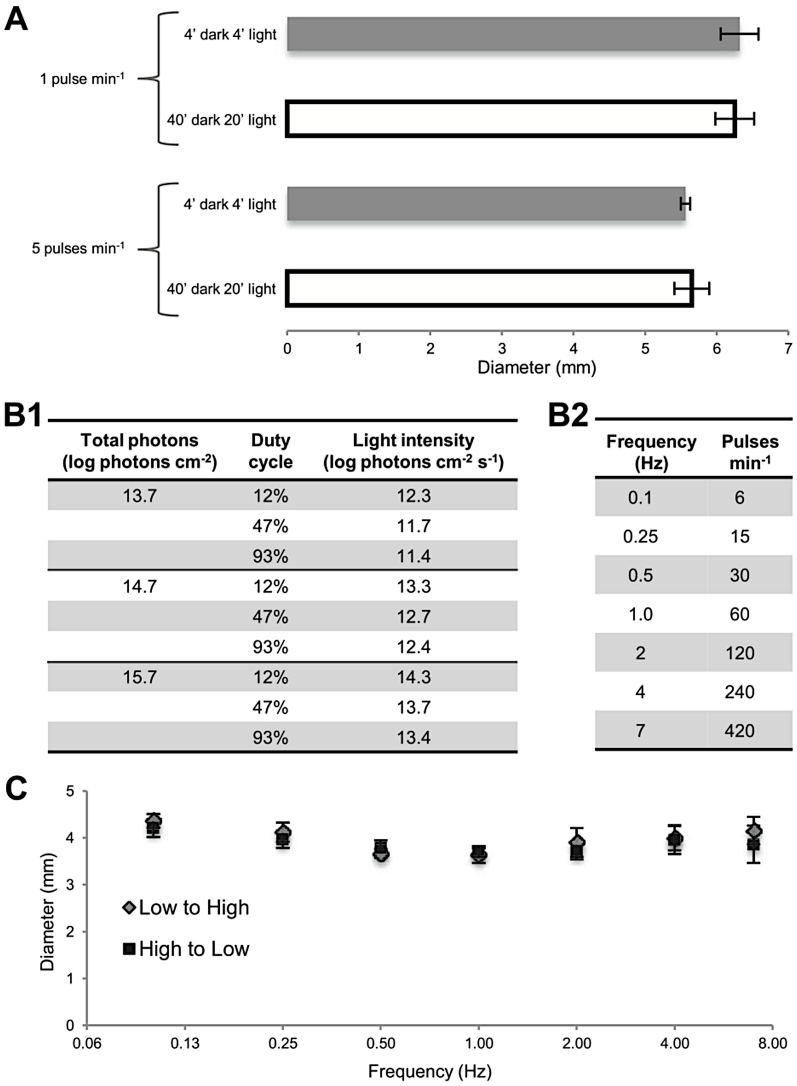

B1

Total photons (log photons cm^{-2})	Duty cycle	Light intensity (log photons cm^{-2} s^{-1})
13.7	12%	12.3
	47%	11.7
	93%	11.4
14.7	12%	13.3
	47%	12.7
	93%	12.4
15.7	12%	14.3
	47%	13.7
	93%	13.4

B2

Frequency (Hz)	Pulses min^{-1}
0.1	6
0.25	15
0.5	30
1.0	60
2	120
4	240
7	420

Figure 3.1 Control experiments and the stimulus matrix. (A) Flickering lights presented for 4 minutes, after 4 minutes of dark adaptation evoked the same steady-state pupil responses as when they were presented for 20 minutes, following 40 minutes of dark adaptation. All stimuli had 12.3 log photons cm^{-2} s^{-1} intensity and a 12% duty cycle. Pupil diameters were averaged over the final minute of each trial. Five subjects were tested, with each person contributing two trials to each of the four conditions. (B) This study tested 63 flickering lights varying in 3 parameters: three total photon counts ([1], left column); three duty cycles ([1], middle column); and seven flicker frequencies (2). To maintain a fixed total photon count, intensity was adjusted according to duty cycle ([1], right column). (C) Responses to the seven flicker frequencies were not influenced by the order of presentation. Light pulses of 12.3 log photons cm^{-2} s^{-1} with a 12% duty cycle were presented either from the lowest to the highest frequency or from the highest to the lowest, and yielded statistically indistinguishable ($P > 0.05$) response magnitudes at all frequencies. Four subjects participated in this control, and each was tested with both presentation orders twice.

by averaging pupil diameter over the final minute of stimulation. These protocols yielded similar ($P > 0.05$) final-minute PLRs for both frequencies (Fig. 3.1A), demonstrating the shorter protocol accurately assessed steady-state responses.

Using the 4-minute dark/4-minute light protocol, we tested a three-dimensional matrix of 63 flickering stimuli: 3 total photon counts, 3 duty cycles, and 7 flicker frequencies (Fig. 3.1B, Fig. 3.2). Each subject was tested by all 63 stimuli, with every stimulus tested twice on 2 separate days. Each person participated in one 56-minute session per day in which 7 flicker frequencies (Fig. 3.1B2) of the same duty cycle and photon count were presented, and the person was always tested at about the same time of day. To determine whether the order of presenting the seven frequencies might influence response amplitude, they were presented in either increasing or decreasing order in another control experiment. They yielded nearly identical results (Fig. 3.1C), indicating no ordering effect. For consistency, we tested the 7 frequencies in increasing order in all experiments.

Data Analysis and Statistics

In Figures 4 through 6, results are expressed as the mean percent change in pupil diameter during the final minute of the 4-minute stimulus presentation:

% change = 100% ×

(baseline diameter – mean pupil diameter during final minute)/baseline diameter

In this equation, baseline diameter refers to the pupil diameter under fully dark-adapted conditions, which presumably allow spiking activity of ipRGCs to completely recover from prior photostimulation. The fully dark-adapted diameter was used because we wanted the percent-change calculation to reflect, as well as possible, the absolute

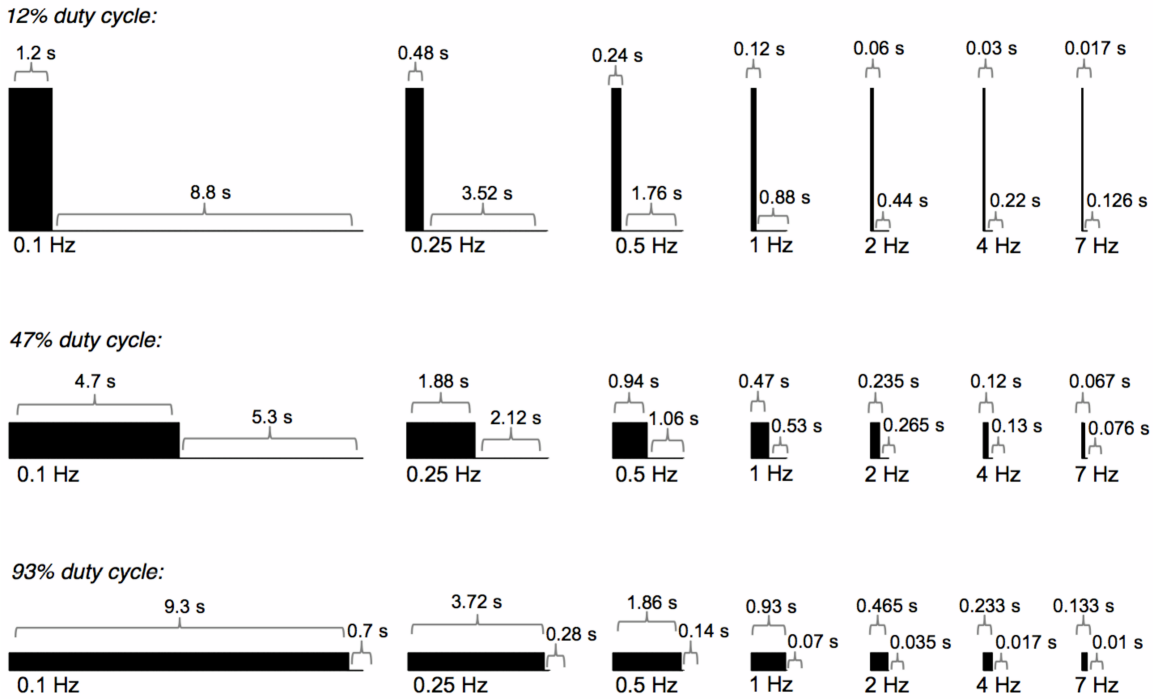

Figure 3.2 Waveforms of the 21 stimuli that contained 13.7 log photons cm^{-2}. One flicker cycle is illustrated for each stimulus. All waveforms are drawn to scale, on both time (x) and intensity (y) axes. Waveforms for the 14.7 log photons cm^{-2} and 15.7 log photons cm^{-2} stimuli (not shown) would be 10- and 100-fold taller, respectively.

firing rate of ipRGCs. Because the 4-minute prestimulus dark adaptation was insufficient for photoreceptors to fully dark-adapt, each subject's baseline pupil diameter was measured in a separate experiment where pupil diameter was measured after 1-hour dark adaptation. Every subject was measured on 4 separate days and the measurements agreed closely (Figure 3.3), indicating the baseline pupil diameter was remarkably constant. The average of the four measurements was used in all calculations based on that subject's data.

In the experiments shown in Figures 5 through 7, statistical comparisons employed a linear mixed model(West, Welch, and Galecki 2006; Gelman and Hill 2006) that accounted for repeated measures within subjects (see next section). Elsewhere, the paired, two-tailed Student's t-test was used. Differences were considered significant if $P < 0.05$. All error estimates are SEM unless stated otherwise.

Detailed Methods for Statistical Analysis

For the experiments shown in Figs. 5 – 7, we used linear mixed models (linear models with random effects) to make statistical comparisons between experimental conditions. Mixed models are defined in terms of a mean structure, describing the expected value of each observation, and a covariance structure, describing the relationships among the observations. For our purposes, the main interest is in the mean structure. However, the covariance structure must also be accounted for in order to make meaningful statistical inferences about the mean structure. We specified the models to have a saturated factorial mean structure, meaning that each of the 63 combinations of experimental factors (photon count, duty cycle and frequency) and each of the 11 constant-light conditions

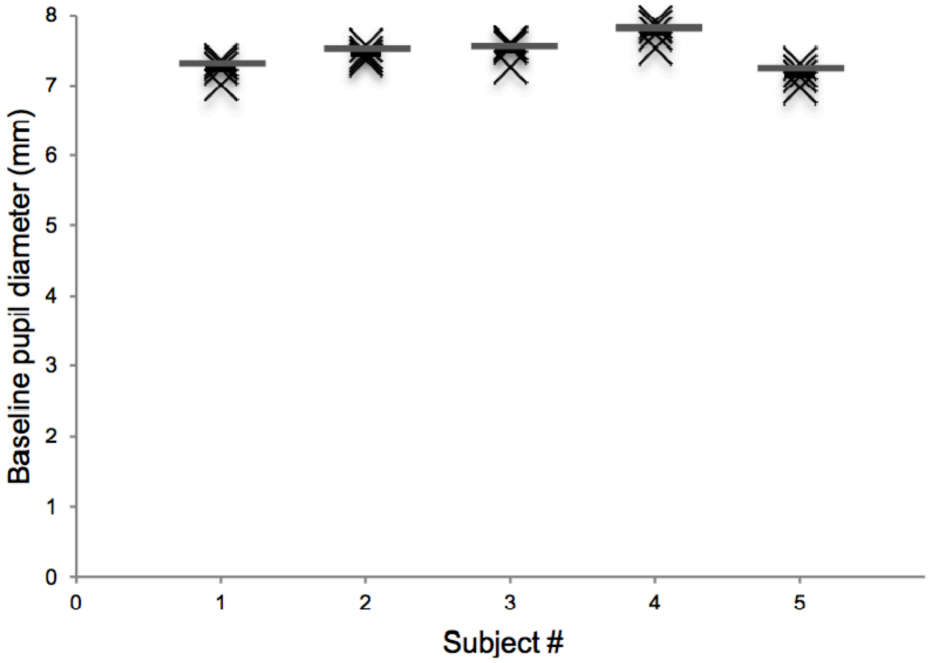

Figure 3.3 The baseline pupil diameters of the five subjects who were tested with the 63 flickering stimuli. For every subject, pupil diameter was measured after 1-hr dark adaptation on four separate days, with each measurement made at about the same time of day. The crosses represent individual measurements, and each horizontal bar indicates the subject's averaged baseline pupil diameter.

has its own mean value that varies independently of the others. Random effects were used to account for within-subject correlations. The random effects structure employed a nested sum of two terms. One of the terms applied to all values for a given subject, while the other applied only to the two replicates made in a single stimulus condition. The variance parameter for the first random effect reflects between-subject variation that appears in all stimulus conditions, whereas the variance parameter for the second random effect accounts for effects that are common to the two replicates of a stimulus condition made for a given subject.

We used likelihood ratio tests to establish the presence of strong effects for each of the three experimental factors. All three factors showed highly statistically significant differences between levels ($p<0.001$ for all 3 factors). Subsequently, we conducted post-hoc mean comparisons between the fitted curves for each condition (expressed as functions of frequency) and their corresponding constant-light conditions, and between selected trials of interest. All error estimates are S.E.M. unless stated otherwise.

We investigated the fit of the mixed model using standard residual diagnostics. Plotting the residuals against the fitted values revealed no relationships, but there were weak trends in which the dispersion of the residuals became lower with both increasing photon count and with decreasing duty cycle. To account for this heteroscedasticity, the variance was allowed to differ among the 9 combinations of two parameters, total photon count and duty cycle (i.e. 3 photon counts × 3 duty cycles). To visualize the results, fitted means were plotted as a function of frequency for each of the 9 combinations of total photon count and duty cycle. Standard errors shown in these plots were derived from the linear effects model.

Electrophysiological Recording From Mouse ipRGCs

All procedures in this experiment were approved by the University Committee on Use and Care of Animals, adhered to the ARVO Statement for the Use of Animals in Ophthalmic and Vision Research, and were described in detail previously(Zhao et al. 2014). Briefly, retinas were isolated from dark-adapted opn4Cre/þ;GFP, mice whose ipRGCs were labeled with green fluorescent protein (GFP). Retinas were superfused by 328C Ames' medium. GFP-labeled ipRGCs were visualized using a multi-photon laser and whole-cell-recorded using a Kþ-based intracellular solution. Cells with dendrites stratifying exclusively in the OFF sublamina of the inner plexiform layer were identified as M1 cells, whereas those with sparse, ON- stratifying dendrites were M2. The stimuli were full-field lights produced by the blue channel (peak emission ~440 nm) of an OLED microdisplay.

Results

Pupillary Responses to Flickering Stimuli

Figure 3.4 shows one subject's single-trial responses to the 7-frequency series with 13.7 log photons cm^{-2} and a 12% duty cycle. The response to the 0.1-Hz flicker clearly tracked the individual flashes, with pupil diameter dropping to ~4 mm at the peak of each flash response and relaxing to ~6 mm just before the next pulse. During the steady state of the response to the 0.25-Hz flicker, minimum pupil diameter was again ~4 mm, but postpulse dilation reached only ~5.5 mm. The 0.5-Hz response still showed

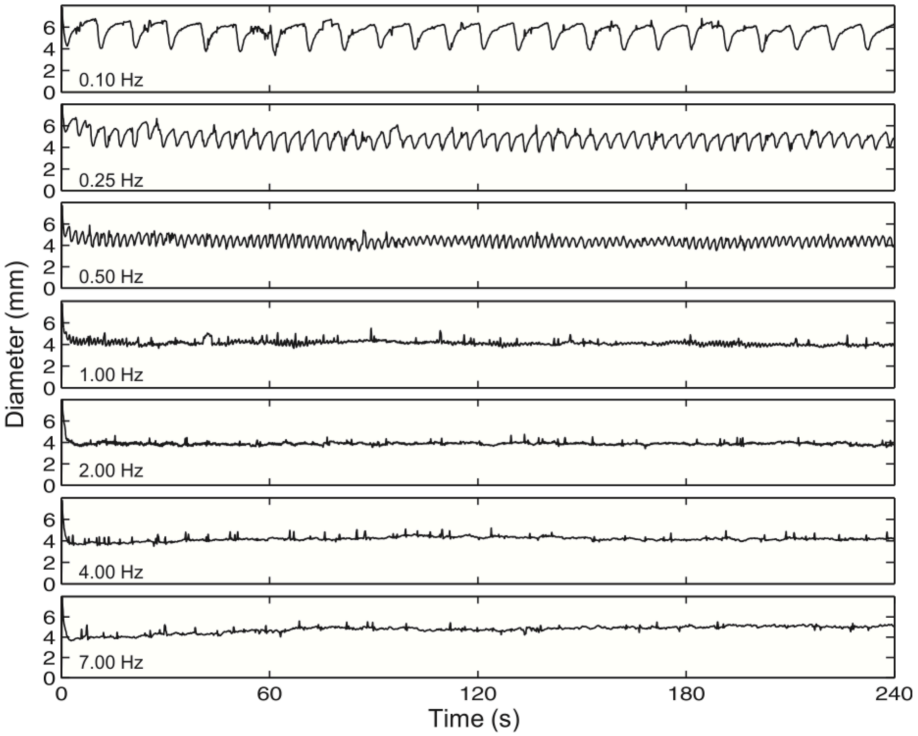

Figure 3.4 Example recordings. One subject's responses to the seven-frequency family of flickering lights with a 12% duty cycle and a photon count of 13.7 log photons cm^{-2}. All responses were filtered using a 4-pole, low-pass Butterworth filter with a cutoff frequency of 3 Hz.

tracking. During the steady state, peak constriction again reduced pupil diameter to ~4 mm, but peak dilation was even less than for the 0.25-Hz response, under ~5 mm. The 1-Hz response was remarkably flat with diameter staying around 4 mm, although small oscillations suggesting pulse tracking were seen intermittently. The 2-Hz response was also very stable with pupil diameter averaging just under 4 mm, but tracking was absent. For the 4-Hz response, pupil diameter dipped below 4 mm during the first half minute and then relaxed slightly over time, stabilizing at just over 4 mm. In the 7-Hz response, pupil diameter also dropped slightly below 4 mm early on, but then showed a more pronounced dilation, with steady-state diameter at nearly 5 mm. Thus, among these 7 stimuli, 2 Hz was optimal because it caused the greatest steady- state constriction. Figure 3.5 summarizes the results from all subjects for all 63 flickering stimuli, showing averaged final-minute percent reductions in pupil diameter. For the 13.7 log photons cm^{-2} stimuli (Fig. 3.5A), the 2-Hz flicker with 12% duty cycle induced the greatest diameter change (48% 6 4%) while the 4-Hz, 93% duty cycle flicker reduced pupil diameter the least (12% 6 5%). All the flickers containing 14.7 log photons cm^{-2} (Fig. 3.5B) induced greater pupil constrictions than their 13.7 log photons cm^{-2} counterparts, with the 2-Hz, 12% duty cycle stimulus being optimal (58% 6 4% diameter change) and the 7-Hz, 93% duty cycle one being the weakest (24% 6 4% diameter change). The 15.7 log photons cm^{-2} flickers induced even larger responses (Fig. 3.5C). For this photon count, the 1-Hz, 47% duty cycle flicker was the most potent (59% 6 4% diameter change), although several other stimuli were almost as effective, producing remarkably flat response versus frequency curves suggestive of response saturation. The least effective 15.7 log photons cm^{-2} flicker (0.1 Hz, 12% duty cycle) evoked a 37% 6 4% diameter change.

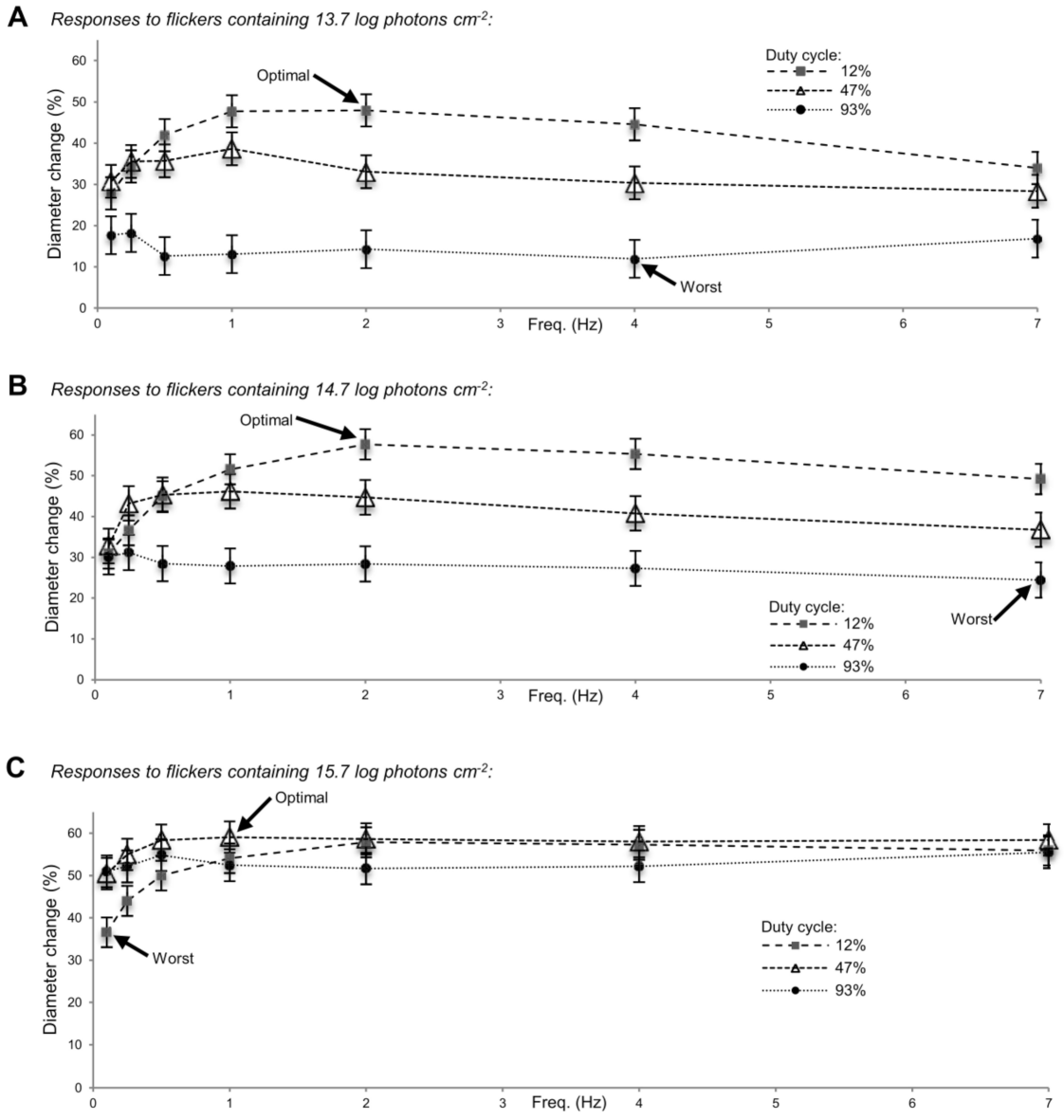

Figure 3.5 Responses to the 63 flickering stimuli. Averaged final-minute responses to the flickers containing 13.7 log photons cm^{-2} (A), the ones containing 14.7 log photons cm^{-2} (B), and those containing 15.7 log photons cm^{-2} (C), expressed as percent reduction in diameter. Five subjects were tested, with each contributing two trials to all 63 conditions.

In summary, responses to stimuli with identical photon counts but different frequencies and/or duty cycles could vary in amplitude up to fourfold. In Figure 3.6, we compared responses to stimuli with different photon counts. The response to the best 13.7 log flicker was nearly twice the response to the worst 14.7 log flicker (Fig. 3.6A). Remarkably, this 13.7 log response was also significantly greater than the response to the worst 15.7 log flicker despite containing 100- fold fewer photons (Fig. 3.6B), although it was smaller than the best 14.7 log response (Fig. 3.6C). The best 14.7 log response was 57% larger than the worst 15.7 log response (Fig. 3.6D), but was statistically comparable to the best 15.7 log response (Fig. 3.6E).

Comparisons With Pupillary Responses to Constant Light

We next compared the most effective flickers (labeled ‘‘optimal’’ in Fig. 3.5) with constant lights that had either the same photon counts as these flickers, or the same intensities as flickers with various duty cycles. Both the optimal 13.7 log and 14.7 log photons cm^{-2} flickers induced significantly greater responses than all the constant lights compared, even though these constant lights had up to 8.5-fold more photons (Figs. 3.7A, 3.7B). While the optimal 15.7 log photons cm^{-2} flicker was significantly more potent than a constant light with an equal number of photons and another with ~10% more photons, it evoked statistically similar response amplitudes as the two highest-intensity constant lights (Fig. 3.7C).

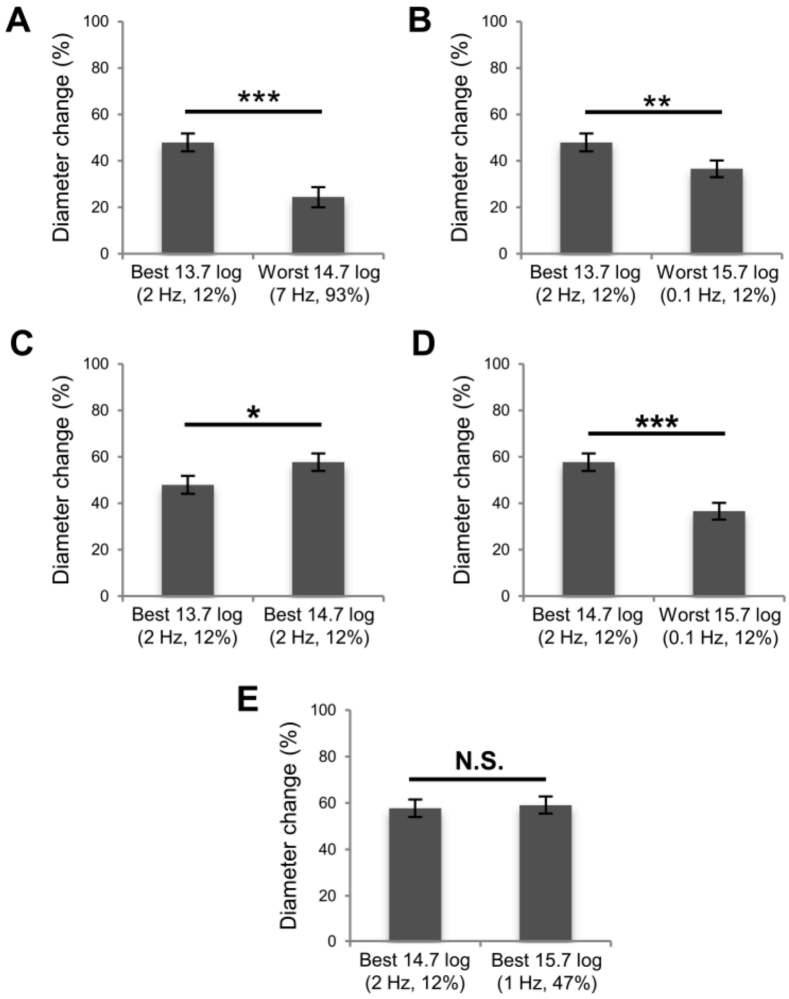

Figure 3.6 Statistical comparisons across different photon counts. (A) The greatest response evoked by a 13.7 log photons cm^{-2} flicker was larger than the smallest response induced by a 14.7 log photons cm^{-2} flicker. (B) The best 13.7 log response was larger than the weakest response evoked by a 15.7 log photons cm^{-2} stimulus. (C) The best 13.7 log response was smaller than the best 14.7 log response. (D) The best 14.7 log response was larger than the weakest 15.7 log response. (E) The best 14.7 log response was not significantly different from the best 15.7 log response (P = 0.7156). * P < 0.05. ** P < 0.01. *** P < 0.001.

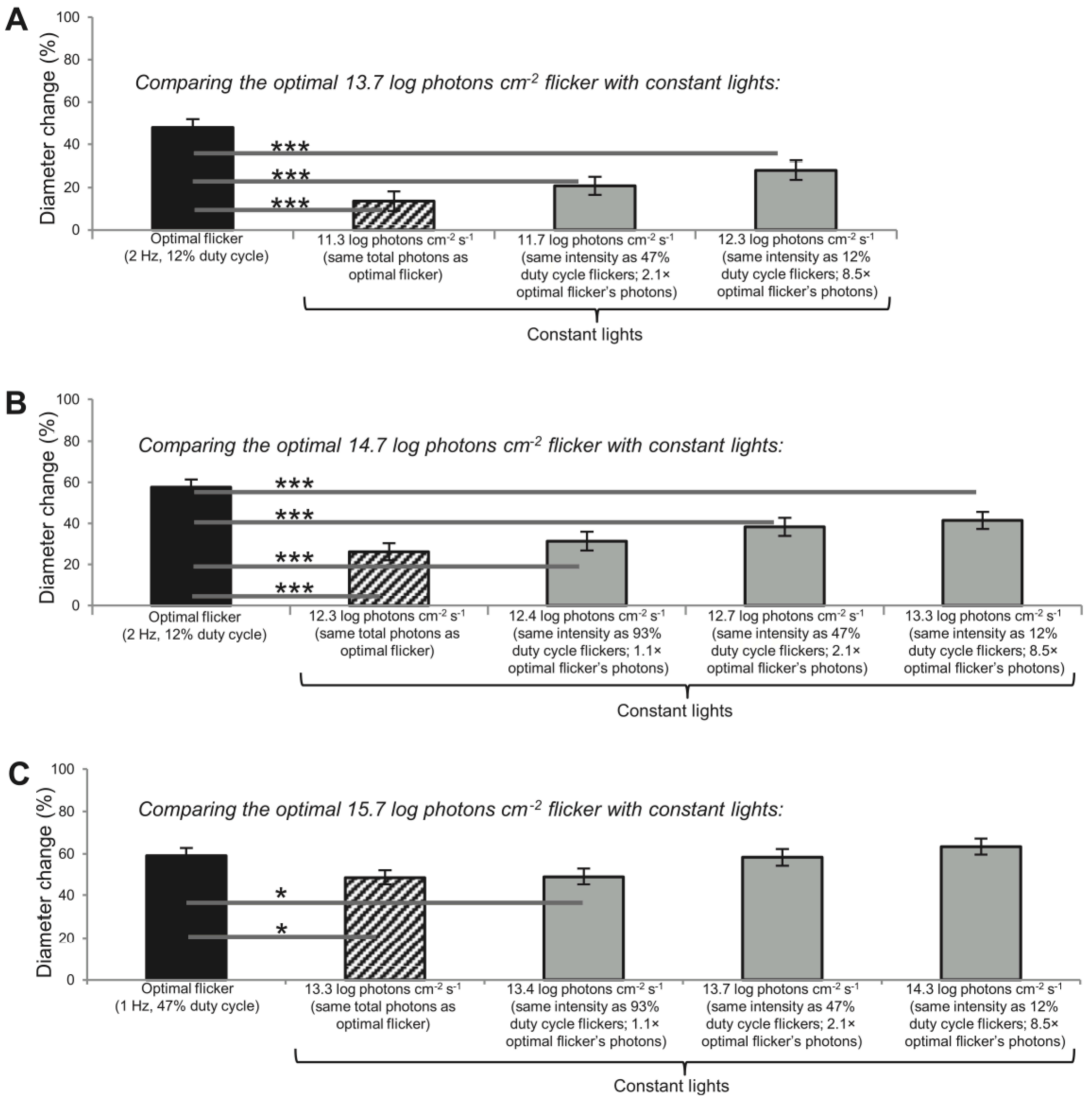

Figure 3.7 Comparisons with responses to constant lights. The optimal flicker responses shown in Fig. 3 are replotted here (black columns) and compared with responses to constant lights that have either the same photon counts as the optimal flickers (hashed columns) or the same intensities as the various flicker duty cycles (gray columns). * P < 0.05. *** P < 0.001. Five subjects participated, each contributing two trials to all 14 conditions.

Prolonged Photostimulation Following Prolonged Dark Adaptation

As mentioned in the Introduction, a potential application of this study is phototherapy. In all the experiments discussed so far, each stimulus was presented to just one eye for 4 minutes, after 4 minutes of dark adaptation. However, phototherapy sessions typically last for much longer and are often performed shortly after waking in the morning from a dark-adapted state, and light is delivered to both eyes. In the final PLR experiment, we simulated a phototherapy session by illuminating both eyes, and increasing the duration of both dark adaptation and photostimulation to 1 hour. We compared the best 14.7 log flicker (13.3 log photons cm^{-2} s^{-1}, 2-Hz, 12% duty cycle) with an equal–photon count constant light (12.3 log photons cm^{-2} s^{-1}). Recordings averaged from three trials by one subject are shown in Figure 3.8. The first several minutes of these recordings should be disregarded because presenting the lights after prolonged dark adaptation caused them to appear uncomfortably bright, resulting in squinting and frequent eye blinks. After the initial discomfort, however, the eyes remained wide open and blinked minimally. Both stimuli induced remarkably stable responses beyond the initial ~10 minutes. The constant light induced a steady-state pupil diameter of ~5 mm (Fig. 3.8A), whereas the response to the flicker stabilized at ~3 mm (Fig. 3.8B). The two responses were significantly different ($P < 0.001$) during the final 10 minutes, inducing 22% ± 4% versus 48% ± 7% (SD) diameter reduction.

Both M1- and M2-Type Mouse ipRGCs Prefer Flickering Light

The above human PLR data may be relevant to other ipRGC- mediated NIF visual responses. Although rodents possess five functionally diverse types of ipRGCs (M1–

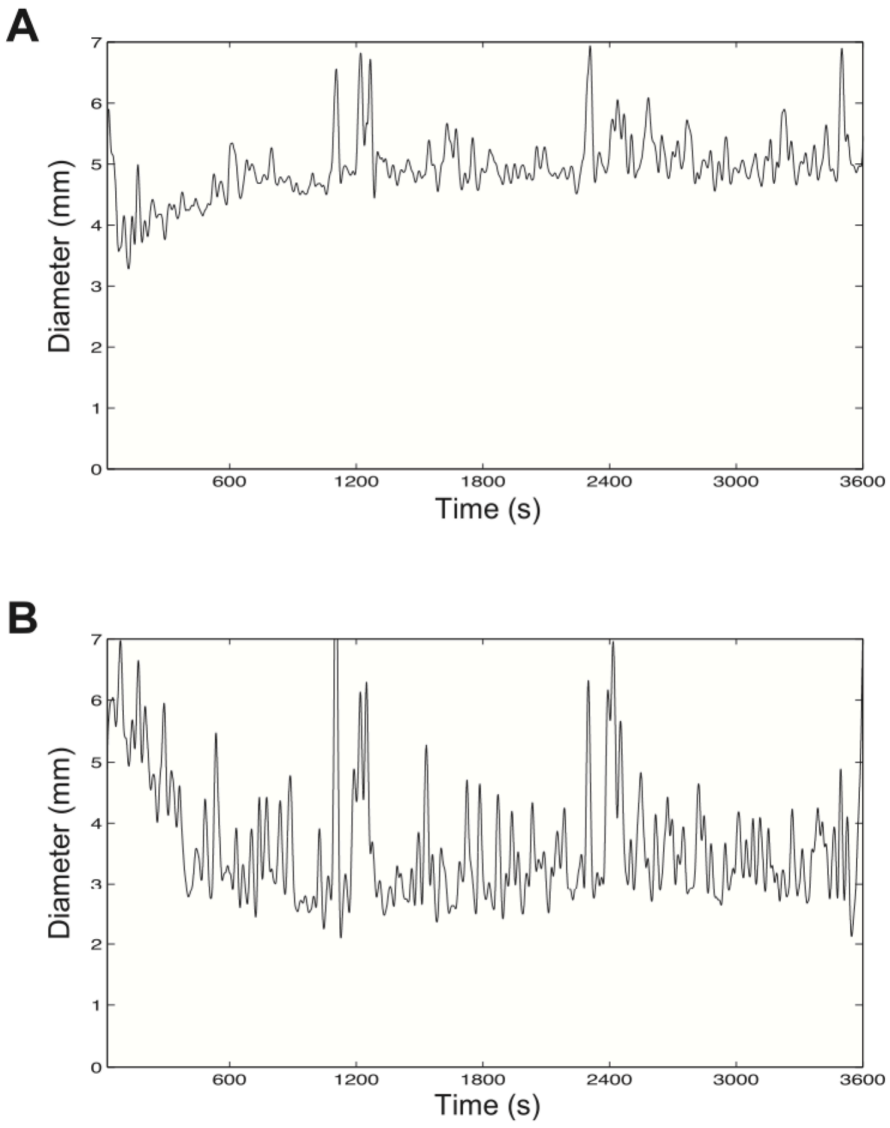

Figure 3.8 Responses to prolonged photostimulation. After 60 minutes of dark adaptation, a subject was exposed to 60 minutes of either a 12.3 log photons cm^{-2} s^{-1} constant light (A) or a 13.3 log photons cm^{-2} s^{-1} stimulus flickering at 2 Hz with a 12% duty cycle (B). In both cases, a total of 15.9 log photons cm^{-2} was delivered per trial. Each trace was generated by averaging three trials, and was filtered using a 4- pole low-pass Butterworth filter with a 0.03-Hz cutoff frequency.

M5)(Zhao et al. 2014; Ecker et al. 2010; Hu, Hill, and Wong 2013; Chen, Badea, and Hattar 2011; Schmidt and Kofuji 2009; Schmidt and Kofuji 2010), only two types are known to exist in primates, one ON-stratifying and the other OFF-stratifying(Dacey et al. 2005; Reifler et al. 2015; Jusuf et al. 2007; GrüNert et al. 2011; S. Neumann, Haverkamp, and Auferkorte 2011; Hannibal et al. 2014). They showed similar responses to a 2-Hz flicker and to longer light steps, and both innervate the olivary pretectal nucleus which drives the PLR(Dacey et al. 2005; Dacey et al. 2003). But it is unknown whether both types prefer flickering light, and whether other NIF visual nuclei are likewise innervated by both(Hannibal et al. 2014). If the two cell types have different preferences for flickering versus constant light and if these other nuclei receive input from just one type, then findings based on the PLR might not be applicable to all other NIF visual responses. To provide a preliminary answer to this question, we whole- cell recorded from mouse M1 and M2 cells, which are thought to be homologous to the OFF- and ON-stratifying primate ipRGCs, respectively(GrüNert et al. 2011; S. Neumann, Haverkamp, and Auferkorte 2011). A flickering light and an equal-photon count constant light were presented, and the former evoked significantly larger spiking responses in both ipRGC types (Fig. 3.9). Assuming that M1 and M2 cells are true homologues of the OFF- and ON-stratifying ipRGCs and that these are the only types of primate ipRGCs, this preliminary result suggests that flickering light is likely more effective than steady light for inducing not only the PLR but also other NIF photoresponses in humans. Indeed, intermittent light phaseshifts human circadian rhythms more efficiently than continuous light(Zeitzer et al. 2011; Gronfier 2004; Rimmer et al. 2000).

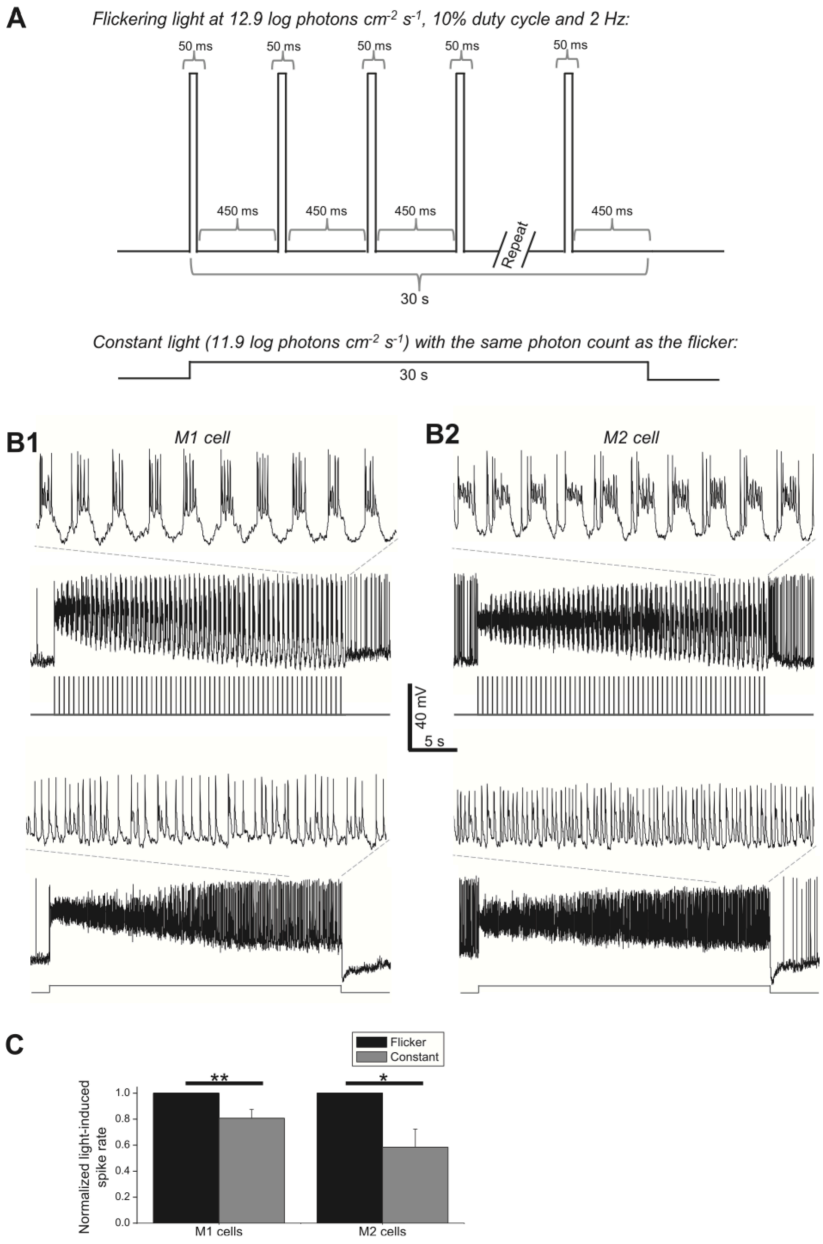

Figure 3.9 Responses of mouse ipRGCs to flickering versus constant lights. Whole-cell current-clamp recordings were made from 11 mouse ipRGCs (seven M1 cells and four M2 cells) under conditions that preserved synaptic input. (A) Two stimuli were presented to each cell, in random order: a 12.9 log photons cm^{-2} s^{-1} light flickering at 2 Hz with a 10% duty cycle, and a steady 11.9 log photons cm^{-2} s^{-1} light with the same photon count as the flicker. All stimuli were full-field 440-nm light. (B) Representative responses from an M1 cell (1) and M2 cell (2). The insets show magnified views of the final 5 seconds of the responses. (C) Averaged data from all cells, illustrating that both ipRGC types displayed larger steady-state spiking responses to the flicker. All mouse ipRGCs spike spontaneously in the dark(Zhao et al. 2014). Thus, to quantify the light-induced spiking increase, spike rate was averaged during the 5 seconds before light onset to calculate the spontaneous spike rate and during the last 5 seconds of photostimulation to calculate the steady-state spike rate, and the former rate was subtracted from the latter rate. In the histogram, each cell's flicker-induced spike rate increase was normalized to 1. * P < 0.05. ** P < 0.01.

Discussion

Flicker Responses of ipRGCs and the Nonimage-Forming Visual System

Intrinsically photosensitive retinal ganglion cells respond to light both directly using melanopsin and indirectly through input from rods and cones(Dacey et al. 2005), and the PLR similarly consists of melanopsin and rod/cone-driven components(Gamlin et al. 2007; Kardon et al. 2009). The different intensity thresholds of rod input, cone input and melanopsin confer ipRGCs with a dynamic range spanning at least 9 log units(Dacey et al. 2005). Rod/cone input and melanopsin also play nonredundant roles in the temporal domain: ipRGCs and the PLR require rod/cone input to track fast irradiance changes but use melanopsin for prolonged integration(Joshua J. Gooley et al. 2012; K. Y. Wong et al. 2007). Melanopsin's response to a brief flash starts slowly and terminates even slower, requiring tens of seconds to return to the baseline(Do et al. 2009). This slow decay provides a window of temporal summation— that is, a second pulse presented during this time induces a response superimposed on the first response, so that the second response peaks higher than the first.

The degree of such paired-pulse facilitation may be expected to increase as the interpulse interval decreases, but another phenomenon must also be taken into account, namely, adaptation. All photoreceptors exhibit light adaptation, meaning they become less sensitive during illumination. After lights off, photoreceptors undergo dark adaptation to regain photosensitivity over time(Fain et al. 2001; Kwoon Y. Wong, Dunn, and Berson 2005). Thus, for a flickering stimulus, a decrease in interpulse interval tends to facilitate temporal summation but reduce the extent of dark adaptation. The flicker frequency that strikes the best balance between these opposing effects presumably

corresponds to the optimal frequency. Here, we have found this frequency to be around 1 to 2 Hz for most intensities and duty cycles. Two previous studies also showed that sinusoidal waves evoked PLRs most effectively within this frequency range(Clarke 2003; Varjú 1964); however, different duty cycles were not explored, and the intensities tested were probably insufficient to activate melanopsin significantly.

Adaptation may also explain why flickering lights induce stronger PLRs than steady lights. During prolonged illumination, ipRGCs lose sensitivity over time and drive a PLR whose amplitude decreases progressively. In comparison, when the stimulus contains a train of short pulses, each pulse desensitizes the photoreceptors only briefly, after which they are allowed to partially recover sensitivity through dark adaptation. Gooley and colleagues(Joshua J. Gooley et al. 2012) reported such steady-versus-flicker difference for the PLR using low-intensity, cone-selective green light. In the current study, we observed a similar difference using blue light that effectively stimulated melanopsin in addition to the classical photoreceptors(Gamlin et al. 2007; J. J. Gooley et al. 2010; McDougal and Gamlin 2010; Park et al. 2011). Differences in the duration of light versus dark adaptation could also partly explain our observation that, for nonsaturating intensities, the 12% duty cycle usually evoked greater PLRs than the longer duty cycles (Figs. 3A, 3B). The duration of each pulse in the 12% duty cycle flicker was about 1/4 and 1/8 of that for the 47% and 93% flickers, respectively, thereby desensitizing photoreceptors the least while allowing the most dark adaptation between pulses.

Potential Strategies for Further Optimization

Our most effective 14.7 log photons cm^{-2} stimulus reduced steady-state pupil diameter by ~60% and increasing light intensity 10-fold did not cause greater constriction, suggesting response saturation. This diameter could reflect the equilibrium point where any increase in ipRGC spiking would be negated by the resultant decrease in the amount of light entering the eye. However, our stimuli were generated using a relatively small light source and illuminated only one eye. Stimulating both eyes using wider-field lights can reduce pupil diameter as much as ~75%(Loewenfeld 1999), more than the ~60% achieved here. Thus, an obvious way to enhance the efficacy of our stimuli is to present them to both eyes through a Ganzfeld system so that the entire visual field is illuminated(Lei et al. 2014).

Additional improvement in efficacy could be achieved by using flickers with shorter duty cycles than the ones we tested. Trains of 2-ms flashes have been shown to phase-shift circadian rhythms far more than prolonged lights with comparable photon counts(Zeitzer et al. 2011; Vidal and Morin 2007; Van Den Pol, Cao, and Heller 1998). If presented as a 2-Hz flicker, these 2-ms pulses would correspond to a duty cycle of 0.4%. Due to hardware limitation, we were unable to test such a short duty cycle.

Finally, the bistable properties of melanopsin could be exploited to further enhance NIF responses to intermittent light. Melanopsin exists in two photosensitive states with different spectral sensitivities(Koyanagi et al. 2005). In the excitable state, melanopsin is most sensitive to short-wavelength blue light and photon absorption activates the photopigment. Once excited, melanopsin becomes more sensitive to longer wavelengths, and the absorption of a second photon reverses melanopsin to its excitable

state. Under certain conditions, NIF photoresponses can be enhanced when the excitation light is preceded by a long-wavelength light, presumably because the latter increases the number of melanopsin molecules ready for photoexcitation(Ludovic S. Mure et al. 2009; L. S. Mure et al. 2007). It would be of interest to test whether pre-exposure to red light enhances the effectiveness of intermittent light.

Conclusions

Potential Applications

As explained in the Results section, the mouse ipRGC recordings suggest that our human PLR data are likely relevant to other NIF visual functions. Thus, these data could inform the design of healthier architectural lighting technologies that promote daytime NIF vision. Another possible application is phototherapy of seasonal affective disorder, non-seasonal depression, and jet lag. All commercially available phototherapy devices emit constant light. Even with intense light, phototherapy typically requires up to 2 hours per session(Golden, R 2005). The discovery that intermittent light induces larger NIF responses than does steady light suggests that intermittent light could enhance the efficiency and/or efficacy of phototherapy. We have determined the best combination of flicker frequency and duty cycle at three light levels. These optimal stimuli induced PLRs with minimal time-dependent decay (Figs. 2, 6), suggesting very sustained, nearly nonadapting spiking in ipRGCs. Assuming the efficacy of phototherapy is proportional to the total number of ipRGC spikes generated per therapy session, such flickers could shorten each session and/or reduce the light intensity required. In this study, the lowest

photon count light causing maximal steady-state pupil constriction was the 2-Hz, 13.3 log photons cm^{-2} s^{-1} flicker with 12% duty cycle. This has the same photon count as a 12.3 log photons cm^{-2} s^{-1} constant light which is roughly 3 to 4 log units less intense than the 10,000 lux light boxes commonly used in phototherapy. Prolonged exposure to intense light could damage retinal photoreceptors(Hunter et al. 2012). By reducing intensity, flickering lights could make phototherapy safer.

Of all the ramifications derived from a dynamic photostimulation paradigm, the largest foreseeable impact falls in the field of general lighting. Since the flickering light schedules studied herein rely on perceivable on-off pulses of blue light, incorporation of the current approach into architectural illumination for home and industry seems infeasible. In order to cross this technological gap, two more steps need to be taken. A pulsing stimulus for contrast-enhanced melanopsin response without a change in contribution from rods and cones will be necessary. If it is possible to stimulate nonimage-forming responses separate from that of conscious vision, i.e., keep the response of rods and cones fixed, while pulsing melanopsin only, a general lighting paradigm that incorporates dynamic photostimulation now becomes possible. One can think of this as an "invisible" flicker. To achieve this aim, a method called silent substitution is employed. The realization of an "invisibly flickering" light is described in the following chapter.

Acknowledgments

We thank Kerby Shedden at the University of Michigan Center for Statistical

Consultation and Research for assistance with statistical analysis; and Adetayo Abdulrazak, Christopher Breuler, Sania Cheema, Benjamin Li, Nenita Maganti, Karun Nair, and Sureel Shah for help with data collection.

Supported by NIH Grants EY013934 (GVV) and EY007003 (Vision Research Core Grant).

Disclosure: G.V. Vartanian, None; X. Zhao, None; K.Y. Wong, None

Chapter 4 – Temporally Modulated Multi-LED Light for Enhanced Subconscious Physiological Responses

Submitted for published as: **Temporally modulated multi-LED light for enhanced subconscious physiological responses,** Garen V. Vartanian, Kwoon Y. Wong, and Pei-Cheng Ku, *APL Photonics*, (submitted July 2016).

Introduction

Photic stimulation of retinal neurons evokes not only conscious vision but also subconscious responses central to our well-being. Because the average person spends >80% of time indoors(Klepeis et al. 2001), the quality of artificial light has far-reaching health impacts. To date, lighting technologies have been designed to improve energy efficiency and visual comfort, but their physiological effects have been largely overlooked. Because the recommended illuminance of indoor lighting is typically ≥100-fold lower than outdoor levels, inadequate daytime light exposure has been linked to various morbidities(Turner, Van Someren, and Mainster 2010). As mentioned previously, the typical indoor inhabitant experiences only 10-20 lux of light at eye level. This is well below intensity levels required to induce proper synchronization of our light dark cycle to the earth's 24-hour light-dark cycle(Gronfier et al. 2007; Middleton, Stone, and Arendt 2002). Here, we present a novel lighting scheme to address this deficiency.

The health impacts of light have been a topic of renewed interest in the 21st century, partly due to the discovery of a new class of photoreceptors: intrinsically photosensitive retinal ganglion cells (ipRGCs)(S Hattar et al. 2002). ipRGCs sense light using the photopigment melanopsin which is most sensitive to blue light, and are the primary neurons mediating nonimage-forming physiological responses to light, e.g. the pupillary light reflex(Gamlin et al. 2007), suppression of nocturnal melatonin release(G. C. Brainard et al. 2001), and entrainment of circadian rhythms such as sleep to the light/dark cycle(Güler et al. 2008). Insufficient daytime light exposure or overexposure during subjective night can result in not only discomfort but also jet lag symptoms, seasonal affective disorder (SAD)(Rosenthal et al. 1984), and general depressive disorders(Naus et al. 2013). Conversely, boosting daytime blue light exposure can decrease reaction times, increase alertness, and ameliorate SAD symptoms(Rahman et al. 2014; Lockley et al. 2006; Viola et al. 2008; Lehrl et al. 2007). But it is unrealistic to promote subconscious photostimulation simply by enhancing blue emission in indoor lighting as that would cause poor color rendering and undesirable color temperature. Thus, having an alternative strategy to make indoor light more potent for subconscious visual stimulation would be highly advantageous.

Several recent studies reported that temporally modulated light stimulated the subconscious visual system more effectively than constant light(Joshua J. Gooley et al. 2012; Lall et al. 2010; Vartanian, Zhao, and Wong 2015; Zeitzer et al. 2011; Walch et al. 2015). For both ipRGCs and downstream targets such as the central circadian pacemaker, melanopsin-based responses to constant light adapt within seconds(K. Y. Wong, Graham, and Berson 2007; Kwoon Y. Wong, Dunn, and Berson 2005). Thus, an intermittently

varying light intensity reduces melanopsin adaptation and enhances ipRGC responses, ultimately stimulating cognitive brain activity(Gilles Vandewalle et al. 2013; Gilles Vandewalle et al. 2006; Rahman et al. 2014). Incorporating temporally modulated blue light into an electric light can therefore boost subconscious responses at a typical indoor illuminance level, but a compensation scheme must be introduced to mask the periodic intensity fluctuation. When temporally modulating the blue component in a white light, two sources of perceived fluctuation are generated: temporal variations in the color coordinates of the light source itself and scenery variations of the illuminated environment. In this paper, we show that by using multiple independently modulated color channels, the silent substitution technique and mathematical optimizations, both sources of visible flickering can be minimized.

Since conscious vision is primarily mediated by cone photoreceptors under daytime lighting conditions, two stimuli with dissimilar spectral power distributions can still look identical to an observer if both spectra produce equivalent responses among the 3 cone channels. Such spectra are called cone metamers. When one metamer is substituted with another, no change in the cone response is evoked; this process is called silent substitution(Ishihara 1906; Mitchell and Rushton 1971a; Mitchell and Rushton 1971b; Cohen and Kappauf 1982; Estévez and Spekreijse 1982; Shapiro, Pokorny, and Smith 1996; Viénot et al. 2012; Barrionuevo et al. 2014; Cao, Nicandro, and Barrionuevo 2015). Our strategy is to introduce four or more color channels implemented using LEDs. When the channel that most strongly stimulates melanopsin is temporally modulated, the other channels are simultaneously modulated such that the overall cone-based color coordinates remain constant. Our proposed light source periodically oscillates between

two cone metamers: one that stimulates melanopsin the most ("maximum melanopsin") and another that stimulates it the least ("minimum melanopsin"). To minimize the environmental flickering, we searched within the "maximum melanopsin" and "minimum melanopsin" solutions such that the pair of spectra generates the least spectral reflection shifts from standardized test color samples (TCS). The algorithm to obtain the "maximum" and "minimum" spectra is illustrated in Figure 4.1. The shift in cone excitation was calculated as a Weber contrast for each TCS and for each of 3 cone responses (short-, mid- and long-wavelength) by integrating the maximum melanopsin spectrum with the cone responses and taking the difference from the value for the minimum melanopsin spectrum.

To further measure the perceived shift in color when alternating between the two spectra, a color inconstancy index (CII) was applied for each TCS and averaged. Here we used the CIE color difference equation (2000), CIEDE2000. Color inconstancy is typically calculated to gauge the degree of color fidelity of a color sample with a change in illuminant. In this case, we estimated the inconstancy of the scene as the lighting spectrum oscillates between the minimum and maximum melanopsin spectra. To calculate the CII, we first applied a chromatic adaptation transform for both minimum and maximum melanopsin spectra with respect to the reference illuminant best suited for use with CIEDE2000(M. Fairchild 2013). Since this difference equation operates on the basis of CIELAB, the reference illuminant is D65 with an illuminance level of 1000 lux. The adaptation transform is necessary for the index to correlate with visual evaluation. The selected transform is CAT02 with sharpened cone fundamentals; it is the most recent recommendation from CIE and can be found in the CIECAM02 specifications. Since

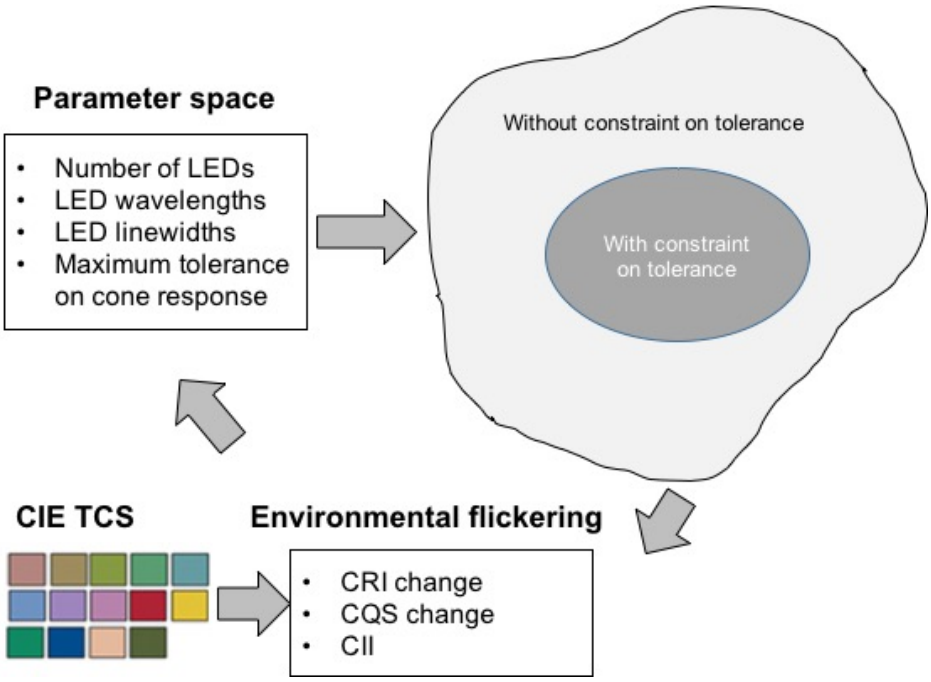

Figure 4.1 The schematic of the algorithm and parameter space used in this work.

cone response to illuminant is fixed, the degree of chromatic adaptation was assumed to be complete and set to 1. This assumption is valid because the color coordinates of the illuminant do not shift and there is no heterogeneous mixing of scene lighting with another source. The TCS spectral reflectances were integrated with the spectral profile of first the minimum-melanopsin and then the maximum-melanopsin illuminant and tristimulus values were calculated. The transform was applied in order to calculate corresponding color coordinates for TCS reflectances under the reference illuminant. Once the corresponding color coordinates under the reference illuminant were specified for a TCS under minimum- and maximum-melanopsin conditions, a CII was calculated.

Methods

In this study, we seek to take the concept of silent substitution one step further by accounting for one's lighting environment. The express purpose is to optimize an indoor light source for maximal ipRGC-mediated response through melanopsin stimulation during daytime. We employ Cohen and Kappauf's formalism to solve for available black metamers and optimize our solution utilizing the simplex method. This allows us to solve for a null space with manifold solutions. That is, any arbitrary number of spectrally independent illuminants greater than 3 can be employed. The calculation provides 2 spectra, one that stimulates melanopsin maximally and one that stimulates melanopsin minimally. The solution is further constrained by taking into account spectral changes in reflections from standardized test color samples used in color rendering calculations("Method of Measuring and Specifying Colour Rendering Properties of Light

Sources" 1995). The temporal alternation between these two metameric stimuli is assumed to induce dynamic stimulation of the melanopsin-only subconscious visual response. In order to minimize disruptions to the viewing environment, certain color rendering and appearance models are taken into consideration during the optimization process.

Color Rendering Index (CRI) is observed, as an important standard in lighting practice. Color Quality Scale is an additional color rendering metric suitable especially for narrowband light sources, such as LEDs(Davis and Ohno 2010). Color inconstancy is calculated using the latest CIE chromatic adaptation transform and color difference formula, CAT02 and CIEDE2000, in order to estimate perceived changes in color appearances of test color samples. With the emergence of non-image-forming theory, metameric blacks can be employed to dynamically stimulate subconscious visual channels by producing melanopsin contrast, while minimizing distortions of conscious color perception.

Mathematical Approach

Both color matching functions and physiological response functions are employed in our approach. In order to prescribe a color coordinate, a color matching function is necessary and most practical. Subsequently, cone fundamentals are used to simultaneously constrain cone responses to the dynamic illuminant–and to changes in the simulated environment–and to optimize melanopsin contrasts. The simulated environment is defined by test color samples used in color rendering calculations, which themselves are selected from Munsell color indices. All spectral functions are specified in

unit wavelength intervals. Spectral functions that are defined at 5 nm increments are interpolated to 1 nm intervals using the Matlab shape-preserving cubic spline function, *cubic interp1*.

The function whose response is to be optimized is the human melanopsin absorption spectra, **I**, taken from Lucas(Lucas et al. 2014). The constraints are derived from 10-degree cone fundamentals calculated by Stockman and Sharpe based on data from Stiles and Burch, found on the Color Vision & Research Laboratory(University College London, website at cvrl.org). The cone fundamentals provide us with the most recent CIE standard with which to constrain our optimization algorithm(Stockman and Sharpe 2000). The cone fundamentals have been weighted and normalized according to MacLeod & Boynton and used by Barrionuevo(Barrionuevo et al. 2014). For an equienergy spectrum, S_E, the L-cone to M-cone excitations have been defined with a ratio of 2:1 and sum to one when integrated and combined. The L+M response function has been factored by a value of 683 lumens for the purposes of calculation. The S-cone ratio is defined as S/(L+M)=1, and the melanopsin spectral sensitivity function, I, is similarly defined as I/(L+M)=1.

Initial Conditions: Utilization of orthogonal projection to calculate spectrum from colorimetric coordinates

We start by specifying our light source. The source spectra are modeled using the equation suggested by Ohno, which closely mimics the spectral output of real multichip LEDs(Ohno 2005).

$$S_{LED}(\lambda, \lambda_0, \Delta\lambda_{0.5}) = \frac{g(\lambda, \lambda_0, \Delta\lambda_{0.5}) + 2g^5(\lambda, \lambda_0, \Delta\lambda_{0.5})}{3},$$

where

$$g(\lambda, \lambda_0, \Delta\lambda_{0.5}) = exp\{-[(\lambda - \lambda_0)/\Delta\lambda_{0.5}]^2\}.$$

The spectra are adjusted so that their integrated optical output is ~1.72 W, typical of real LEDs. The peak wavelengths and full width half max (FWHM) of *n* individual color LEDs is specified. The resulting spectra are each represented by an *m* x 1 vector $\mathbf{P}_i$,

$$\boldsymbol{P_i} = \left[P_{i,\lambda 1}\ P_{i,\lambda 2} \ldots P_{i,\lambda m}\right]' \quad i = 1,2, \ldots n$$

A superposition of independent LED contributions results in an illuminant with spectrum N,

$$\boldsymbol{N} = L_1\boldsymbol{P_1} + L_2\boldsymbol{P_2} + \cdots + L_n\boldsymbol{P_n}$$

where **L** is a *n* x 1 vector and **N** is a *m* x 1 vector. This can be represented in matrix form as

$$\boldsymbol{N} = \boldsymbol{PL}\ .$$

Metameric black decomposition uses the formalism devised by Cohen and Kappauf and further described by Vienot(Cohen and Kappauf 1982; Viénot et al. 2012; Viénot and Brettel 2014). In order to manipulate a light stimulus, we first decompose the spectrum into its fundamental light stimulus, **N***, and a metameric black component, **B**,

$$\boldsymbol{N} = \boldsymbol{N}^* + \boldsymbol{B}$$

N is a matrix, which describes the spectral power distribution of the stimulus in equal increments across the spectrum,

$$\boldsymbol{N} = [\ N_{\lambda 1}\ \ N_{\lambda 2} \ldots N_{\lambda k}]'\ .$$

A color-matching basis is chosen in Euclidean space as a k x 3 matrix **A**, which contains 3 observer color-matching functions, where

$$\boldsymbol{A} = [\boldsymbol{X_{10}}\ \boldsymbol{Y_{10}}\ \boldsymbol{Z_{10}}].$$

We have chosen the color matching functions of the 10 degree CIE 1964 supplemental observer, since this is better suited for general lighting purposes than the 2 degree observer. This becomes of little practical importance when we utilize color appearance models to calculate color differences equations, since uncertainty in scaling color appearance is much larger than any difference in color match predictions due to selection of standard observer(M. Fairchild 2013).

V is the luminous spectral luminous efficiency function for the 1924 standard photometric observer, as defined by the CIE, with a maximum of 683 lumens defined to be its maximum value. $\mathbf{Y_{10}}$ is here defined as 683 lumens at its maximum value with the caveat that luminance is photometrically defined within the 1931 standard observer functions, where **Y** is equal to **V**. However, this is allowed as it approximates luminance sufficiently well(Stockman and Sharpe 2000). $\mathbf{X_{10}}$ and $\mathbf{Z_{10}}$ have been normalized to $\mathbf{Y_{10}}$.

Tristimulus values, **T**, are obtained as a 3-vector by first specifying xyY values, defining luminance, $\mathbf{Y_{10}}$, in candela/m^2 as 100.

$$\boldsymbol{T} = (\boldsymbol{Y_{10}}/\boldsymbol{y_{10}}) \begin{bmatrix} \boldsymbol{x_{10}} \\ \boldsymbol{y_{10}} \\ \mathbf{1} - \boldsymbol{x_{10}} - \boldsymbol{y_{10}} \end{bmatrix},$$

Since the values of **P** and **A** are fixed by our initial conditions, the problem is simplified by solving

$$\boldsymbol{A_n} = \boldsymbol{P'A}\ ,$$

again where *n* equals the number of independent LED components and $\mathbf{A_n}$ is an *n* x 3 matrix. The motivation here is to produce an orthogonal projector, $\mathbf{R_n}$, which projects a spectral stimulus, **N,** onto the plane defined by the additive mixtures of all possible colors, or range, of the component LED weighted color matching functions. That is, the distance

between an arbitrary spectrum and the plane is minimized. The projected spectrum is defined as the fundamental metamer, **N***(Cohen and Kappauf 1982). (The minimization itself is of minor consequence, since our intention is to simply supply the linear optimization algorithm with a starting point.) The *n* x *n* symmetric matrix $\mathbf{R_n}$ is calculated by

$$\boldsymbol{R}_n = \boldsymbol{A}_n(\boldsymbol{A}_n'\boldsymbol{A}_n)^{-1}\boldsymbol{A}_n' \ .$$

The fundamental metamer is mathematically defined by

$$\boldsymbol{N}^* = \boldsymbol{R_n N} \ ,$$

and

$$\boldsymbol{L}^* = \boldsymbol{R_n L} \ ,$$

where **L*** is the vector between 0 and 1 with relative contributions of each of the *n* LEDs required to produce the fundamental metamer. Since also,

$$\boldsymbol{T} = \boldsymbol{A'N} = \boldsymbol{A'PL} \ ,$$

relative contributions can be calculated in our algorithm by the more suitable form

$$\boldsymbol{L}^* = \boldsymbol{A}_n(\boldsymbol{A}_n'\boldsymbol{A}_n)^{-1}\boldsymbol{T} \ .$$

Finally, the fundamental metamer is calculated,

$$\boldsymbol{N}^* = \boldsymbol{PL}^* \ .$$

Linear Programming for Melanopsin Contrast Optimization

A range of colorimetric coordinates is provided for the optimization algorithm. One batch of coordinates is defined within a small range of values surrounding the

equienergy point, with chromaticity coordinates (0.3333,0.3333)±0.01. A second set of coordinates is derived from blackbody spectra within a temperature range from 3,000 K to 10,000 K.

$$\boldsymbol{T = A' N_T} \ ,$$

where $\mathbf{N_T}$ is the blackbody spectrum calculated using Planck's law. Thirdly, 2 chromaticity coordinates with matching correlated color temperature are calculated above and below the planckian locus for each point on the locus. The corresponding coordinates are calculated in the 1960 uniform chromaticity space, by calculating orthogonal isotemperature lines and making sure the Euclidean distance between isotemperature and blackbody chromaticity coordinates falls below 5.4×10^{-3}.

For the complete set of tristumulus values, the fundamental metamers are calculated. The optimization algorithm employed to maximize melanopsin contrast for each fundamental metamer is Dantzig's simplex algorithm(Cherney, Denton, and Waldron 2013). The algorithm *linprog* provided by Matlab is used for this purpose. The inputs to this algorithm include our constraints in matrix form and the response function to be maximized or minimized. The algorithm has constraints, which follow the two forms

$$\boldsymbol{M_{eq} x = b_{eq}}$$

and

$$\boldsymbol{Mx \leq b} \ .$$

As we seek to manipulate melanopsin and cone opsins, we have defined our constraints within a physiological space, that is with respect to photoreceptor fundamentals(Schanda 2007). The cone response functions, S, M & L, are vectorized into columns, C_i, to build the *k* x 3 fundamental matrix, **C**, and

$$\boldsymbol{M_{eq} = C'P} \ .$$

The cone responses to the fundamental metamer are calculated as

$$\boldsymbol{M_{eq}L^* = b_{eq}}$$

The cone responses are specified as fixed in the output vector, $\mathbf{b}_{eq}$, where $\mathbf{b}_{eq}$ is the 3 x 1 matrix describing S, M, & L cone excitation responses, respectively. The response function to be minimized and maximized is

$$\boldsymbol{f = I'P} \ .$$

The linear programming algorithm then calculates LED contribution values, $\mathbf{L}_{min}$, which results in minimal interaction with the melanopsin response function.

$$\boldsymbol{mel_{min} = fL_{min}} \ .$$

$\mathbf{mel}_{max}$ is calculated similarly. This is chosen as a starting condition, against which subsequent calculations are compared. The first constraint is required in order to fix the cone response of both the minimum and maximum excitation spectra with respect to direct illumination by the two spectra,

$$\boldsymbol{M_{eq}L_{min} = M_{eq}L_{max} = b_{eq}} \ .$$

The solutions to $\mathbf{mel}_{max}$ and $\mathbf{mel}_{min}$ allow us to calculate a contrast for melanopsin stimulation before consideration of reflections from surfaces in a viewing environment.

Environmental Considerations – Linear programming with tolerances

Subsequently, we seek to model a typical viewing environment by introducing constraints into our optimization algorithm. It has been shown that generalization of simplified surface color experiments from a simplified laboratory scene to the natural viewing environment is possible(D. H. Brainard and Maloney 2011). Since the color difference equation, i.e. CIEDE2000 is difficult to linearize, we have employed a surrogate constraint with which to limit noticeable differences due to a change in illuminant. In order to do this we select the 14 canonical test color samples (TCS) recommended by the CIE for use in calculating the 14 special color rendering indexes (CRI R_i)("Method of Measuring and Specifying Colour Rendering Properties of Light Sources" 1995). The spectral reflectances of the TCS, $\mathbf{TCS(\lambda)}$, are integrated with our LED contributions, $\mathbf{P}$, and cone excitations in order to describe a physiological response metric to each illuminant-color sample combination. Anywhere from the first 8 to first 12 TCS samples are included in the construction of our constraint matrix (see Figure 1.13). This heuristic approach is reasonable given experiments in constant luminance-cone space showing the invariance of discrimination threshold contour shape with respect to chromaticity, observer, and experimental conditions(Nagy, Eskew, and Boynton 1987).

Using the first 8 TCS samples, our matrix elements for each cone class are defined as

$$\boldsymbol{Gc_{i,j}} = \sum_{\boldsymbol{\lambda=1}}^{\boldsymbol{\Lambda}} \boldsymbol{TCS_{i,\lambda}} \cdot \boldsymbol{P_{j,\lambda}} \cdot \boldsymbol{C_{c,\lambda}} \;\; for\; i = 1,2,\dots,8, j = 1,2,\dots,n \; and \; c = s,m,l \;\; .$$

In this example system, **G** is a 24 row by *n* matrix.

$$\boldsymbol{G} = [\boldsymbol{G}\mathbf{s}\ \mathbf{Gm}\ \mathbf{Gl}]'$$

where the first 8 rows define an s-cone response to *n* LED reflectances from 8 independently viewed color samples. The second set of 8 rows represents m-cone response, and the third set of 8 rows represents l-cone response. If the cone responses to sample reflectances are fixed during the melanopsin contrast optimization, a solution is not possible. In order to increase contrast, we condition a tolerance within our cone response constraints with respect to reflections. Our cone response output vector is then defined in our inequality as

$$\boldsymbol{b^+} = (\mathbf{1} + \boldsymbol{tol})\boldsymbol{b_{eq}} \;,\; 0 \leq \boldsymbol{tol} \leq 2 \;.$$

This represents a positive deviation with an upper limit of 200%. We also define a lower bound,

$$\boldsymbol{b^-} = (\mathbf{1} + \boldsymbol{tol^-})\boldsymbol{b_{eq}} \;,\; -1 \leq \boldsymbol{tol^-} \leq 0 \;.$$

The lower bound goes no lower than 0, to prevent negative excitation values. Our lower and upper tolerances values are identical up to ±100%. Then our lower bounds and upper bound are combined to define the linear programming constraints,

$$\boldsymbol{M} = \begin{bmatrix} \boldsymbol{G} \\ -\boldsymbol{G} \end{bmatrix} \text{ and } \boldsymbol{b} = \begin{bmatrix} \boldsymbol{b^+} \\ \boldsymbol{b^-} \end{bmatrix},$$

Finally,

$$\boldsymbol{Mx} \leq \boldsymbol{b} \ .$$

The melanopsin contrast is optimized, with the spectral reflectance constraints outlined above. The initial condition is chosen as a linear combination of the min and max excitation spectrum prior to the environmental constraints imposed above. After this linear combination has been specified, the melanopsin response is maximized or minimized in order to find the largest melanopsin contrast.

The change in photoreceptor excitation is calculated as a Weber contrast for each of 8 color samples and for each of 3 cone responses by integrating the maximum melanopsin spectrum with the cone responses and taking the difference from the minimum melanopsin spectrum responses as

$$\%\ \boldsymbol{cone\ change}_{\boldsymbol{c,i}} = \frac{\sum_{\lambda=1}^{\Lambda} \boldsymbol{TCS}_{i,\lambda} \cdot \boldsymbol{N}_{max,s} \cdot \boldsymbol{C}_{c,\lambda} - \sum_{\lambda=1}^{\Lambda} \boldsymbol{TCS}_{i,\lambda} \cdot \boldsymbol{N}_{min,\lambda} \cdot \boldsymbol{C}_{c,\lambda}}{\sum_{\lambda=1}^{\Lambda} \boldsymbol{TCS}_{i,\lambda} \cdot \boldsymbol{N}_{min,\lambda} \cdot \boldsymbol{C}_{c,\lambda}} \quad for\ i = 1,2,\dots,8\ and\ c = s,m,l\ .$$

The percent physiological change does not exceed the tolerance value specified (see figure). For each iteration, special color rendering indexes and a general color rendering index is calculated for the minimum melanopsin and maximum melanopsin spectra using the original recommendations by the CIE on color rendering index calculations (CRI) by employing the 1964 uniform chromaticity space, CIEUVW (G Wyszecki and Stiles 1982). The CQS values are calculated in turn. CQS employs a different set of reflectance functions specified by that particular index.

Also, for each iteration, a color inconstancy index (CII) is applied for each of the 14 TCS(Hunt and Pointer 2011; Berns 2000). The results are subsequently averaged to

find a mean index value. Here we use the CIE color difference equation (2000), CIEDE2000. Color inconstancy is typically calculated to gauge the degree of color fidelity of a color sample with a change in illuminant. In this case, we are estimating the inconstancy of the scene as the lighting spectrum oscillates between the minimum and maximum melanopsin spectral states. In order to calculate the CII, we first apply a chromatic adaptation transform for both the minimum and maximum melanopsin spectrum with respect to the reference illuminant best suited for use with CIEDE2000(M. Fairchild 2013). Since this difference equation operates on the basis of CIELAB, the reference illuminant is D65 with an illuminance level of 1000 lux. The adaptation transform is necessary in order for the index to correlate with visual evaluations upon which the CII scaling is based. The selected transform is CAT02 with sharpened cone fundamentals. It is the most recent recommendation from CIE and can be found in the CIECAM02 specifications. Since cone response to illuminant is fixed, the degree of chromatic adaptation (D) is assumed to be complete and D is set to 1. This is because the color coordinates of the illuminant do not shift and there is no heterogeneous mixing of scene lighting with another source. The TCS spectral reflectances are integrated with the spectral profile of first the min and then the max illuminant and tristumulus values are calculated. The transform is applied in order to calculate corresponding color coordinates for TCS reflectances under the reference illuminant. Once the corresponding color coordinates under the reference illuminant are specified for a TCS sample under min and max conditions, a CII is calculated.

The CII provides an approximate quantity for predicting just noticeable differences (JND) of color change. A value of one describes a change in color that is just

barely perceivable in side-by-side sample comparisons by the average viewer. Larger values reflect more noticeable changes in color and a higher likelihood of perceived difference by a viewer selected randomly from the population.

The melanopsin contrast optimization is run as an iterative process with a combination of various parameter inputs. The parameters specified are tolerance values, number of component LEDs, and the full width half maximum (FWHM) values of the component LEDs. The tolerance values range from 0 to 200%. Initially, we use a 5 LED model and select the 5 peak wavelengths from Cao's 5 LED photostimulator. We also look at 4,6, 10, and "delta function" LED models. In the case of a 4 LED system, we specify the model to have a long wavelength peak that falls in between the amber and red LED peak of the 5 LED system. For the 6 and 10 LED systems, we optimize the peak wavelengths iteratively for a color coordinate of (0.3333,0.3333). There is a special case considered, referred to as the delta function LED set. In this case, the LED inputs are 400 evenly spaced impulse functions, with integer wavelength values spanning from 400 to 799 nm. FWHM values span the range from 1 to 100 nm.

Results

We varied the number of LED channels from 4 to 400 and the spectral full width at half maximum (FWHM) from 1 nm to 100 nm. We also varied the maximum allowable shift in cone response between the maximum and minimum melanopsin spectra. A small tolerance in the cone shift is needed for the light source to be suitable for general illumination while this constraint can be greatly relaxed for a therapeutic light source. We

considered white light sources along the Planckian locus and its isotemperature lines with color temperatures ranging from 3000 to 10000 K in 100 K intervals (Figure 4.2)(Gunter Wyszecki and Stiles 1982). For each condition, we calculated the color rendering index (CRI) ("Method of Measuring and Specifying Colour Rendering Properties of Light Sources" 1995), color quality scale (CQS) (Davis and Ohno 2010), and CII. The CII value provides an approximate quantity for predicting "just noticeable differences" in color. A CII of 1 describes a barely perceptible color difference in side-by-side sample comparisons by an average viewer, while larger values reflect greater, more readily perceived color differences. Figure 4.3 summarizes the results for an illuminant system containing 5 LEDs, each with a 10 nm FWHM. To facilitate discussions, we focus on three tolerance levels in Figure 4.4: no constraints, 50% tolerance, and 5% tolerance. The first case is relevant to phototherapeutic devices while the others have potential applications in general lighting.

Light source without constraint on cone response change

There is a tradeoff between melanopsin contrast and illuminant quality measured by CRI (or CQS) and CII. As expected, the highest melanopsin contrast can be obtained when there is no constraint on the tolerable cone response shift between the two spectra. When the maximum number (400) of LED channels is used, the highest melanopsin contrast is achieved: a Michelson contrast of 87.4%, corresponding to a maximum-to-minimum melanopsin response ratio of 14.9. However, this system also produces the worst CRI and CQS values: the CRI of the maximum and minimum spectra oscillates between -26 and

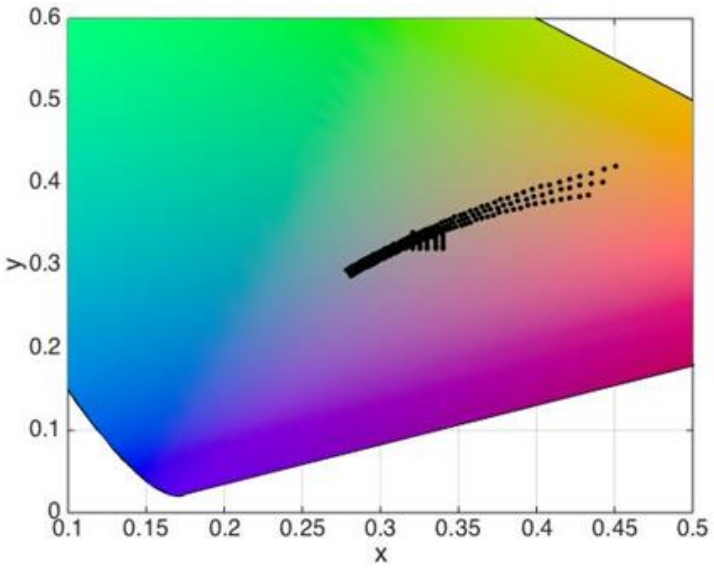

Figure 4.2 Color temperatures explored in this study fall along the Planckian locus and its isotemperature lines from 3000 to 10000 K in 100 K intervals as well as near and around the equi-energy point, i.e. a square bounded by (0.3203,0.3203) and (0.3403,0.3403). Sampled points are plotted here using the 10º response functions of the 1964 supplemental observer.

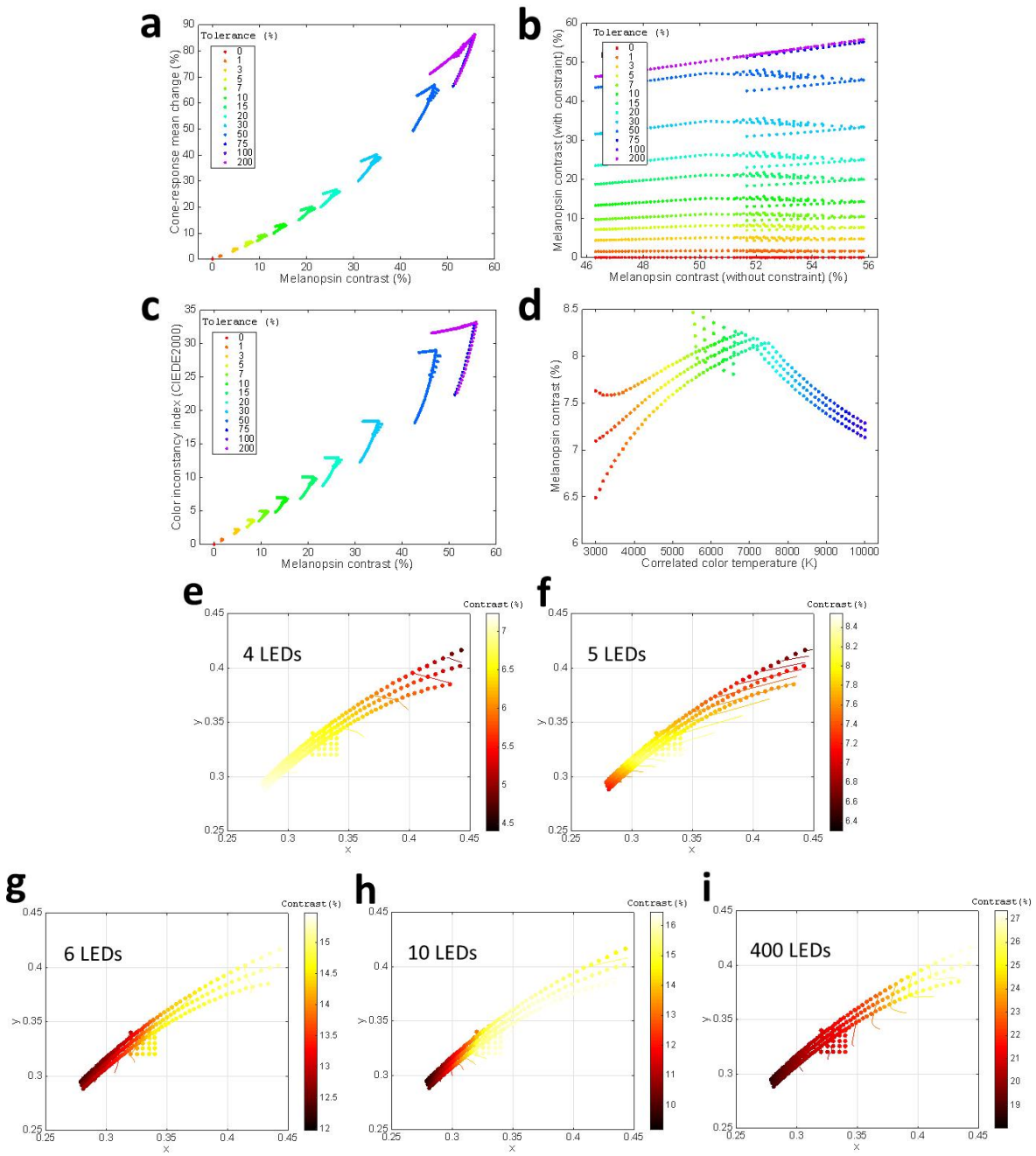

Figure 4.3. A survey of trends in melanopsin contrast with relaxation of cone response constraints for a light with specified system parameters. *a – d:* In this example, the system consists of 5 LEDs (peak wavelengths 456, 488, 540, 592 and 632 nm; 10 nm FWHM) with color coordinates along the Planckian locus, and the cone response change is calculated with respect to the oscillation of white light between the maximum- and minimum-melanopsin spectra. When calculating cone response changes in this case, the first 8 TCSs are used. The tolerance to change in cone response ranges from 0% to 200%. As tolerance is increased, the optimized melanopsin contrast increases with mean cone response changes increasing concomitantly (*a*), ultimately matching the unconstrained contrast as tolerance approaches 200% (*b*). However, CII also increases as tolerance goes up (*c*). Melanopsin contrast reaches a maximum at 7000 K correlated color temperature (*d*). *e – i:* Melanopsin Michelson contrasts for simulations with 4, 5, 6, 10, and 400 LED channels, respectively, plotted on the CIE chromaticity diagram using 10° cone fundamentals. The correlated color temperature of maximum

contrast shifts when number of independent LED channels is adjusted. In *d* – *i*, isotemperature results are presented, as seen by the 3 contour-matched scatter plot groupings in each panel.

-306, and the CQS value is 0 for both spectra. The mean CII is 34, which will produce an obviously fluctuating and hence unpleasant lighting environment.

Light source with 5% tolerance in cone response change

When searching for the smallest CRI shift, many conditions from our iteration qualify with no change in CRI value. These conditions can also demonstrate high melanopsin contrasts. For example, a 6-LED system with a tolerance of ±50% and FWHM of 10 nm has a contrast of 47%. However, CRI values can be very low, in this case 33, with CII at 16 and CQS oscillating between 9 and 32.

A small tolerance in visual shift usually leads to a low CII. In combination with a large FWHM, the light source can produce a moderate melanopsin contrast with hard-to-notice oscillation. Recent *in vitro* recordings suggested that the optimal modulation frequency for melanopsin-based photoresponses in rat ipRGCs was ~0.1 Hz(Walch et al. 2015). Hence even with the worst case scenario, say a room dominated by the color similar to TCS12 (deep blue), the change generated by a light source oscillating sinusoidally at ~0.1 Hz will be slow and probably barely noticeable. Figure 2 and Table 1 show the results of two illuminants containing four LEDs. Each illuminant is spectrally and temporally modulated between two spectra shown in Fig. 2a and 2b. For example, a 4-LED system with a 100 nm FWHM (Fig 4a) yields a high CRI of 92. The CII mean for all TCSs is 1.6 (Fig 4c). This system has a melanopsin contrast of 4.7%. A 5-LED system can give a slightly higher contrast of 6.4% but also a higher CII of 3.

Light source with 50% tolerance in cone response change

The illuminant in Fig 4b contains 4 LEDs with chromaticity coordinates (0.4370,0.4042), corresponding to a CCT of ~3200 K. Its melanopsin contrast is 30.1%, and its maximum-to-minimum melanopsin response ratio is 1.86. The CRI values of its minimum and maximum spectra are 65 and 80. Its CQS values are poorer and range from 37 to 68, and the mean CII for 14 TCSs is 8.2. The CII for TCS 12 is 26.7, more than twice the second largest value of 12.0, for TCS 10 (Fig 4d). However, for viewers suffering SAD or other conditions arising from poor ipRGC stimulation, the therapeutic benefits of a high melanopsin contrast might take priority over color inconstancy, i.e. these individuals may be willing to tolerate subtle changes in the shades of objects in exchange for better therapeutic effects from their interior lighting. These subtle shifts can probably be reduced by using a light source that alternates between the maximum and minimum spectra in a smooth, sinusoidal fashion. Existing light therapies are inefficient and require prolonged dedicated viewing. Incorporating phototherapy into general lighting would circumvent such inconvenience, by allowing users to receive therapy while engaging in normal daily activities.

Discussion

We have provided theoretical predictions of the impact of dynamic lighting parameters on visual disturbance; psychophysical testing in architectural environments will be needed to assess real-life impacts. Our biggest concern is perceived flicker and

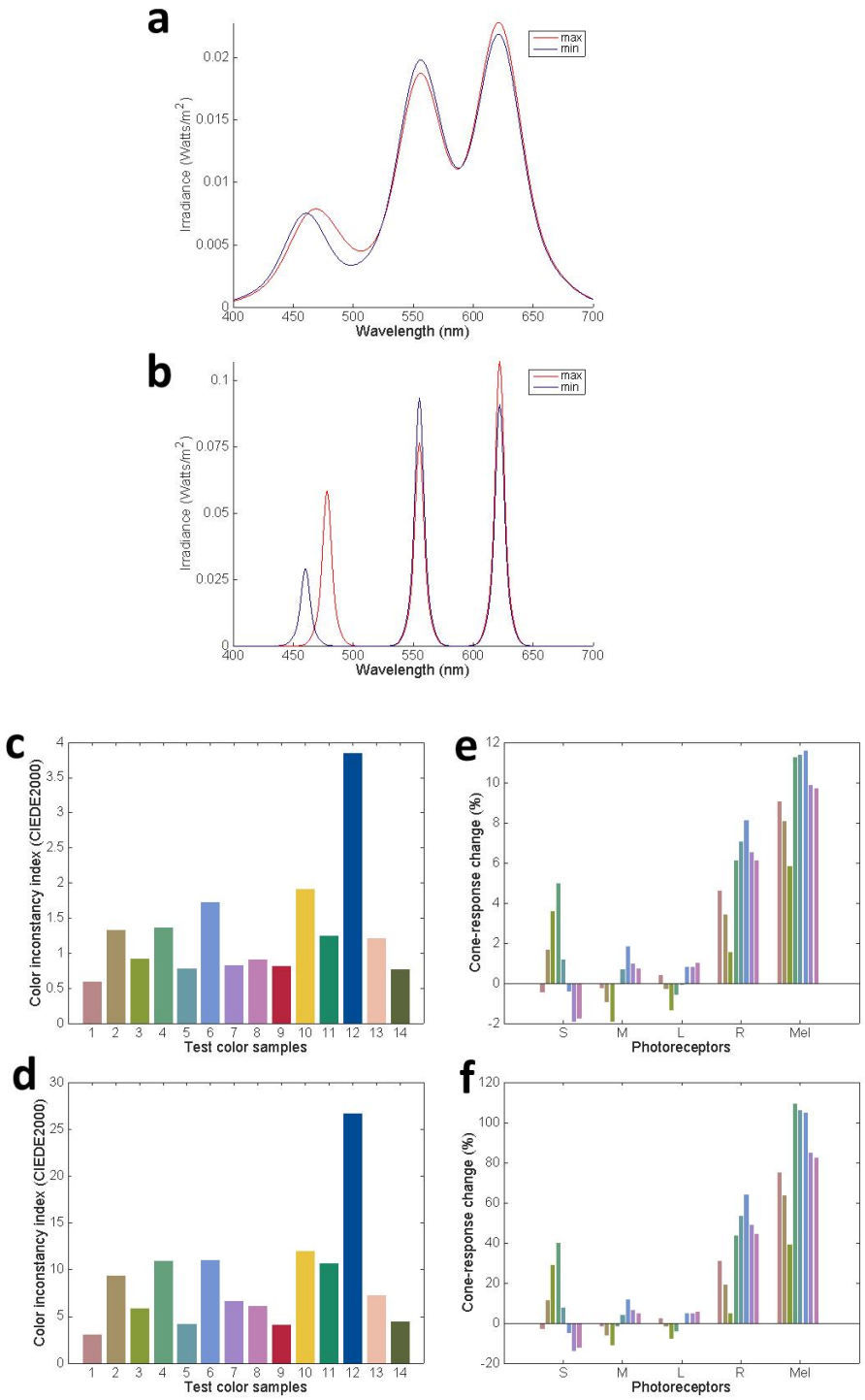

Figure 4.4 Spectra and metrics for general and therapeutic lighting. *a,b:* Spectra of two example light sources with different applications: general lighting (*a*) and therapeutic lighting (*b*). *c,d:* Individual CII values for 14 TCSs specified in CRI calculations for the general (*c*) and therapeutic (*d*) light sources. *e,f:* Amount of cone response change to the first 8 TCSs, as spectra oscillate between the maximum- and minimum-melanopsin states for general (*e*) and therapeutic (*f*) lights.

	x_{10} , y_{10}	CCT	Michelson contrast	Max/min ratio	Mean CII	CRI min	CRI max	CQS min	CQS max
General	(0.437, 0.404)	3200 K	4.7 %	1.10	1.22	79	85	64	72
Therapeutic	(0.437, 0.404)	3180 K	30.1 %	1.86	8.18	65	80	37	68

Table 4.1. Values of key lighting parameters for the general and therapeutic lights shown in Fig 3. "CCT": the correlated color temperature of the illuminant. "Max/min ratio", the ratio of the melanopsin response induced by the maximum- *vs*. the minimum-melanopsin spectrum. "Mean CII", the average color inconstancy index with respect to all 14 TCSs. "CRI min", "CRI max", "CQS min" and "CQS max", the color rendering index and color quality scale values of the minimum- and maximum-melanopsin illuminants.

noticeable hue, chroma, and lightness changes in illuminated objects. The well-known phenomenon of "discounting the illuminant," in which retinal and cortical processes allow the viewer to perceive an object's color as constant under varying lighting conditions, does not readily apply to our illuminant. Thus, a novel question arises regarding color and brightness constancy, heretofore unexplored. Since the illuminant is fixed to a specified cone-based color coordinate throughout the spectral oscillation, it is unknown if the mechanism of color constancy will reduce perceived color shifts. In terms of evolution, there is no teleological purpose for a neural color mechanism that could adjust for a change in illuminant, yet maintains the same level of cone excitation. Fortunately, color memory is relatively weak in humans and it has been reported that larger environments help minimize perceived color changes(Berns 2000). The dynamic light will oscillate at 0.05 – 0.2 Hz, well below the frequencies that trigger the Broca-Sulzer effect(Hart 1987). With respect to brightness instability, this "decoupling" of conscious and subconscious responses may thus be advantageous.

Chromatic adaptation can be described by a superposition of fast and slow processes. 50% adaptation is observed within 4 sec of illuminant transition, and 90% within 60 sec(M. D. Fairchild and Reniff 1995). Our dynamic light will oscillate between two states on the order of once every 10 seconds. Chromatic adaptation may not apply directly to our scenario, but may partly explain it. Firstly, though illuminant color remains the same, the spectral shift in illumination will be uniform throughout the environment. Thus, chromatic adaptation should hold. Secondly, color constancy takes place before conscious adaptation to a change-in-illuminant(Hunt 1981; Brill and West 1986). If there is indeed inertia of perception when it comes to hue discrimination, then there may also

be leeway in the color shifts caused by dynamic lighting, in the absence of being primed for tasks requiring active color discrimination. This is aided by the fact that our light does not oscillate discontinuously, but follows a sinusoidal path. The gradual transition provides preconscious visual modalities additional time to adapt to changes in lighting.

Any single simulation will not account for or control for all the possible contrast effects, which can arise in daily experience. Ultimately, the near-infinite number of environments with their unique geometries, object arrangements, and interplay with outdoor lighting provide for a near-infinite range of lighting situations. Observer variability adds an additional confounding factor. Environmental variability is a reason we avoided the most recent CIE color appearance model, CIECAM02, in our initial simulation design. CIECAM02 provides a streamlined and effective means to describe color appearance with respect to scene context, but would require known background and surround conditions. Mesopic visual responses become relevant at lower lighting levels. The melanopsin contrast optimization algorithm does not consider rod responses whatsoever, as rods are likely saturated or at least nearly saturated under our dynamic lighting. Utilizing a more complicated model that takes into account mesopic vision such as the Hunt model may add unnecessary complications to our algorithm(Hunt and Pointer 2011). Adding rod response to our model would also add to our list of constraints and hence severely reduce melanopsin contrast. One can envision more advanced illuminant designs where the color coordinates of the illuminant itself are allowed to vary. The motivation would be to reduce the just noticeable differences (JNDs) in color sample tests to below threshold. However, a favorable shift in JND for one color would be offset by unfavorable shifting for other colors. There are numerous contrast phenomena, which

could take place based on the arbitrary arrangements of objects, such as simultaneous contrast and crispening effects. Ultimately, quantifying true melanopsin contrast would be impossible without knowing scene context. An accurate assessment of contrast will consider not only the direct illuminant itself, but the summation of all reflections in a given environment. Self-restraint from overmodeling not only allows for conceptual and computational simplicity, but also is no less accurate on balance than a highly refined simulation when it comes to general modeling.

Instead, a broad approach gives us a practical yet sound footing to begin initial designs of dynamic illumination. We observed general trends through statistical analysis of the data. It is clear that more LEDs will provide more contrast, but with more LEDs comes more instability in color appearance as a high proportion of simulation states cause an increase in CII as well as larger changes in CRI and CQS. One remedy to counteract this instability is to decrease the independence of the LED channels by broadening the spectral width of each LED. Surprisingly, spectral broadening does not impact the contrast values significantly. Setting a narrow cone-change tolerance range with respect to our environmental constraints, say ±5%, results in permitted contrast solutions that remain smaller than those that are solely limited by the effects of spectral broadening – up to FWHM values as high 50 nm. The benefit of large spectral width was demonstrated in our general lighting example. In practice, large FWHM can be obtained from LED chips of relatively low quality. If needed, phosphors can be incorporated into the lighting design.

As seen from the considerable spread in outputs, even when correlations are relatively high, our method benefits from a large number of iterations from which one

can cherry-pick the combination of system traits providing the best contrast, constancy, and color rendering. One clear limitation is apparent: no matter how well the light is optimized, there will be a certain amount of color instability in the spectral region where melanopsin is most sensitive. This is unavoidable and its effects are apparent when TCS 12 (strong blue) is employed as a constraint: contrast values drop most dramatically relative to the addition of other high chroma color samples in our constraint matrix (Figure 4.5). How detrimental this limitation to blue color reproduction in reality remains to be determined.

To control for nonlinear outputs such as CRI and CII in addition to contrast during the optimization process, further mathematical work accommodating the nonlinear nature of these devices will be needed. Examples include null space analysis and subspace optimization, using our linear model to conduct calculus of several variables and find extrema with respect to variables, and manifold analysis of the hyperspace of x,y– doublets which overlap in chromaticity space.

Dynamic lighting could prove especially advantageous in settings with a general lack of sunlight, such as settlements in and around the Arctic Circle where winters can be almost entirely devoid of light, and inside submarines. Dynamic lighting would also be beneficial at work and school where alertness and productivity is key. Environments such as factories could rely on such lighting to boost productivity or maintain alertness in order to minimize workplace injury.

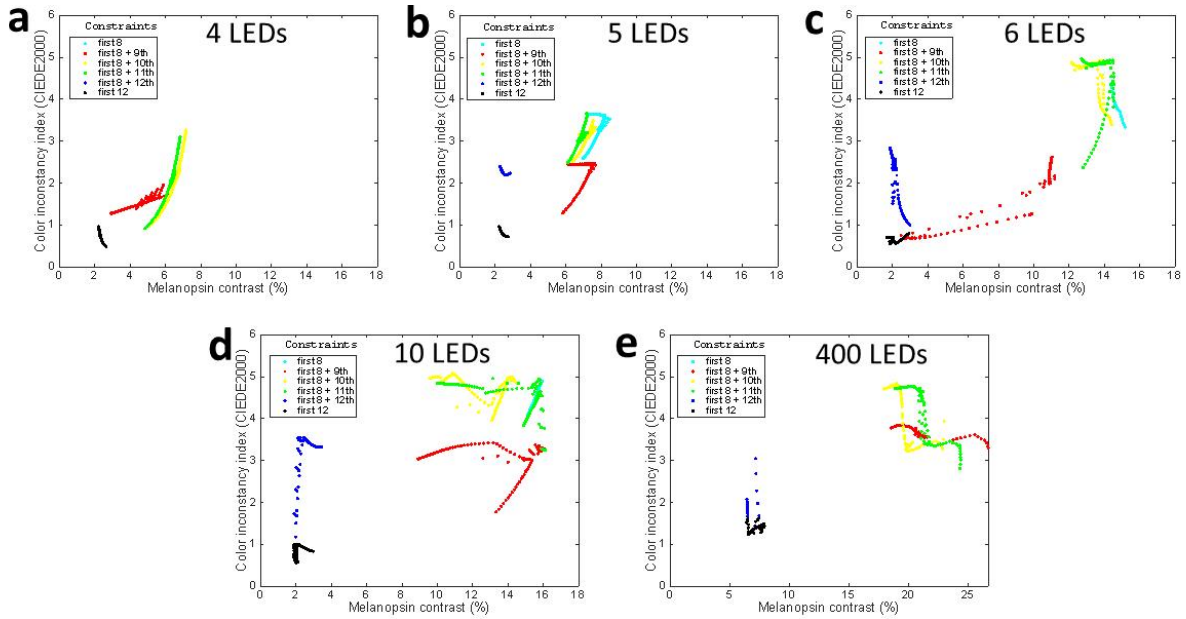

Figure 4.5 Mean CII vs. melanopsin contrast as TCS boundary conditions are expanded for lights with 4 – 400 independent LED channels. TCS 9-12 are high chroma red, yellow, green, and blue colors respectively, which are excluded from the calculation of general CRIs but are regularly encountered in real life. In the legend, "first 8" refers to the inclusion of the first 8 TCSs in the constraint matrix, "first 8 + 9th" means including the first 8 TCSs plus the 9th TCS, etc. The panels reveal trends toward reduced CII and contrast as additional TCSs are included in the constraints. Including TCS 12 (strong blue) in the boundary conditions shows the largest drop in melanopsin contrast, often with little benefit to reduction in mean CII.

Conclusions

Incorporating dynamic modulation into a general illuminant presents an exciting yet complex challenge. The complexity of incorporating silent substitution, which heretofore had been used solely in scientific experimentation, arises from the multiple environmental variables we seek to control. Vision research employing silent substitution considers only direct light exposure using optical instruments. However, the environment consists of subtractive objects, each with its unique reflectance properties. In selecting a light source to accomplish our intended purpose, we must balance three metrics: melanopsin contrast, color fidelity and/or quality, and constancy of scene appearance. Using four or more independently controlled LED channels, an optimization scheme has been presented to maximize melanopsin contrast while maintaining good quality for color rendering and color temperature. A moderate melanopsin contrast of 5% can be achieved with excellent CRI and CII. Such a light source could replace existing interior lighting to improve well-being and productivity.

Acknowledgements

This work was supported in part by NIH grants EY013934 (Vision Training Grant to GVV) and EY007003 (Vision Research Core Grant to the Department of Ophthalmology and Visual Sciences).

Chapter 5 – Conclusions

Our knowledge of ipRGC's existence has a timespan of only 15 years, and so, the field of study dedicated to elucidating its structure and function is relatively young. Accordingly, translation of scientific knowledge in this area into health and architectural lighting is in its nascent stages.

Throughout this dissertation, mention is made of the suboptimal effects of understimuluation of our subconscious visual system due to inadequate lighting. In chapter 2, however, we demonstrate the highly sensitive nature of this very system. Melatonin suppression was seen with light levels of 10.3 log photons cm^{-2} s^{-1}. This is 5 orders of magnitude lower than outdoors lighting intensities(Turner, Van Someren, and Mainster 2010) and what has been suggested for light therapy(Glickman et al. 2006). What explains this discrepancy? An important question to be answered is how does the threshold and sensitivity of subconscious vision change within the 24 hour daily cycle? Are there long term seasonal changes in sensitivity? McIntyre found that melatonin suppression sensitivity is phase dependent. Specifically, he showed that this sensitivity is higher at midnight then early evening(McIntyre et al. 1989). Rea et al. also found that the sensitivity of pupillary light reflex and melatonin suppression changes throughout the night with a spectral shift showing increased sensitivity to blue light(Figueiro et al. 2005). His results show a heightened sensitivity at midnight compared to early morning. More

studies will be needed to show the dynamic sensitivity variation throughout the day. Full studies of sensitivity and thresholds will be expensive and time-consuming, but must be undertaken if a full mapping of the human subconscious visual response is to take place.

In chapter 3, we looked at the use of pulsed light in order to enhance subconscious visual adaptation by preventing light adaptation. The studies show an enhanced effect on pupillary constriction with pulsed light, compared to steady light with an increased efficacy of about ten fold. The light pulses stimulate rods and cones in addition to ipRGCs vis-à-vis melanopsin. Since all 3 cone types are involved in modulating ipRGCs, the question arises, do ipRGCs respond differently to various colors? Frequencies? Two groups presented opposing results. One group claimed that S-cones provided an on signal to ipRGCs(Rea et al. 2005), while the other claimed an S-cone off and L+M-cone on system(Dacey et al. 2005). Recent evidence has led to the latter claim holding true, although antagonistic S-cone contributions seem to be weak and masked by a strong melanopsin-mediated response(Cao, Nicandro, and Barrionuevo 2015; Spitschan et al. 2014). Perhaps alternating between a blue and yellowish light can enhance non-image-forming responses further. The optimal temporal spacing must be determined in this scheme since timing the yellow and blue flashes too close together may activate an opponency process, diminishing response magnitude(*Webvision: The Organization of the Retina and Visual System* 2016). Frequency optimization for melanopsin appears to fall into a slower pulse regime, revealing different requirements for maximizing melanopsin-only responses, when rod and cone stimuli are to remain static(Walch 2015; McDougal and Gamlin 2010; Spitschan et al. 2014)

Another recent finding is light-mediated melanopsin tristability(Emanuel and Do 2015). In the light-activation pathway of the visual system, rod and cone photopigments isomerize after absorption of photons. They rely upon enzymatic processes in order to transform spent photopigments back into an active isomeric form. Melanopsin has an additional pathway, which allows for photo-mediated reisomerization into an active form. When reisomerized by light instead of enzymatic processes, melanopsin takes on a slightly blue shifted absorption profile to 454 nm(Emanuel and Do 2015). The inactive isomer is most sensitive to photoisomerization by amber light around 590 nm. Utilizing an amber light in order to reactivate melanopsin in between blue pulses can enhance responsiveness of the subconscious visual system. Preliminary studies on amber-enhanced pupillary response were undertaken in the Wong lab. 4 minutes of amber light were interspersed between 4 minutes of steady blue light. The results were inconclusive (unpublished data). However, another group was able to show an enhancement in pupillary response using the same methods(Ludovic S. Mure et al. 2009).

In chapter 3, a comprehensive simulation was designed in order to create a light with the ability to pulse melanopsin while maintaining a steady response from the cones. The challenge of such a design is apparent in the inherent tradeoff between melanopsin contrast and lighting quality. In order to determine the feasibility of such a light source, studies must focus on two areas: (1) suitability for use as a general light and (2) physiological and psychological benefits. To assess whether or not such a light is suitable for everyday use, straightforward experiments can measure an observer's satisfaction with the appearance of the light in the context of a viewing environment such as a room. Object colors can be judged. Subjects can be asked to comment on any perceived changes

in brightness or color of the empty scene during trials. Metameric objects with saturated color profiles can be judged in side-by-side comparisons and perceived changes in brightness and color can be measured(Royer and Houser 2012). A point scale can be used to separately measure the conscious visual discrimination of color and of brightness under dynamic illumination, i.e., a scale that ranks color changes between no perceivable differences, and at worst, an obvious strobe like effect. Discrimination tasks will answer the question of color instability as the light oscillates from the low to high melanospin excitation state. The more difficult task lies in the design of optics to suitably mix the output of the various LED color channels, which is absolutely necessary in order to present a light that performs in line with specifications derived from computer simulations. Observer variability must be considered, the degree to which can affect the validity of theoretical calculation and the feasibility of the light. This concern is mitigated by the fact that uncertainty of observer variability is overshadowed, since the scaling of color appearance–and by extension color difference formulas–is larger than the differences in observer(M. Fairchild 2013). EEG measurements and quantitative psychological testing can be used to measure its capacity to affect human health(Rahman et al. 2014; Lehrl et al. 2007; Weissman et al. 2015).

All uncertainty aside, first steps have been taken to construct a light source implementing ideas put forth in chapter 4. A light has been constructed with 5 LED color channels. Each color channel consists of 4 LEDs of the same type for a total of 20 LEDs. The light is controlled by a pulse width modulation scheme and programmed to oscillate sinusoidally between two melanopsin-stimulating states (see Figure 5.1). Optics mix the color channels at the output stage. This device and future iterations are intended to test

the feasibility of an “invisibly” pulsing light source. Regardless of the success of such a lighting paradigm, this is an important first step in rethinking approaches to synthetic light and applying recent findings in the field of vision into practice.

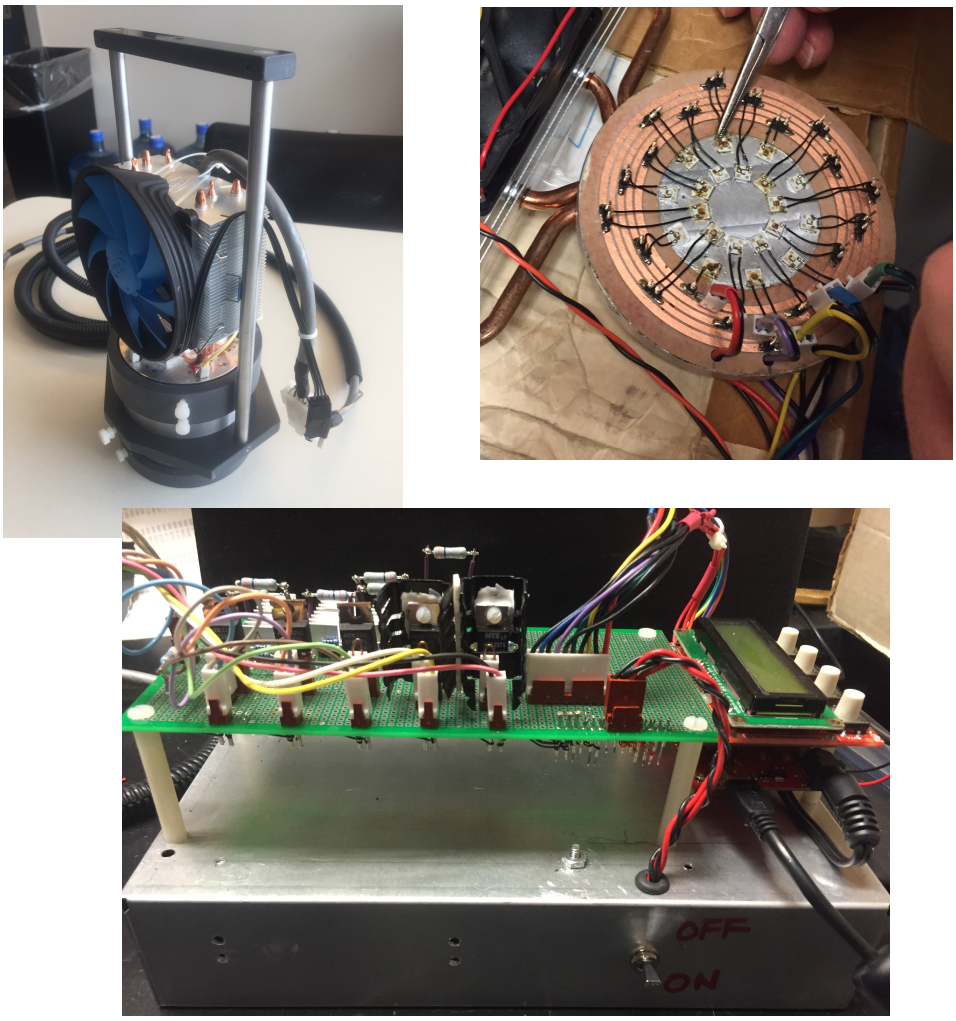

Figure 5.1 Design of light with PWM capabilities of independent LED channels.

Appendix – Waveforms Results

In addition to pulsed light of a simple nature, i.e., square waves(Vartanian, Zhao, and Wong 2015), we decided to investigate the effect of more complex temporal amplitude envelopes. In the literature very few, if any, investigations into the effects of complex waveforms on the subconscious visual response have been published. Physiological studies of pupillary light reflex (PLR) in the past have employed pulses that are square wave or sinusoid(Gronfier 2004; Munch et al. 2012; Rüger et al. 2013; Swanson et al. 1987; Joshua J. Gooley et al. 2012; Spitschan et al. 2014; Cao, Nicandro, and Barrionuevo 2015; Varjú 1964; Barrionuevo et al. 2014; Alexandridis and Manner 1977).

The light pulses we have chosen for this follow-up study employ waveforms found typically in electrical engineering applications: we use amplitude envelopes that are either saw up, saw down, triangle, or sinusoid in nature (Appendix Figure 1). The measured response is PLR, again. Preferential enhancement of the PLR response by any one of the waveforms makes that waveform a prime candidate for employment in dynamic lighting intended to boost subconscious visual stimulation.

Experimental Methods

The same protocol was employed as is from chapter 3, unless otherwise indicated. Again, using the 4-minute dark/4-minute light protocol, we tested each of these

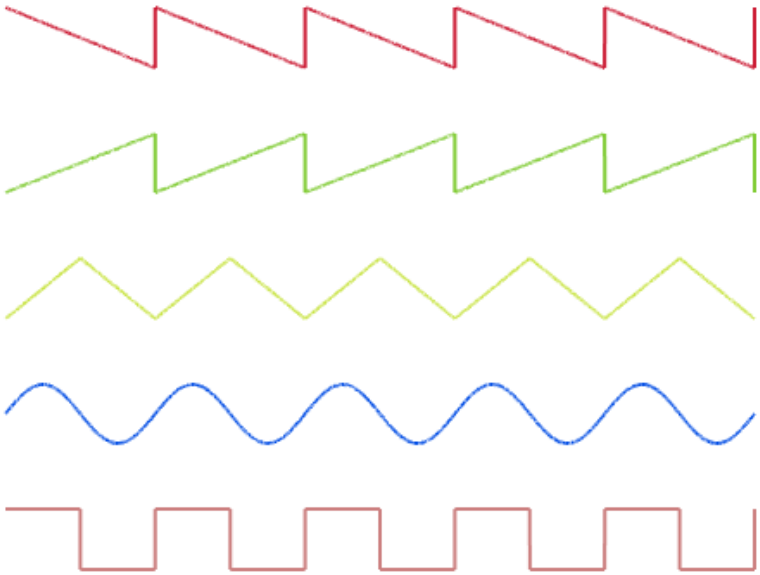

Appendix Figure 1 Waveform envelopes used for stimulus presentation. The stimulus waveforms as shown from top to bottom are saw down, saw up, triangle, sinusoid, and square (Olivia Walch 2016).

waveforms during a one hour session. Each subject attended two sessions during the week at approximately the same time, when circadian rhythm effects are essentially negligible on PLR. In these trials, we set the maximum stimulus light intensity to one setting. The maximum light intensity at the peak of each waveform was fixed to 12.3 log photons cm^{-2} s^{-1} (0.01 W m^{-2}) for all trials. We tested pulse frequencies of 0.1, 1, and 2 Hz. The last minute of pupil diameter data has been averaged. For the 0.1 Hz trial condition, only saw down and saw up waveforms were tested.

Each condition was repeated 3 times per subject. The 3 replicates per condition were then averaged. Paired student two-tailed t-tests were used to assess significance of each waveform stimulus in comparison to a steady light of equal energy density. The same t-test was also used to compare all combination of waveforms with each other.

Experimental Results and Discussion

At 0.1 Hz, pulsing light showed suppression compared to the steady light control. Only the saw up protocol revealed any statistical significance ($p<0.01$) (Appendix Figure 2, top). At 1 Hz, all waveforms showed a significant downward change in pupil size compared to steady light ($p<0.05$) (Appendix Figure 2, middle). At 2 Hz, only the saw up data showed a reduced pupil diameter with statistical significance at the 0.05 level (Appendix Figure 2, bottom). This was the case even though saw up had a mean pupil diameter larger in value than the other waveforms. However, all other waveforms had p-values less than $p = 0.6$ (except saw down $p \cong 0.7$) and are considered marginally significant. None of the t-tests among waveforms revealed any significances.

All waveforms showed a downward effect in pupil size in comparison to the steady light control. However, not all waveform comparisons to the control light revealed a significance. This is expected and can be explained by two obvious reasons. Human subject data is notoriously noisy and is subject to changes in alertness, drowsiness, and focus. This can even affect pupil states(Yoss, Moyer, and Hollenhorst 1970). The second explanation is tied in part to the noisiness of the data. Small subject sets reduce the power of statistical analysis and result in less significant findings. It is not uncommon for researchers working with small groups of subjects to set significance alpha level to 0.10 instead of 0.05. These findings are usually preliminary in nature and further testing is always encouraged in order to validate early findings. In our case, future testing with additional subjects will help reduce the noisy fluctuation in pupil data and increase the power of analysis.

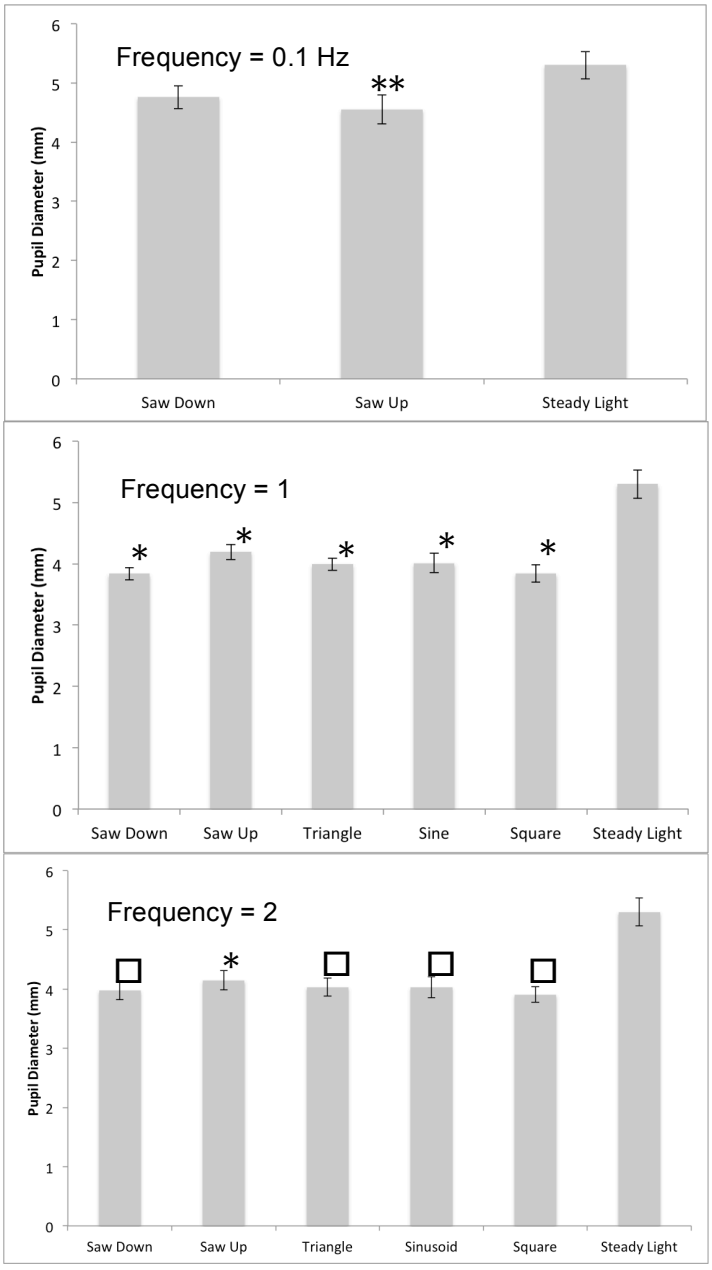

Appendix Figure 2 Mean pupil responses after exposure to light with distinct waveform envelopes. The pupil response is given in pupil diameter and waveforms are indicated below the bars. Paired two-tailed student t-tests were made between the steady light and pulsing lights at each frequency. (P < 0.01, * P < 0.05, ■ P ≅ 0.05)**

Acknowledgement

Special thanks to Olivia Walch for discussions on pupil response modeling and for the use of her waveforms figure.

Bibliography

Alexandridis, E., and M. Manner. 1977. "Folgefrequenz Der Pupille Bei Flimmernden Lichtreizen." *Albrecht von Graefes Archiv Für Klinische Und Experimentelle Ophthalmologie* 202 (3): 175–80.

Altimus, Cara M, Ali D Güler, Nazia M Alam, A Cyrus Arman, Glen T Prusky, Alapakkam P Sampath, and Samer Hattar. 2010. "Rod Photoreceptors Drive Circadian Photoentrainment across a Wide Range of Light Intensities." *Nature Neuroscience* 13 (9): 1107–12. doi:10.1038/nn.2617.

Amaral, F. G., A. M. Castrucci, J. Cipolla-Neto, M. O. Poletini, N. Mendez, H. G. Richter, and M. T. Sellix. 2014. "Environmental Control of Biological Rhythms: Effects on Development, Fertility and Metabolism." *Journal of Neuroendocrinology* 26 (9): 603–12. doi:10.1111/jne.12144.

Andersen, Monica L., Tathiana F. Alvarenga, Renata Mazaro-Costa, Helena C. Hachul, and Sergio Tufik. 2011. "The Association of Testosterone, Sleep, and Sexual Function in Men and Women." *Brain Research* 1416 (October): 80–104. doi:10.1016/j.brainres.2011.07.060.

Bailes, Helena J., and Robert J. Lucas. 2010. "Melanopsin and Inner Retinal Photoreception." *Cellular and Molecular Life Sciences* 67 (1): 99–111. doi:10.1007/s00018-009-0155-7.

Barrionuevo, Pablo, Nicandro Nathaniel, J. McAnany, Andrew Zele, Paul Gamlin, and Dingcai Cao. 2014. "Assessing Rod, Cone and Melanopsin Contributions to Human Pupil Flicker Responses." *Investigative Ophthalmology & Visual Science*.

Bedrosian, T. A., and R. J. Nelson. 2013. "Influence of the Modern Light Environment on Mood." *Molecular Psychiatry* 18 (7): 751–57.

Berns, R. 2000. *Billmeyer and Saltzman's Principles of Color Technology*. 3rd ed. Wiley-Interscience.

Berson, DM, FA Dunn, and M Takao. 2002. "Phototransduction by Retinal Ganglion Cells That Set the Circadian Clock." *Science*, no. 295: 1070–73.

"Blue Light Hazard for Light Sources and Luminaires (IECTR62778{ED1.0}B)." 2013.

Bouma, H. 1962. "Size of the Static Pupil as a Function of Wave-Length and Luminosity of the Light Incident on the Human Eye." *Nature* 193 (4816): 690–91.

Brainard, D. H., and L. T. Maloney. 2011. "Surface Color Perception and Equivalent Illumination Models." *Journal of Vision* 11 (5): 1–1. doi:10.1167/11.5.1.

Brainard, George C., John P. Hanifin, Jeffrey M. Greeson, Brenda Byrne, Gena Glickman, Edward Gerner, and Mark D. Rollag. 2001. "Action Spectrum for Melatonin Regulation in Humans: Evidence for a Novel Circadian Photoreceptor." *The Journal of Neuroscience* 21 (16): 6405–12.

Brainard, George C., John P. Hanifin, Benjamin Warfield, Marielle K. Stone, Mary E. James, Melissa Ayers, Alan Kubey, Brenda Byrne, and Mark Rollag. 2015. "Short-Wavelength Enrichment of Polychromatic Light Enhances Human Melatonin Suppression Potency." *Journal of Pineal Research* 58 (3): 352–61. doi:10.1111/jpi.12221.

Brentano, F. 1874. *Psychologie Vom Empirischen Standpunkte (in German)*. Leipzig: Duncker & Humblot.

Brill, Michael H., and Gerhart West. 1986. "Chromatic Adaptation and Color Constancy: A Possible Dichotomy." *Color Research & Application* 11 (3): 196–204.

Butler, M. P., and R. Silver. 2011. "Divergent Photic Thresholds in the Non-Image-Forming Visual System: Entrainment, Masking and Pupillary Light Reflex." *Proceedings of the Royal Society B: Biological Sciences* 278 (1706): 745–50. doi:10.1098/rspb.2010.1509.

Cajochen, Christian, Mirjam Münch, Szymon Kobialka, Kurt Kräuchi, Roland Steiner, Peter Oelhafen, Selim Orgül, and Anna Wirz-Justice. 2005. "High Sensitivity of Human Melatonin, Alertness, Thermoregulation, and Heart Rate to Short Wavelength Light." *The Journal of Clinical Endocrinology & Metabolism* 90 (3): 1311–16. doi:10.1210/jc.2004-0957.

Cao, Dingcai, N. Nicandro, and P. A. Barrionuevo. 2015. "A Five-Primary Photostimulator Suitable for Studying Intrinsically Photosensitive Retinal Ganglion Cell Functions in Humans." *Journal of Vision* 15 (1): 27–27. doi:10.1167/15.1.27.

Chen, S.-K., T. C. Badea, and S. Hattar. 2011. "Photoentrainment and Pupillary Light Reflex Are Mediated by Distinct Populations of ipRGCs." *Nature* 476 (7358): 92–95. doi:10.1038/nature10206.

Cherney, David, Tom Denton, and Andrew Waldron. 2013. *Linear Algebra*. First Edition. Davis.

"CIE (2009) Ocular Lighting Effects on Human Physiology and Behaviour." 2009. Commission Internationale de l'E´ clairage.

CIE No. 15. 2004. "Colorimetry." Vienna: Commission Internationale de l'Éclairage.

CIE No. 15.2. 1986. "Colorimetry." Vienna: Commission Internationale de l'Éclairage.

CIE No. 17.4. 1987. "International Lighting Vocabulary." Vienna: Commission Internationale de l'Éclairage.

CIE No. 86. 1990. "2º Spectral Luminous Efficiency Function for Photopic Vision." Vienna: Commission Internationale de l'Éclairage.

CIE No. 142. 2001. "Improvement to Colour Difference Evaluation." Vienna: Commission Internationale de l'Éclairage.

CIE No. 160. 2004. "A Review of Chromatic Adaptation Transforms." Vienna: Commission Internationale de l'Éclairage.

Clarke, R. J. 2003. "Characteristics of the Pupillary Light Reflex in the Alert Rhesus Monkey." *Journal of Neurophysiology* 89 (6): 3179–89. doi:10.1152/jn.01131.2002.

Cohen, Jozef B., and William E. Kappauf. 1982. "Metameric Color Stimuli, Fundamental Metamers, and Wyszecki's Metameric Blacks." *The American Journal of Psychology*, 537–64.

Czeisler, Charles A., Theresa L. Shanahan, Elizabeth B. Klerman, Heinz Martens, Daniel J. Brotman, Jonathan S. Emens, Torsten Klein, and Joseph F. Rizzo. 1995. "Suppression of Melatonin Secretion in Some Blind Patients by Exposure to Bright Light." *New England Journal of Medicine* 332 (1): 6–11.

Dacey, Dennis, HW Liao, Beth Peterson, Farrel Robinson, Vivianne Smith, Joel Pokorny, KW Yau, and Paul D. Gamlin. 2005. "Melanopsin-Expressing Ganglion Cells in Primate Retina Signal Colour and Irradiance and Project to the LGN." *Nature* 433 (7027): 741–45. doi:10.1038/nature03344.

Dacey, Dennis, Beth B. Peterson, Farrel R. Robinson, and Paul D. Gamlin. 2003. "Fireworks in the Primate Retina: In Vitro Photodynamics Reveals Diverse LGN-Projecting Ganglion Cell Types." *Neuron* 37 (1): 15–27.

Davis, Wendy, and Yoshi Ohno. 2010. "Color Quality Scale." *Optical Engineering* 49 (3): 033602. doi:10.1117/1.3360335.

DiLaura, D.L. 2011. "Lighting Handbook. Reference and Application (10th Ed.)." Illuminating Engineering Society of North America.

"DIN (2009) Optical Radiation Physics and Illuminating Engineering – Part 100: Non-Visual Effects of Ocular Light on Human Beings – Quantities, Symbols and Action Spectra." 2009. Deutsches Institut fur Normung.

Do, Michael Tri H., Shin H. Kang, Tian Xue, Haining Zhong, Hsi-Wen Liao, Dwight E. Bergles, and King-Wai Yau. 2009. "Photon Capture and Signalling by Melanopsin Retinal Ganglion Cells." *Nature* 457 (7227): 281–87. doi:10.1038/nature07682.

Dowling, John. 2012. *The Retina: An Approachable Part of the Brain*. Cambridge: Belknap Press.

Ecker, Jennifer L., Olivia N. Dumitrescu, Kwoon Y. Wong, Nazia M. Alam, Shih-Kuo Chen, Tara LeGates, Jordan M. Renna, Glen T. Prusky, David M. Berson, and Samer Hattar. 2010. "Melanopsin-Expressing Retinal Ganglion-Cell Photoreceptors: Cellular Diversity and Role in Pattern Vision." *Neuron* 67 (1): 49–60. doi:10.1016/j.neuron.2010.05.023.

Edgar, Nicole, and Colleen A. McClung. 2013. "Major Depressive Disorder: A Loss of Circadian Synchrony?" *BioEssays* 35 (11): 940–44. doi:10.1002/bies.201300086.

Emanuel, Alan Joseph, and Michael Tri Hoang Do. 2015. "Melanopsin Tristability for Sustained and Broadband Phototransduction." *Neuron* 85 (5): 1043–55. doi:10.1016/j.neuron.2015.02.011.

Ernst, Michael D. 2004. "Permutation Methods: A Basis for Exact Inference." *Statistical Science* 19 (4): 676–85. doi:10.1214/088342304000000396.

Estévez, O, and H Spekreijse. 1982. "The 'Silent Substitution' Method in Visual Research." *Vision Research* 22: 681–91.

Fain, Gordon L., Hugh R. Matthews, M. Carter Cornwall, and Yiannis Koutalos. 2001. "Adaptation in Vertebrate Photoreceptors." *Physiological Reviews* 81 (1): 117–51.

Fairchild, Mark. 2013. *Color Appearance Models*. 3rd ed. Wiley-Interscience.

Fairchild, Mark D., and Lisa Reniff. 1995. "Time Course of Chromatic Adaptation for Color-Appearance Judgments." *JOSA A* 12 (5): 824–33.

Fechner, GT. 1860. *Elemente Der Psychophysik (in German)*. Leipzig: Breitkopf und Härtel.

Figueiro, Mariana G., Andrew Bierman, and Mark S. Rea. 2008. "Retinal Mechanisms Determine the Subadditive Response to Polychromatic Light by the Human Circadian System." *Neuroscience Letters* 438 (2): 242–45. doi:10.1016/j.neulet.2008.04.055.

Figueiro, Mariana G., John D. Bullough, Robert H. Parsons, and Mark S. Rea. 2005. "Preliminary Evidence for a Change in Spectral Sensitivity of the Circadian System at Night." *Journal of Circadian Rhythms* 3 (1): 14.

Fotios, Houser, Cheal, and Royer. 2010. "A Comparison of Simultanous and Sequential Evaluations of Spatial Brightness Suggests the Pupil Size Mechanism Is Not Responsible for Spatial Brightness: Proceedings of CIE 2010 'Lighting Quality and Energy Efficiency.'" *Vienna: CIE*, 428–38.

Freedman, MS, JL Lucas, B Soni, Malcolm von Schantz, M Muñoz, Zoe David-Gray, and R Foster. 1999. "Regulation of Mammalian Circadian Behavior by Non-Rod, Non-Cone, Ocular Photoreceptors." *Science* 284: 502–4.

Gaddy, JR, MD Rollag, and GC Brainard. 1993. "Pupil Size Regulation of Threshold of Light-Induced Melatonin Suppression." *Journal of Clinical Endocrinology and Metabolism*, no. 77: 1398–1401.

Gamlin, PD, DH McDougal, J Pokorny, VC Smith, KW Yau, and DM Dacey. 2007. "Human and Macaque Pupil Responses Driven by Melanopsin-Containing Retinal Ganglion Cells." *Vision Research* 47 (7): 946–54.

García-Fernández, JM, AJ Jimenez, and RG Foster. 1995. "The Persistence of Cone Photoreceptors within the Dorsal Retina of Aged Retinally Degenerate Mice (rd/rd): Implications for Circadian Organization." *Neuroscience Letters*, no. 187: 33–36.

Gelman, A, and J Hill. 2006. *Data Analysis Using Regression and Multilevel/Hierarchical Models*. Cambridge: Cambridge University Press.

Gibson, KS. 1926. "The Relative Visibility Function." *Proceedings of the CIE 6th Session, Geneva, Switzerland, July 1924*, 232–38.

Glickman, Gena, Brenda Byrne, Carissa Pineda, Walter W. Hauck, and George C. Brainard. 2006. "Light Therapy for Seasonal Affective Disorder with Blue Narrow-Band Light-Emitting Diodes (LEDs)." *Biological Psychiatry* 59 (6): 502–7.

Golden, R. 2005. "The Efficacy of Light Therapy in the Treatment of Mood Disorders: A Review and Meta-Analysis of the Evidence." *Am J Psychiatry*, no. 162: 656–62.

Gooley, J. J., S. M. W. Rajaratnam, G. C. Brainard, R. E. Kronauer, C. A. Czeisler, and S. W. Lockley. 2010. "Spectral Responses of the Human Circadian System Depend on the Irradiance and Duration of Exposure to Light." *Science Translational Medicine* 2 (31): 31ra33–31ra33. doi:10.1126/scitranslmed.3000741.

Gooley, Joshua J., Ivan Ho Mien, Melissa A. St Hilaire, Sing-Chen Yeo, Eric Chern-Pin Chua, Eliza van Reen, Catherine J. Hanley, Joseph T. Hull, Charles A. Czeisler, and Steven W. Lockley. 2012. "Melanopsin and Rod–Cone Photoreceptors Play Different Roles in Mediating Pupillary Light Responses during Exposure to Continuous Light in Humans." *The Journal of Neuroscience* 32 (41): 14242–53.

Göz, Didem, Keith Studholme, Douglas A. Lappi, Mark D. Rollag, Ignacio Provencio, and Lawrence P. Morin. 2008. "Targeted Destruction of Photosensitive Retinal Ganglion Cells with a Saporin Conjugate Alters the Effects of Light on Mouse

Circadian Rhythms." Edited by Ernest Greene. *PLoS ONE* 3 (9): e3153. doi:10.1371/journal.pone.0003153.

Gronfier, C. 2004. "Efficacy of a Single Sequence of Intermittent Bright Light Pulses for Delaying Circadian Phase in Humans." *AJP: Endocrinology and Metabolism* 287 (1): E174–81. doi:10.1152/ajpendo.00385.2003.

Gronfier, Claude, Kenneth Wright Jr., Richard Kronauer, and Charles Czeisler. 2007. "Entrainment of the Human Circadian Pacemaker to Longer-than-24-H Days." *Proceedings of the National Academy of Sciences* 104 (21): 9081–86

GrüNert, Ulrike, Patricia R. Jusuf, Sammy C.S. Lee, and Dung Than Nguyen. 2011. "Bipolar Input to Melanopsin Containing Ganglion Cells in Primate Retina." *Visual Neuroscience* 28 (01): 39–50. doi:10.1017/S095252381000026X.

Güler, Ali D., Jennifer L. Ecker, Gurprit S. Lall, Shafiqul Haq, Cara M. Altimus, Hsi-Wen Liao, Alun R. Barnard, et al. 2008. "Melanopsin Cells Are the Principal Conduits for Rod–cone Input to Non-Image-Forming Vision." *Nature* 453 (7191): 102–5. doi:10.1038/nature06829.

Hannibal, J., L. Kankipati, C.E. Strang, B.B. Peterson, D. Dacey, and P.D. Gamlin. 2014. "Central Projections of Intrinsically Photosensitive Retinal Ganglion Cells in the Macaque Monkey: Central Projections of Intrinsically Photosensitive RGCs in Macaque." *Journal of Comparative Neurology* 522 (10): Spc1–Spc1. doi:10.1002/cne.23588.

Hart, W.M. 1987. *Adler's Physiology of the Eye, Clinical Application*. St. Louis: The C. V. Mosby Company,.

Hashimoto, Kenjiro, Tadashi Yano, Masanori Shimizu, and Yoshinobu Nayatani. 2007. "New Method for Specifying Color-Rendering Properties of Light Sources Based on Feeling of Contrast." *Color Research & Application* 32 (5): 361–71. doi:10.1002/col.20338.

Hatori, Megumi, Hiep Le, Christopher Vollmers, Sheena Racheal Keding, Nobushige Tanaka, Christian Schmedt, Timothy Jegla, and Satchidananda Panda. 2008. "Inducible Ablation of Melanopsin-Expressing Retinal Ganglion Cells Reveals Their Central Role in Non-Image Forming Visual Responses." Edited by Michael Hendricks. *PLoS ONE* 3 (6): e2451. doi:10.1371/journal.pone.0002451.

Hattar, Samer, Robert J. Lucas, N. Mrosovsky, S. Thompson, R. H. Douglas, Mark W. Hankins, J. Lem, et al. 2003. "Melanopsin and Rod–cone Photoreceptive Systems Account for All Major Accessory Visual Functions in Mice." *Nature* 424 (6944): 75–81.

Hattar, S, HW Liao, M Takao, DM Berson, and KW Yau. 2002. "Melanopsin-Containing Retinal Ganglion Cells: Architecture, Projections, and Intrinsic Photosensitivity." *Science*, no. 295: 1065–70.

Hecht, Eugene. 1987. *Optics*. 2nd ed. Addison Wesley.

Helmholtz. 1911. *Treatise on Physiological Optics*. Vol. ii.

Ho Mien, Ivan, Eric Chern-Pin Chua, Pauline Lau, Luuan-Chin Tan, Ivan Tian-Guang Lee, Sing-Chen Yeo, Sara Shuhui Tan, and Joshua J. Gooley. 2014. "Effects of Exposure to Intermittent versus Continuous Red Light on Human Circadian Rhythms, Melatonin Suppression, and Pupillary Constriction." Edited by Henrik Oster. *PLoS ONE* 9 (5): e96532. doi:10.1371/journal.pone.0096532.

Hu, C., D. D. Hill, and K. Y. Wong. 2013. “Intrinsic Physiological Properties of the Five Types of Mouse Ganglion-Cell Photoreceptors.” *Journal of Neurophysiology* 109 (7): 1876–89. doi:10.1152/jn.00579.2012.

Hunter, Jennifer J., Jessica I.W. Morgan, William H. Merigan, David H. Sliney, Janet R. Sparrow, and David R. Williams. 2012. “The Susceptibility of the Retina to Photochemical Damage from Visible Light.” *Progress in Retinal and Eye Research* 31 (1): 28–42. doi:10.1016/j.preteyeres.2011.11.001.

Hunt, RWG. 1981. “A Theory of Hue Appearance.” *Proceedings of the 4th Congress of the International Color Association, AIC Color 81 Berlin*, J7.

Hunt, RWG, and MR Pointer. 2011. *Measuring Colour*. 4th ed. Wiley-Interscience.

“IES (2008) Light and Human Health: An Overview of the Impact of Optical Radiation on Visual, Circadian, Neuroendocrine and Neurobehavioural Responses.” 2008. Illuminating Engineering Society of North America.

Ishihara, M. 1906. “Analysis Test of the Photoelectric Fluctuations in a Frog’s Eye.” *ARCHIV FUR DIE GESAMTE PHYSIOLOGIE DES MENSCHEN UND DER TIERE* 114 (11/12): 569–618.

Jusuf, Patricia R., Sammy C. S. Lee, Jens Hannibal, and Ulrike Grünert. 2007. “Characterization and Synaptic Connectivity of Melanopsin-Containing Ganglion Cells in the Primate Retina: Melanopsin Ganglion Cells in Primate Retina.” *European Journal of Neuroscience* 26 (10): 2906–21. doi:10.1111/j.1460-9568.2007.05924.x.

Kankipati, L., C. A. Girkin, and P. D. Gamlin. 2009. “Post-Illumination Pupil Response in Subjects without Ocular Disease.” *Investigative Ophthalmology & Visual Science* 51 (5): 2764–69. doi:10.1167/iovs.09-4717.

Kardon, R, SC Anderson, TG Damarjian, E Grace, E Stone, and A Kawasaki. 2009. “Chromatic Pupil Responses: Preferential Activation of the Melanopsin-Mediated versus Outer Photoreceptor-Mediated Pupil Light Reflex.” *Ophthalmology* 116 (8): 1564–73.

Klepeis, Neil E., William C. Nelson, Wayne R. Ott, John P. Robinson, Andy M. Tsang, Paul Switzer, Joseph V. Behar, Stephen C. Hern, William H. Engelmann, and others. 2001. “The National Human Activity Pattern Survey (NHAPS): A Resource for Assessing Exposure to Environmental Pollutants.” *Journal of Exposure Analysis and Environmental Epidemiology* 11 (3): 231–52.

Kolla, B. P., and R. R. Auger. 2011. “Jet Lag and Shift Work Sleep Disorders: How to Help Reset the Internal Clock.” *Cleveland Clinic Journal of Medicine* 78 (10): 675–84. doi:10.3949/ccjm.78a.10083.

Koyanagi, Mitsumasa, Kaoru Kubokawa, Hisao Tsukamoto, Yoshinori Shichida, and Akihisa Terakita. 2005. “Cephalochordate Melanopsin: Evolutionary Linkage between Invertebrate Visual Cells and Vertebrate Photosensitive Retinal Ganglion Cells.” *Current Biology* 15 (11): 1065–69. doi:10.1016/j.cub.2005.04.063.

Lall, Gurprit S., Victoria L. Revell, Hiroshi Momiji, Jazi Al Enezi, Cara M. Altimus, Ali D. Güler, Carlos Aguilar, et al. 2010. “Distinct Contributions of Rod, Cone, and Melanopsin Photoreceptors to Encoding Irradiance.” *Neuron* 66 (3): 417–28. doi:10.1016/j.neuron.2010.04.037.

La Morgia, Chiara, Fred N. Ross-Cisneros, Jens Hannibal, Pasquale Montagna, Alfredo A. Sadun, and Valerio Carelli. 2011. “Melanopsin-Expressing Retinal Ganglion

Cells: Implications for Human Diseases." *Vision Research* 51 (2): 296–302. doi:10.1016/j.visres.2010.07.023.
Lam, Raymond W., and Anthony J. Levitt. 2000. "Pathophysiology of Seasonal Affective Disorder: A Review." *Retrieved November* 3: 2007.
Lee, Sang-il, Akiko Hida, Shingo Kitamura, Kazuo Mishima, and Shigekazu Higuchi. 2014. "Association between the Melanopsin Gene Polymorphism OPN4* Ile394Thr and Sleep/wake Timing in Japanese University Students." *Journal of Physiological Anthropology* 33 (1): 1.
LeGates, Tara A., Cara M. Altimus, Hui Wang, Hey-Kyoung Lee, Sunggu Yang, Haiqing Zhao, Alfredo Kirkwood, E. Todd Weber, and Samer Hattar. 2012. "Aberrant Light Directly Impairs Mood and Learning through Melanopsin-Expressing Neurons." *Nature* 491 (7425): 594–98.
Lehrl, S., K. Gerstmeyer, J. H. Jacob, H. Frieling, A. W. Henkel, R. Meyrer, J. Wiltfang, J. Kornhuber, and S. Bleich. 2007. "Blue Light Improves Cognitive Performance." *Journal of Neural Transmission* 114 (4): 457–60. doi:10.1007/s00702-006-0621-4.
Lei, Shaobo, Herbert C. Goltz, Mano Chandrakumar, and Agnes M. F. Wong. 2014. "Full-Field Chromatic Pupillometry for the Assessment of the Postillumination Pupil Response Driven by Melanopsin-Containing Retinal Ganglion Cells." *Investigative Opthalmology & Visual Science* 55 (7): 4496. doi:10.1167/iovs.14-14103.
Lockley, Steven W., George C. Brainard, and Charles A. Czeisler. 2003. "High Sensitivity of the Human Circadian Melatonin Rhythm to Resetting by Short Wavelength Light." *J Clin Endocrinol Metab* 88 (9): 4502–5.
Lockley, Steven W., Erin E. Evans, FAJL Scheer, George C. Brainard, Charles A. Czeisler, and Daniel Aeschbach. 2006. "Short-Wavelength Sensitivity for the Direct Effects of Light on Alertness, Vigilance, and the Waking Electroencephalogram in Humans." *SLEEP-NEW YORK THEN WESTCHESTER*- 29 (2): 161.
Loewenfeld, IE. 1999. *The Pupil: Anatomy, Physiology, and Clinical Applications*. 2nd ed. Oxford: Butterworth-Heinemann.
Lok, Corie. 2011. "Seeing without Seeing." *Nature* 469 (7330): 284–85.
Lucas, Robert J., Stuart N. Peirson, David M. Berson, Timothy M. Brown, Howard M. Cooper, Charles A. Czeisler, Mariana G. Figueiro, et al. 2014. "Measuring and Using Light in the Melanopsin Age." *Trends in Neurosciences* 37 (1): 1–9. doi:10.1016/j.tins.2013.10.004.
Malacara, Daniel. 2011. *Color Vision and Colorimetry: Theory and Applications*. 1st ed. SPIE.
Marks, Lawrence. 1974. *Sensory Processes: The New Psychophysics*. Elsevier.
McDougal, David H., and Paul D. Gamlin. 2010. "The Influence of Intrinsically-Photosensitive Retinal Ganglion Cells on the Spectral Sensitivity and Response Dynamics of the Human Pupillary Light Reflex." *Vision Research* 50 (1): 72–87.
McIntyre, IM, TR Norman, GD Burrows, and SM Armstrong. 1989. "Human Melatonin Response to Light at Different Times of the Night." *Psychoneuroendocrinology*, no. 14: 187–93.
Medina, John. 2008. *Brain Rules*. Pear Press.

Meesters, Ybe, Vera Dekker, Luc JM Schlangen, Elske H. Bos, and Martine J. Ruiter. 2011. “Low-Intensity Blue-Enriched White Light (750 Lux) and Standard Bright Light (10 000 Lux) Are Equally Effective in Treating SAD. A Randomized Controlled Study.” *BMC Psychiatry* 11 (1): 17.

“Method of Measuring and Specifying Colour Rendering Properties of Light Sources.” 1995. CIE 13.3 (TC-3.2). Vienna: Commission Internationale de l’Éclairage.

Middleton, Benita, Barbara M. Stone, and Josephine Arendt. 2002. “Human Circadian Phase in 12: 12 H, 200:< 8 Lux and 1000:< 8 Lux Light-Dark Cycles, without Scheduled Sleep or Activity.” *Neuroscience Letters* 329 (1): 41–44.

Mitchell, DE, and WAH Rushton. 1971b. “The Red/green Pigments of Normal Vision.” *Vision Research* 11: 1045–56.

———. 1971a. “Visual Pigments in Dichromats.” *Vision Research* 11: 1033–43.

Mori, L, H Sobagaki, H Komatsubara, and K Ikeda. 1991. “Field Trials on CIE Chromatic Adaptation Formula.” Proceedings of the CIE 22nd Session. Vienna: Commission Internationale de l’Éclairage.

Morin, L.P., and K.M. Studholme. 2011. “Separation of Function for Classical and Ganglion Cell Photoreceptors with Respect to Circadian Rhythm Entrainment and Induction of Photosomnolence.” *Neuroscience* 199 (December): 213–24. doi:10.1016/j.neuroscience.2011.09.057.

Munch, M, L Leon, S Crippa, and A Kawasaki. 2012. “Circadian and Wake-Dependent Effects on the Pupil Light Reflex in Response to Narrow-Bandwidth Light Pulses.” *Visual Neuroscience* 53 (8): 4546–55.

Mure, L. S., C. Rieux, S. Hattar, and H. M. Cooper. 2007. “Melanopsin-Dependent Nonvisual Responses: Evidence for Photopigment Bistability In Vivo.” *Journal of Biological Rhythms* 22 (5): 411–24. doi:10.1177/0748730407306043.

Mure, Ludovic S., Pierre-Loic Cornut, Camille Rieux, Elise Drouyer, Philippe Denis, Claude Gronfier, and Howard M. Cooper. 2009. “Melanopsin Bistability: A Fly’s Eye Technology in the Human Retina.” Edited by Christophe Egles. *PLoS ONE* 4 (6): e5991. doi:10.1371/journal.pone.0005991.

Nagy, Allen L., Rhea T. Eskew, and Robert M. Boynton. 1987. “Analysis of Color-Matching Ellipses in a Cone-Excitation Space.” *JOSA A* 4 (4): 756–68.

Naus, Tess, Andreas Burger, Ayse Malkoc, Marc Molendijk, and Judith Haffmans. 2013. “Is There a Difference in Clinical Efficacy of Bright Light Therapy for Different Types of Depression? A Pilot Study.” *Journal of Affective Disorders* 151 (3): 1135–37. doi:10.1016/j.jad.2013.07.017.

Neumann, A., J. J. Wierer, Jr., W. Davis, Y. Ohno, S. R. J. Brueck, and J. Y. Tsao. 2011. “Four-Color Laser White Illuminant Demonstrating High Color-Rendering Quality.” *Optics Express* 19 (S4): A982–90.

Neumann, S., S. Haverkamp, and O.N. Auferkorte. 2011. “Intrinsically Photosensitive Ganglion Cells of the Primate Retina Express Distinct Combinations of Inhibitory Neurotransmitter Receptors.” *Neuroscience* 199 (December): 24–31. doi:10.1016/j.neuroscience.2011.10.027.

Ohno, Yoshi. 2005. “Spectral Design Considerations for White LED Color Rendering.” *Optical Engineering* 44 (11): 111302. doi:10.1117/1.2130694.

Panda, S, I Provencio, D Tu, and S Pires. 2003. “Melanopsin Is Required for Non-Image-Forming Photic Responses in Blind Mice.” *Science* 301: 526–27.

Park, J. C., A. L. Moura, A. S. Raza, D. W. Rhee, R. H. Kardon, and D. C. Hood. 2011. "Toward a Clinical Protocol for Assessing Rod, Cone, and Melanopsin Contributions to the Human Pupil Response." *Investigative Ophthalmology & Visual Science* 52 (9): 6624–35. doi:10.1167/iovs.11-7586.

Provencio, Ignacio, Mark D. Rollag, and Ana Maria Castrucci. 2002. "Photoreceptive Net in the Mammalian Retina." *Nature* 415 (6871): 493–493.

Rahman, Shadab A., Erin E. Flynn-Evans, Daniel Aeschbach, George C. Brainard, Charles A. Czeisler, and Steven W. Lockley. 2014. "Diurnal Spectral Sensitivity of the Acute Alerting Effects of Light." *SLEEP*, February. doi:10.5665/sleep.3396.

Rea, Mark S., Mariana G. Figueiro, John D. Bullough, and Andrew Bierman. 2005. "A Model of Phototransduction by the Human Circadian System." *Brain Research Reviews* 50 (2): 213–28. doi:10.1016/j.brainresrev.2005.07.002.

Reifler, Aaron N., Andrew P. Chervenak, Michael E. Dolikian, Brian A. Benenati, Benjamin S. Meyers, Zachary D. Demertzis, Andrew M. Lynch, et al. 2015. "The Rat Retina Has Five Types of Ganglion-Cell Photoreceptors." *Experimental Eye Research* 130 (January): 17–28. doi:10.1016/j.exer.2014.11.010.

Revell, Victoria L., Daniel C. G. Barrett, Luc J. M. Schlangen, and Debra J. Skene. 2010. "PREDICTING HUMAN NOCTURNAL NONVISUAL RESPONSES TO MONOCHROMATIC AND POLYCHROMATIC LIGHT WITH A MELANOPSIN PHOTOSENSITIVITY FUNCTION." *Chronobiology International* 27 (9-10): 1762–77. doi:10.3109/07420528.2010.516048.

Rimmer, DW, DB Boivin, TL Shanahan, RE Kronauer, JF Duffy, and CA Czeisler. 2000. "Dynamic Resetting of the Human Circadian Pacemaker by Intermittent Bright Light." *Am J Physiol Regul Integr Comp Physiol* 279 (5): 1574–79.

Robertson, AR. 1978. "CIE Guidelines for Coordinated Research on Color-Difference Evaluation." *Color Research & Application*, no. 3: 149–51.

Roecklein, Kathryn, Patricia Wong, Natalie Ernecoff, Megan Miller, Shannon Donofry, Marissa Kamarck, W. Michael Wood-Vasey, and Peter Franzen. 2013. "The Post Illumination Pupil Response Is Reduced in Seasonal Affective Disorder." *Psychiatry Research* 210 (1): 150–58. doi:10.1016/j.psychres.2013.05.023.

Rosenthal, Norman E., David A. Sack, J. Christian Gillin, Alfred J. Lewy, Frederick K. Goodwin, Yolande Davenport, Peter S. Mueller, David A. Newsome, and Thomas A. Wehr. 1984. "Seasonal Affective Disorder: A Description of the Syndrome and Preliminary Findings with Light Therapy." *Archives of General Psychiatry* 41 (1): 72.

Royer, M, and K Houser. 2012. "Spatial Brightness Perception of Trichromatic Stimuli." *LEUKOS* 9 (2): 89–108.

Rüger, Melanie, Melissa A. St Hilaire, George C. Brainard, Sat-Bir S. Khalsa, Richard E. Kronauer, Charles A. Czeisler, and Steven W. Lockley. 2013. "Human Phase Response Curve to a Single 6.5 H Pulse of Short-Wavelength Light." *The Journal of Physiology* 591 (1): 353–63.

Ryer, Alex. 1997. *Light Measurement Handbook*. Newburyport, MA: International Light.

Schanda, János. 2007. *Colorimetry: Understanding the CIE System*. 1st Ed. John Wiley & Sons.

Schmidt, T. M., and P. Kofuji. 2009. "Functional and Morphological Differences among Intrinsically Photosensitive Retinal Ganglion Cells." *Journal of Neuroscience* 29 (2): 476–82. doi:10.1523/JNEUROSCI.4117-08.2009.
———. 2010. "Differential Cone Pathway Influence on Intrinsically Photosensitive Retinal Ganglion Cell Subtypes." *Journal of Neuroscience* 30 (48): 16262–71. doi:10.1523/JNEUROSCI.3656-10.2010.
Shapiro, Arthur G., Joel Pokorny, and Vivianne C. Smith. 1996. "Cone–rod Receptor Spaces with Illustrations That Use CRT Phosphor and Light-Emitting-Diode Spectra." *JOSA A* 13 (12): 2319–28.
Spitschan, M., S. Jain, D. H. Brainard, and G. K. Aguirre. 2014. "Opponent Melanopsin and S-Cone Signals in the Human Pupillary Light Response." *Proceedings of the National Academy of Sciences* 111 (43): 15568–72. doi:10.1073/pnas.1400942111.
Stein, J.F. 2006. *Neuroscience: An Introduction*. Chichester: Wiley.
Stephenson, Kathryn M., Carmen M. Schroder, Gilles Bertschy, and Patrice Bourgin. 2012. "Complex Interaction of Circadian and Non-Circadian Effects of Light on Mood: Shedding New Light on an Old Story." *Sleep Medicine Reviews* 16 (5): 445–54. doi:10.1016/j.smrv.2011.09.002.
Stevens, Richard G. 2009. "Electric Light Causes Cancer? Surely You're Joking, Mr. Stevens." *Mutat Res* 682 (1): 1–6.
Stockman, Andrew, Herbert Jägle, Markus Pirzer, and Lindsay Sharpe. 2007. "Vμ*(λ): A Generalized Luminous Efficiency Function for Any Condition of Chromatic Adaptation." *Journal of Vision* 7 (9): 793–793. doi:10.1167/7.9.793.
Stockman, Andrew, and Lindsay T. Sharpe. 2000. "The Spectral Sensitivities of the Middle- and Long-Wavelength-Sensitive Cones Derived from Measurements in Observers of Known Genotype." *Vision Research*, no. 40: 1711–37.
———. 2006. "Into the Twilight Zone: The Complexities of Mesopic Vision and Luminous Efficiency." *Ophthalmic and Physiological Optics* 26 (3): 225–39.
Swanson, William H., Takehiro Ueno, Vivianne C. Smith, and Joel Pokorny. 1987. "Temporal Modulation Sensitivity and Pulse-Detection Thresholds for Chromatic and Luminance Perturbations." *JOSA A* 4 (10): 1992–2005.
Tapia-Osorio, Araceli, Roberto Salgado-Delgado, Manuel Angeles-Castellanos, and Carolina Escobar. 2013. "Disruption of Circadian Rhythms due to Chronic Constant Light Leads to Depressive and Anxiety-like Behaviors in the Rat." *Behavioural Brain Research* 252 (September): 1–9. doi:10.1016/j.bbr.2013.05.028.
Thapan, Kavita, Josephine Arendt, and Debra J. Skene. 2001. "An Action Spectrum for Melatonin Suppression: Evidence for a Novel Non-Rod, Non-Cone Photoreceptor System in Humans." *The Journal of Physiology* 535 (1): 261–67.
Toga, Arthur. 2015. *Brain Mapping: An Encyclopedic Reference*. London: Academic Press.
Tsujimura, S.-i., K. Ukai, D. Ohama, A. Nuruki, and K. Yunokuchi. 2010. "Contribution of Human Melanopsin Retinal Ganglion Cells to Steady-State Pupil Responses." *Proceedings of the Royal Society B: Biological Sciences* 277 (1693): 2485–92. doi:10.1098/rspb.2010.0330.
Turner, Patricia L., Eus J.W. Van Someren, and Martin A. Mainster. 2010. "The Role of Environmental Light in Sleep and Health: Effects of Ocular Aging and Cataract

Surgery." *Sleep Medicine Reviews* 14 (4): 269–80. doi:10.1016/j.smrv.2009.11.002.
Tuunainen, Arja, Daniel F Kripke, and Takuro Endo. 2004. "Light Therapy for Non-Seasonal Depression." In *Cochrane Database of Systematic Reviews*, edited by The Cochrane Collaboration. Chichester, UK: John Wiley & Sons, Ltd. http://doi.wiley.com/10.1002/14651858.CD004050.pub2.
Van Den Pol, Anthony N., Vinh Cao, and H. Craig Heller. 1998. "Circadian System of Mice Integrates Brief Light Stimuli." *American Journal of Physiology-Regulatory, Integrative and Comparative Physiology* 275 (2): R654–57.
Vandewalle, G., S. Gais, M. Schabus, E. Balteau, J. Carrier, A. Darsaud, V. Sterpenich, G. Albouy, D. J. Dijk, and P. Maquet. 2007. "Wavelength-Dependent Modulation of Brain Responses to a Working Memory Task by Daytime Light Exposure." *Cerebral Cortex* 17 (12): 2788–95. doi:10.1093/cercor/bhm007.
Vandewalle, Gilles, Evelyne Balteau, Christophe Phillips, Christian Degueldre, Vincent Moreau, Virginie Sterpenich, Geneviève Albouy, et al. 2006. "Daytime Light Exposure Dynamically Enhances Brain Responses." *Current Biology* 16 (16): 1616–21. doi:10.1016/j.cub.2006.06.031.
Vandewalle, Gilles, Olivier Collignon, Joseph T. Hull, Véronique Daneault, Geneviève Albouy, Franco Lepore, Christophe Phillips, et al. 2013. "Blue Light Stimulates Cognitive Brain Activity in Visually Blind Individuals." *Journal of Cognitive Neuroscience* 25 (12): 2072–85. doi:10.1162/jocn_a_00450.
Varjú, Von Dezsö. 1964. "Der Einflu Sinusförmiger Leuchtdichteänderungen Auf Die Mittlere Pupillenweite Und Auf Die Subjektive Helligkeit." *Biological Cybernetics* 2 (2): 33–43.
Vartanian, Garen, Xiwu Zhao, and K. Y. Wong. 2015. "Using Flickering Light to Enhance Non-Image Forming Visual Stimulation in Humans." *Investigative Ophthalmology & Visual Science* 56 (8): 4680–88. doi:10.1167/iovs.15-16468.
Vidal, L., and L. P. Morin. 2007. "Absence of Normal Photic Integration in the Circadian Visual System: Response to Millisecond Light Flashes." *Journal of Neuroscience* 27 (13): 3375–82. doi:10.1523/JNEUROSCI.5496-06.2007.
Viénot, Françoise, and Hans Brettel. 2014. "The Verriest Lecture: Visual Properties of Metameric Blacks beyond Cone Vision." *Journal of the Optical Society of America A* 31 (4): A38. doi:10.1364/JOSAA.31.000A38.
Viénot, Françoise, Hans Brettel, Tuong-Vi Dang, and Jean Le Rohellec. 2012. "Domain of Metamers Exciting Intrinsically Photosensitive Retinal Ganglion Cells (ipRGCs) and Rods." *JOSA A* 29 (2): A366–76.
Viola, A, L James, L Schlangen, and D.J. Dijk. 2008. "Blue-Enriched White Light in the Workplace Improves Self-Reported Alertness, Performance, and Sleep Quality." *Scandinavian Journal of Work, Environment & Health* 34 (4): 297–306.
Von Kries, JA. 1911. *Handbuch Der Physiologisches Optik, Vol. II (in German)*. Hamburg: Leopold Voss.
Walch, Olivia J., L. Samantha Zhang, Aaron N. Reifler, Michael E. Dolikian, Daniel B. Forger, and Kwoon Y. Wong. 2015. "Characterizing and Modeling the Intrinsic Light Response of Rat Ganglion-Cell Photoreceptors." *Journal of Neurophysiology* 114 (5): 2955–66. doi:10.1152/jn.00544.2015.

Webvision: The Organization of the Retina and Visual System. 2016. http://webvision.med.utah.edu.

Weissman, Daniel H., Tobias Egner, Zoë Hawks, and Jacqueline Link. 2015. "The Congruency Sequence Effect Emerges When the Distracter Precedes the Target." *Acta Psychologica* 156 (March): 8–21. doi:10.1016/j.actpsy.2015.01.003.

West, BT, KB Welch, and AT Galecki. 2006. *Linear Mixed Models: A Practical Guide Using Statistical Software*. London: Chapman & Hall/CRC.

Wong, Kwoon Y., Felice A. Dunn, and David M. Berson. 2005. "Photoreceptor Adaptation in Intrinsically Photosensitive Retinal Ganglion Cells." *Neuron* 48 (6): 1001–10. doi:10.1016/j.neuron.2005.11.016.

Wong, K. Y., F. A. Dunn, D. M. Graham, and D. M. Berson. 2007. "Synaptic Influences on Rat Ganglion-Cell Photoreceptors." *The Journal of Physiology* 582 (1): 279–96. doi:10.1113/jphysiol.2007.133751.

Wong, K. Y., D. M. Graham, and D. M. Berson. 2007. "The Retina-Attached SCN Slice Preparation: An In Vitro Mammalian Circadian Visual System." *Journal of Biological Rhythms* 22 (5): 400–410. doi:10.1177/0748730407305376.

Wyszecki, G, and W. S. Stiles. 1982. *Color Science: Concepts and Methods, Quantitative Data and Formulae*. 2nd ed. Wiley-Interscience.

Wyszecki, Gunter, and Walter Stanley Stiles. 1982. *Color Science: Concepts and Methods, Quantitative Data and Formulae*. Vol. 8. Wiley New York.

Yoss, Robert E., Norma J. Moyer, and Robert W. Hollenhorst. 1970. "Pupil Size and Spontaneous Pupillary Waves Associated with Alertness, Drowsiness, and Sleep." *Neurology* 20 (6): 545–545.

Zaidi, Farhan H., Joseph T. Hull, Stuart N. Peirson, Katharina Wulff, Daniel Aeschbach, Joshua J. Gooley, George C. Brainard, et al. 2007. "Short-Wavelength Light Sensitivity of Circadian, Pupillary, and Visual Awareness in Humans Lacking an Outer Retina." *Current Biology* 17 (24): 2122–28. doi:10.1016/j.cub.2007.11.034.

Zeitzer, Jamie M., Derk-Jan Dijk, Richard E. Kronauer, Emery N. Brown, and Charles A. Czeisler. 2000. "Sensitivity of the Human Circadian Pacemaker to Nocturnal Light: Melatonin Phase Resetting and Suppression." *The Journal of Physiology* 526 (3): 695–702.

Zeitzer, Jamie M., Norman F. Ruby, Ryan A. Fisicaro, and H. Craig Heller. 2011. "Response of the Human Circadian System to Millisecond Flashes of Light." Edited by Shin Yamazaki. *PLoS ONE* 6 (7): e22078. doi:10.1371/journal.pone.0022078.

Zele, Andrew J., Beatrix Feigl, Simon S. Smith, and Emma L. Markwell. 2011. "The Circadian Response of Intrinsically Photosensitive Retinal Ganglion Cells." Edited by Stuart Dryer. *PLoS ONE* 6 (3): e17860. doi:10.1371/journal.pone.0017860.

Zhao, Xiwu, Ben K. Stafford, Ashley L. Godin, W. Michael King, and Kwoon Y. Wong. 2014. "Photoresponse Diversity among the Five Types of Intrinsically Photosensitive Retinal Ganglion Cells: Light Responses of Melanopsin Ganglion Cells." *The Journal of Physiology* 592 (7): 1619–36. doi:10.1113/jphysiol.2013.262782.